

INTELLIGENT POWER ALLOCATION STRATEGY FOR ELECTRIC VEHICLES

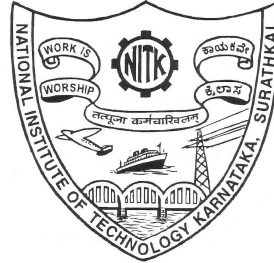
Thesis

Submitted in partial fulfillment of the requirement for the award of the degree of

DOCTOR OF PHILOSOPHY

by

VISHNU SIDHARTHAN P




DEPARTMENT OF ELECTRICAL AND ELECTRONICS ENGINEERING
NATIONAL INSTITUTE OF TECHNOLOGY KARNATAKA
SRINIVASNAGAR, MANGALORE - 575025

OCTOBER, 2023

DECLARATION

by the Ph.D. Research Scholar

I hereby *declare* that the Research Thesis entitled “**Intelligent Power Allocation Strategy for Electric Vehicles**” which is being submitted to the **National Institute of Technology Karnataka, Surathkal** in partial fulfillment of the requirement for the award of the Degree of **Doctor of Philosophy in Electrical and Electronics Engineering** is a *bonafide report of the research work carried out by me*. The material in this Research Thesis has not been submitted to any University or Institution for the award of any degree.



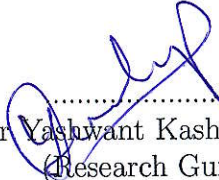
.....
VISHNU SIDHARTHAN P, 187119
Department of Electrical and Electronics Engineering


Place: NITK-Surathkal
Date: October 17, 2023

CERTIFICATE

by the *Ph.D. Research Scholar*

This is to *certify* that the Research Thesis entitled "**Intelligent Power Allocation Strategy for Electric Vehicles**" submitted by **Vishnu Sidharthan P** (Register Number: 187119) as the record of the research work carried out by him, is *accepted as the Research Thesis submission* in partial fulfillment of the requirements for the award of degree of **Doctor of Philosophy**.


.....
Dr. Yashwant Kashyap
(Research Guide)


.....
Dr. Dattatraya Narayan Gaonkar
(Chairman-DRPC, EEE dept.)

PROFESSOR AND HEAD

DEPARTMENT OF ELECTRICAL AND ELECTRONICS ENGINEERING
NATIONAL INSTITUTE OF TECHNOLOGY KARNATAKA
SRINIVASNAGAR, SURATHKAL, MANGALORE - 575 025, INDIA

Acknowledgments

It gives me immense pleasure and great satisfaction to express my heartfelt gratitude to those who made this dissertation possible.

Firstly, I thank *almighty God* for always giving me strength.

I want to express my sincere gratitude to *Dr. Yashwant Kashyap* for his guidance, unending support, and encouragement and for having been my Ph.D. supervisor. He has been a constant source of inspiration throughout this journey. I feel proud to have worked under his guidance.

I thank *National Institute of Technology Karnataka, Surathkal (NITK)* for allowing me to do research and *Ministry of Human Resource Department, Government of India* for awarding a research scholarship.

I thank my research progress assessment committee (RPAC) members, *Dr. Krishnan Chemmangat Manakkal Cherya* and *Dr Prabu K*, for their constructive feedback and guidance.

Thanks also go to former HODs, *Prof. B Venkatesa Perumal, Prof. Shubhanga K N, Prof. Gururaj S Punekar*, and HOD, *Dr. Dattatraya Narayan Gaonkar*, for providing the necessary resources in the department to carry out my research.

I would like to offer my sincere thanks to *Dr. Dileep. G, Mr. Asif Abdullah, Mr. Roystan Castelino, Mr. Vishnu Vishwambharan* and *Mr. Stejin C J* for their valuable supports at every stage of the research work.

I want to extend my deepest gratitude to my mother, father, and sister for their love and patience, which kept me on this journey. Their faith and unconditional love towards me are the reason for my achievements.

Finally, these last words are specially for my wife, who has been with me from the beginning of this process. Thank you for supporting me and making me strong to face any situation.

Vishnu Sidharthan P

Abstract

Transportation plays a significant role in the global economy, and its energy requirement has increased tremendously to reach 29 %, with massive growth in the past decade. Meanwhile, the transportation industry has consumed almost $2/3^{rd}$ of oil demand and nearly $1/4^{th}$ of global carbon dioxide emissions from fossil fuel combustion. Moreover, a hike in fossil fuel costs and their reduced availability are other major issues that motivated the development of a green and clean mode of transportation. In that context, vehicles with an alternative energy source are essential.

This highly motivated the development of battery electric vehicles and hybrid electric vehicles. Researchers have focused on investigating innovations with EVs. Although EVs are developed with improved performance and comfort, certain issues hinder their wider adoption. The Lithium-ion battery is one of the primary energy sources for electrified transportation. The battery performance of BEVs is affected by variations in different driving profiles and conditions. Vital factors that decide the performance of the EVs are 1) Battery life, 2) Range or mileage 3) Battery capacity fade costs. Hence investigation of these parameters is necessary for analyzing BEVs performance.

Considering the recent advanced BEV technologies, the performance parameters are not up to the mark. Battery life - Battery degradation affects the maximum power handling capability of the BEV battery, thus leading to poor performance of the vehicle. It reduces the life cycle of the battery and may initiate battery replacement. Range anxiety - The EV's range or mileage decides the user's anxiety. A reduced range creates range anxiety while driving since the charging stations are not ubiquitous. Capacity fade cost - This is an after-effect of battery life depletion. However, these are not similar for all users. It differs based on different driving conditions such as 1) **Vehicle** (starting, velocity, acceleration, and braking), 2) **Driver** (driving behaviors, route selection, charging, and usage patterns), 3) **Environment** (irradiance, ambient temperature, wind speed, road, and traffic conditions). Whenever the battery's capacity reaches less than 75%, it is called the battery's end of life. The battery fade costs must be reduced to increase the popularity of BEVs. The solution to such impacts on the BEVs highlights the usage of hybrid sources in EVs.

A supercapacitor coupled with a battery handles the transient load current of the EV traction. The SC response time and power density are higher than batteries; thus, it can ensure battery safety. Moreover, the regenerative braking energy can be recuperated in the SC, which improves energy efficiency. The energy utilization of the transportation industry is increasing tremendously. $2/3^{rd}$

of total energy consumption will be occupied by renewable energy (wind, solar, bioenergy, geothermal, and hydro energy) by the end of 2050. Electrified transportation combined with renewable energy sources reduces emissions by 60 %. Utilizing renewable sources in the vehicle ensures a green, clean, and sustainable transportation sector. Developing countries with higher solar insolation can employ solar panels to charge the EV sources during the daytime. They can achieve their daily commute with less number of charging from the grid. Therefore the contribution of Hybrid Source Electric Vehicles (HSEV) will be a significant step toward a sustainable future.

The SC and PV are the auxiliary sources coupled with the Lithium-ion battery in a proposed hybrid source system in EVs. An Intelligent Hybrid Source Energy Management Strategy (IHSEMS) employing a fuzzy logic-based controller is successfully introduced to overcome the issues and drawbacks of the existing electric vehicle systems ensuring an optimal source operations. The proposed algorithm ensures absolute energy sharing among each source and diminishes the impact of varying driving and environmental conditions. The proposed energy management strategy for HSEV improves the battery charge levels, increases the vehicle range, eliminates high C-rate instants, avoids frequent charge and discharging (fluctuations) in battery current profile, and improves the battery life. Moreover a modified energy management algorithm (EMA) is proposed for a high energy-dense SC and high conversion efficient PV panels based on a new hybrid energy vehicle. Investigations on different locations with varying driving and environmental conditions are conducted to highlight the significance of the proposed hybrid source model. A detailed techno-economic assessment shows the significance of the proposed hybrid models and respective proposed energy management algorithms compared to BEVs and existing EMSs. Moreover, in countries with underdeveloped grid infrastructure, Solar PV in electric vehicle applications can be highly beneficial.

Contents

Acknowledgements	i
Abstract	iii
List of Figures	vi
List of Tables	x
List of Abbreviations	xii
List of Symbols	xiv
1 Introduction	1
1.1 Background	1
1.2 Issues in Battery Electric Vehicles	3
1.3 Characteristics of Hybrid Sources	4
1.3.1 Lithium-ion battery	4
1.3.2 Supercapcitor	5
1.3.3 Solar Photovoltaic	6
1.3.4 Future significance of PV and SC	7
1.4 Motivation for the Work	9
1.5 Problem Statement	9
1.6 Outline of the Thesis	9
2 Literature Review on Hybrid Sources in Electric Vehicles	11
2.1 Introduction	11
2.2 Hybrid Energy Source System	13
2.3 DC-DC Converter Topologies	14
2.3.1 Passive topology	15
2.3.2 Semi-active topology	16
2.3.3 Full-active topology	17
2.4 Hybrid Energy Management Strategies	20
2.4.1 Rule-based EMS	22
2.4.1.1 Deterministic-based energy management strategy	22
2.4.1.2 Fuzzy logic-based energy management strategy	24
2.4.2 Optimization based EMS	26
2.4.2.1 Offline optimization based EMS	26
2.4.2.2 Online optimization based EMS	31
2.4.3 Learning-based EMS	34
2.4.3.1 Reinforcement learning	34

2.4.3.2	Neural network	36
2.5	Identified Research Gaps	39
2.6	Objectives	39
3	Proposed Intelligent Energy Management Strategy for Hybrid Electric Vehicle	41
3.1	Introduction	41
3.2	Electric Vehicle Modeling	42
3.2.1	Dynamics of electric vehicle	43
3.3	Proposed Hybrid Source Model	45
3.4	Proposed Energy Management Strategy	52
3.4.1	Technical evaluation	58
3.4.2	Economy evaluation	62
3.5	Simulation Results	63
3.5.1	Impact of PV power	65
3.5.2	Techno-economic analysis	69
3.5.2.1	Technical performance comparison of EMSs	70
3.5.2.2	Economy analysis of EMSs	74
3.6	Summary	74
4	Proposed SC-PV Hybrid Electric Vehicle	77
4.1	Introduction	77
4.2	Proposed Hybrid Source Model	78
4.3	Proposed Energy Management Algorithm	78
4.4	Simulation Results	83
4.4.1	Cases of EV run under varying PV irradiance	83
4.4.2	Cases of EV run under varying driving locations	91
4.4.3	Cases of sudden load demand fluctuations in EV drive	99
4.4.4	Technical parametric analysis	101
4.5	Summary	103
5	Conclusion and Future Scope	105
5.1	Conclusion	105
5.2	Contributions	107
5.3	Future Scope of Work	107
A	Resistive Forces Opposing Electric Vehicle Motion	109
A.1	Frictional Force	109
A.2	Aerodynamic Drag Force	109
A.3	Grading Force	110
A.4	Acceleration Force	110
	Bibliography	112
	Publications based on the thesis	131

List of Figures

1.1	Characteristics of energy sources - Ragones plot	4
2.1	Topology classification of hybrid sources for powering EV.	15
2.2	Schematic of the passive topology of hybrid sources in electric vehicles.	16
2.3	Schematic of the semi-active converter topology of HPSS (a) SC-battery (b) Battery-SC.	17
2.4	Schematic of the fully-active converter topology of HPSS (a) series (b) parallel (c) multi-input type.	18
2.5	Primary targets of EMS in EV, HEV, PHEV.	20
2.6	Classification of EMS employed in hybrid source EVs.	21
2.7	Algorithm for battery-SC hybrid source system using Rule-based EMS.	23
2.8	Fuzzy logic control (FLC) based EMS for battery-SC hybrid source powered EV.	27
3.1	Overall block diagram of hybrid source system in electric 3W.	42
3.2	Dynamics of electric 3W vehicle.	44
3.3	Velocity profile of NYCC, Artemis Urban, and WLTP class-1.	44
3.4	Circuit diagram of proposed EMS of hybrid source electric vehicle.	46
3.5	Irradiance (blue), ambient temperature (red)(March).	47
3.6	Perturb and Observe (P & O) MPPT algorithm.	48
3.7	Input and output membership functions of fuzzy controller (a) Absolute low frequency energy (b) Absolute high frequency energy (c) SC SOC (d) Battery cell temperature (e) Cut-off frequency of LPF	53
3.8	Flowchart of absolute energy sharing algorithm.	55
3.9	System controller block diagram.	58
3.10	Absolute energy sharing profiles.	63
3.11	Cut off frequency derived for the CDP.	64
3.12	Comparison of battery,SC,PV and load power(BEV) with IHSEMS.	65
3.13	Comparison of source energy consumption of IHSEMS under CDP.	65
3.14	PV energy generation (kWh).	66
3.15	Power allocation of IHSEMS for sudden variation in solar irradiance (a), zero PV power (b) under NYCC driving cycle.	68
3.16	Comparison of BEV, SMC, FDS, and IHSEMS in terms of battery current (a), battery capacity loss (b) under NYCC driving cycle.	70

3.17	Comparison of BEV, SMC, FDS and proposed IHSEMS under NYCC driving cycle.	71
3.18	Comparison of SC_{SOC} with SMC, FDS, and IHSEMS under NYCC driving cycle.	72
3.19	Comparison of DC_{BVF} bus voltage fluctuations with SMC, FDS and IHSEMS under NYCC driving cycle.	73
3.20	Comparison of DC_{BVF} bus voltage fluctuations with SMC, FDS and IHSEMS under NYCC driving cycle.	74
4.1	Complete schematic structure of hybrid source energy management in Electric-3W	79
4.2	Algorithm of proposed energy management strategy for SC-PV hybrid system in EV(modify the algorithm further)	81
4.3	Control block diagram of the SC reference current calculation under proposed modified EMS	82
4.4	Combined 34 repeated IDC test profile	84
4.5	Energy consumption comparison for varying PV irradiance cases under 34 IDC cycles (a) Case-I (b) Case-II (c) Case-III.	85
4.6	Power flow analysis for varying PV irradiance cases under 34 IDC cycles (a) Case-I (b) Case-II (c) Case-III	86
4.7	SOC comparison for varying PV irradiance cases under 34 IDC cycles (a) Case-I (b) Case-II (c) Case-III.	87
4.8	Capacity loss comparison for varying PV irradiance cases under 34 IDC cycles (a) Case-I (b) Case-II (c) Case-III.	89
4.9	DC bus voltage comparison for varying PV irradiance cases under 34 IDC cycles (a) Case-I (b) Case-II (c) Case-III.	90
4.10	PV energy generation (kWh) and standard driving profile (WLTP class-1) in New South Wales, Australia (31.2532° S, 146.9211° E).	92
4.11	PV energy generation (kWh) and standard driving profile (IDC) in Bangalore, India (12.9716° N, 77.5946° E).	93
4.12	PV energy generation (kWh) and ECE driving profile in Scotland (56.4907° N, 4.2026° W).	94
4.13	EV Performance analysis of BEV and SC-PV vehicle at New South Wales, Australia under WLTP class-1 driving cycle (a) Energy consumption (b)Source SOC (c) Source capacity loss (d) DC bus voltage.	95
4.14	EV Performance analysis of BEV and SC-PV vehicle at Bangalore, India under Indian driving cycle (a) Energy consumption (b)Source SOC (c) Source capacity loss (d) DC bus voltage.	96
4.15	Performance analysis of BEV and SC-PV vehicle at Scotland under ECE driving cycle (a) Energy consumption (b)Source SOC (c) Source capacity loss d) DC bus voltage.	96
4.16	Power flow analysis for varying driving locations cases (a) NSW (b) Bangalore (c) Scotland.	98
4.17	Comparison of BEV and SC-PV vehicle under sudden load fluctuations.	100

4.18 Comparison of source capacity loss for BEV and SC-PV vehicle under unexpected load demand fluctuations	101
--	-----

List of Tables

1.1	Characteristics of source systems that can be utilized in EV, HEV	5
1.2	Comparison of EV sources	8
2.1	Analysis of different topologies of coupling battery-SC hybrid system	19
2.2	Summary of EMS in EV with significant merits and demerits	38
3.1	Design parameters of electric vehicle.	43
3.2	Parameters of hybrid sources	45
3.3	Converter design parameters of hybrid sources	51
3.4	Controller parameters and specifications of hybrid source system.	58
3.5	Performance and economy analysis of EMSs.	67
3.6	Performance and economy analysis of EMSs.	73
4.1	Operating modes and reference currents	80
4.2	Cases of electric vehicle drive	84
4.3	Performance analysis of EMSs under various locations	102
4.4	Economic analysis of energy storage in electric vehicle [Eaton, 2022]	102
A.1	Reference values for the rolling resistance coefficient	110

List of Abbreviations

AESA	Absolute energy sharing algorithm
Ah	Ampere hour throughput
BEVs	Battery Electric vehicles
BIR	Battery di/dt reduction
BDC	Battery degradation cost
BMS	Battery management system
BLSI	Battery life span improvement
DP	Dynamic programming
DOD	Depth of discharge
EV	Electric vehicle
EC	Electricity cost
ECR	Energy consumption rate
EM	Energy Management
EMA	Energy management algorithm
EMS	Energy management strategies
ECMS	Equivalent consumption minimization strategy
EJ	Exajoule
FCEVs	Fuel cell electric vehicles
FDS	Frequency decoupling strategy
FLC	Fuzzy logic controller
GA	Genetic algorithm
HESS	Hybrid energy source system
HPSS	Hybrid Power Source System
HSEV	Hybrid source electric vehicles
IHSEMS	Intelligent Hybrid Source Energy Management Strategy
LPF	Low pass filter
MPPT	Maximum power point tracking
MPC	Model predictive control
NDC	Nationally Determined Contribution
NYCC	Newyork city cycle
N	Battery cycle number
OCV	Open circuit voltage
PSO	Particle swarm optimization
P& O	Perturb and observe
PV	Photovoltaic
RES	Renewable energy sources
RMS	Root mean square
SMC	State machine control
STEPS	Stated Policies Scenario
SC	Supercapacitor
SDS	Sustainable Development Scenario
3W	Three-wheeler

TOC	Total operation cost
WLTP	Worldwide Harmonized Light Vehicles Test Procedure

List of Symbols

M	Gross weight
g	Acceleration due to gravity
α	Gradeability
λ	Air density
V	Velocity of vehicle
f_r	Rolling resistance coefficient
C_D	Drag coefficient
η_R	Regenerative braking efficiency
η_{HESS}	Efficiency of hybrid system
η_T	Transmission efficiency
η_M	Motor drive efficiency
η_T	Transmission efficiency
η_{PV}	PV panel efficiency
n_{pBc}	Number of parallel cells
n_{sBc}	Number of series cells
B_C	Nominal capacity of battery pack
C_{Bc}	Nominal capacity of battery cell
V_B	Nominal voltage of battery pack
V_{Bc}	Nominal voltage of battery cell
R_B	Resistance of battery pack
B_{SOC}	Battery state of charge
B_{SOC0}	Initial battery state of charge
SC_{SOC}	SC state of charge
C_r	Charge/discharge rate
DOD	Depth of discharge
B_{Qloss}	Battery capacity loss
C_{SC}	Nominal capacitance of SC module
V_{SC}	Nominal voltage of SC module
V_{Sc}	Nominal voltage of SC cell
C_{Sc}	Nominal capacity of SC cell
C_{SC}	Nominal capacitance of SC module
R_{Sc}	Resistance of SC cell
R_{SC}	Resistance of SC module
D	Minimum EV driving range
U_{SC}	Working voltage of SC module
V_{PV}	Output voltage of PV module
I_{PV}	Output current of PV module
I_{PH}	Photo current
I_{RS}	Reverse saturation current
V_{TH}	Diode thermal voltage
R_S	Series PV resistance

R_{SH}	Shunt PV resistance
W_p	Maximum PV panel output
LEC_{Day}	Load energy consumption per day
EC_{Dc}	Energy consumption per driving cycle
N_{Dc}	Number of driving cycles per day
BEC_M	Battery energy consumption per month
TEC_M	Total energy consumption per month
E_{PVM}	PV energy per month
E_{PVday}	PV energy per day
PV_{Range}	PV range per day
P_H	Hybrid power
P_L	Load demand power
P_B	Battery power
P_{SC}	SC power
P_{PV}	PV power
P_C	Combined battery and SC power
I_C	Combined battery and SC current
T_C	Battery cell temperature
Abs E_{HF}	High-frequency absolute energy
Abs E_{LF}	Low-frequency absolute energy
Abs E_L	Load absolute energy
I_{Load}	Load current
I_{LF}	Low frequency current
I_{HF}	High frequency current
P_{LF}	Low frequency power
P_{HF}	High frequency power
f_c	Cut-off frequency
B_P	Battery peak power of BEV
B_{PEMS}	Battery peak power of hybrid EMSs
B_{PPR}	Battery peak power reduction
B_{CL}	Battery capacity loss
B_{CR}	Battery capacity reduction
di/dt	Rate of change of battery current
B_{RI}	Battery RMS current
B_{RIR}	Battery RMS current reduction
DC_{BVF}	DC bus voltage fluctuation
$B_{\delta Q_{loss}}$	Instantaneous battery capacity loss
B_{CEMS}	Battery capacity of hybrid EMS
I_{max}	Discharging peak battery current
I_{min}	Charging peak battery current
t_{max}	$I_{max}time_{instant}$
t_{min}	$I_{min}time_{instant}$
di/dt_{EMS}	Battery di/dt ratio of EMS
di/dt_{BEV}	Battery di/dt ratio of BEV
I_{RMSEMS}	Battery RMS current under EMS

I_{RMSBEV}	Battery RMS current under BEV
z	Power law factor-0.828
Ah	Ampere hour throughput
B_{LS}	Battery lifespan in years
BLSI	Battery life span improvement
N	Battery cycle number
T_s	Sampling interval-1S
Q_{lossD}	Capacity loss at each distance
D_{Day}	Average travelled distance in a day (km)
V_{max}	Maximum DC bus voltage
V_{min}	Minimum DC bus voltage
B_{OS}	Optimum battery size
R	Gas constant- 8.314 J/mol K
T	Absolute temperature in Kelvin

Chapter 1

Introduction

Contents

1.1	Background	1
1.2	Issues in Battery Electric Vehicles	3
1.3	Characteristics of Hybrid Sources	4
1.3.1	Lithium-ion battery	4
1.3.2	Supercapcitor	5
1.3.3	Solar Photovoltaic	6
1.3.4	Future significance of PV and SC	7
1.4	Motivation for the Work	9
1.5	Problem Statement	9
1.6	Outline of the Thesis	9

The current chapter introduces the thesis, including background, research overview, features, and drawbacks of existing electric vehicles and energy management. Moreover, the organization of the thesis as chapters is given.

1.1 Background

Oil resource depletion, fuel cost hikes, and environmental pollution from poisonous gases are major issues in the transportation industry. It contributes more than 26% of total CO₂ across the globe. The increase of private transport modes in the growing economy plays a significant contribution creates a fast increment in such issues to the environment. [Subhash and Reinhard, 2016]. An alternative mode of transportation is essential and handles the recent trends in the automotive sector. Electric vehicle (EV) plays a significant role by setting themselves as an excellent mode of transportation that can solve those problems [Boulanger et al., 2011]. This leads to improved technologies in EVs, which emphasizes them in

the transportation industry. It focuses on improving energy utilization, comfort, vehicle life, and an eco-friendly environment. Recent trends and technologies towards EV are improving year by year [Chan et al., 2009] .

The energy requirement for transportation has increased tremendously to reach 29 %, with massive growth in the past decade [Jia et al., 2021a]. Meanwhile, the transportation industry has contributed almost $2/3^{rd}$ of oil demand and nearly $1/4^{th}$ of global carbon dioxide emissions from fuel combustion [IEA-REA, 2019] By 2050, renewable energy will occupy $2/3^{rd}$ of total energy consumption. By incorporating renewable electricity with electrified transportation, carbon emissions can be reduced by 60 % in 2050 and ensure a sustainable and green mode of transportation [GEO, 2020]. For the next two decades, the energy demand for road transport is expected to double in the STEPS. Moreover, increasing two/three-wheeled vehicles indicates such policies toward less energy-intensive options. [Sonali et al., 2021]. A shift towards electrification limits the growth in oil demand to less than 1 mb/d under the SDS [IEA-Oil and Gas, 2020]. In SDS, additional capital of \$1.4 trillion above the level in the STEPS needed for clean energy technologies to 2040 [Peter et al., 2018]. India’s clean energy transition lays the foundation for energy security.

In the present scenario, an energy predicament and environmental pollution are critical issues caused due to the acceleration in global energy demand. Energy utilization has doubled in India since 2000, and the 80% share is still from coal, oil, and biomass [IEA, 2020]. The significance of alternate sustainable and green energy sources is essential due to fossil fuel energy’s exhausting resource and environmental impacts. India’s ambitions in energy policy are to reach a target of 450 GW of renewable energy by 2030 with a surplus improvement in battery energy storage and cost-competitiveness in solar PV. By 2040, India expects to have the largest battery capacity globally, 140 GW in the Stated Policies Scenario and 200 GW in the Sustainable Development Scenario [IEA-World, 2021]. The intensity of emissions in India’s economy is projected to improve by 40 % from 2000 to 2030. The electricity generation capacity from non-fossil fuels is expected to reach around 60 % and above the Nationally Determined Contribution of 40 %. India leads in expanding clean energy technologies and exhibits in its market for solar PV, wind turbines, and lithium-ion battery equipment to over \$40 billion per year by 2040 [IEA-India, 2021]. This tremendous growth enables India to be a highly sustainable nation with industrial and commercial opportunities from clean energy that are even more prominent in the future.

The transition of transportation mode is highly essential where Lithium-ion batteries are the widely used energy source in battery electric vehicles due to their higher energy density (250 – 400 Wh/kg), high energy efficiency (90 % – 95 %), wide operating temperature range (- 20°C – 60°C), and low self-discharge (0.5% – 2%) per month [Agrawal and Pandey, 2008] [Amin et al., 2017] [Schuster et al., 2017]. Although BEVs are developed with improved performance and comfort, specific issues with lithium-ion batteries hinder their wider adoption. As per the

research, 30-50% of consumers today are interested in purchasing BEVs. However, the adoption rate remains low due to various barriers. High and fluctuating C-rates (I_B/C_B), cell temperature, number of discharge and charge cycles, and depth of discharge cause depletion of the battery life cycle and still exists as a significant issue in lithium-ion batteries [Pedro et al., 2019]. The severity of these battery issues is not similar for all users and varies based on the different driving and environmental conditions [Zhang et al., 2020]. Battery management systems limit such issues to an extent by monitoring and ensuring the safety of battery packs [Bonfiglio and Roessler, 2009]. The automotive industry’s strategy to increase range is with the addition of battery packs but, in return, increases the weight, the need for high-power charging stations, and increases CO2 emissions. The requirement for a high-power charging station needs infrastructure and heavily constrains the adoption of electric vehicles. Since the battery is the single source to handle sudden and fluctuating load demands in BEVs due to varying driving profiles, alternate strategies are necessary to ensure optimal battery operation [Sun et al., 2017].

1.2 Issues in Battery Electric Vehicles

Batteries are the typical electrical energy source utilized in EVs. Lithium-ion types are widely used in EVs compared to all the other types of batteries (lead-acid, Ni-Cd batteries) due to their lifespan, safety, energy, and power density advantages [Agrawal and Pandey, 2008] [Amin et al., 2017] [Schuster et al., 2017]. However, alternate sources must be considered for sustainable transportation due to the numerous disadvantages of high battery degradation, higher maintenance and replacement costs, slow response, higher charging time, and harmful materials deposited in landfills (like cobalt and lithium) [Yuqing et al., 2021]. The most significant drawback of batteries is the response toward sudden peak power demands. Operating the battery under small charge/discharge currents is recommended, and as a consequence, peak sudden power demands adversely affect the battery life span [Amin et al., 2017]. Even though BEVs are designed with high-performance source systems, specific challenges hinder the wider adoption of EVs. The deterioration of li-ion cells occurs due to the effect of fluctuating peak C-rates (I_B/C_B), cell temperature, number of discharge and charge cycles, and depth of discharge [Pedro et al., 2019]. The reduction in battery life varies from user to user and highly depends on the driving and environmental conditions across the globe [Zhang et al., 2020]. The battery management system has limitations in solving the issues since the battery is the only source in BEV. Therefore, a hybrid source system is essential to handle the varying load conditions [Sun et al., 2017].

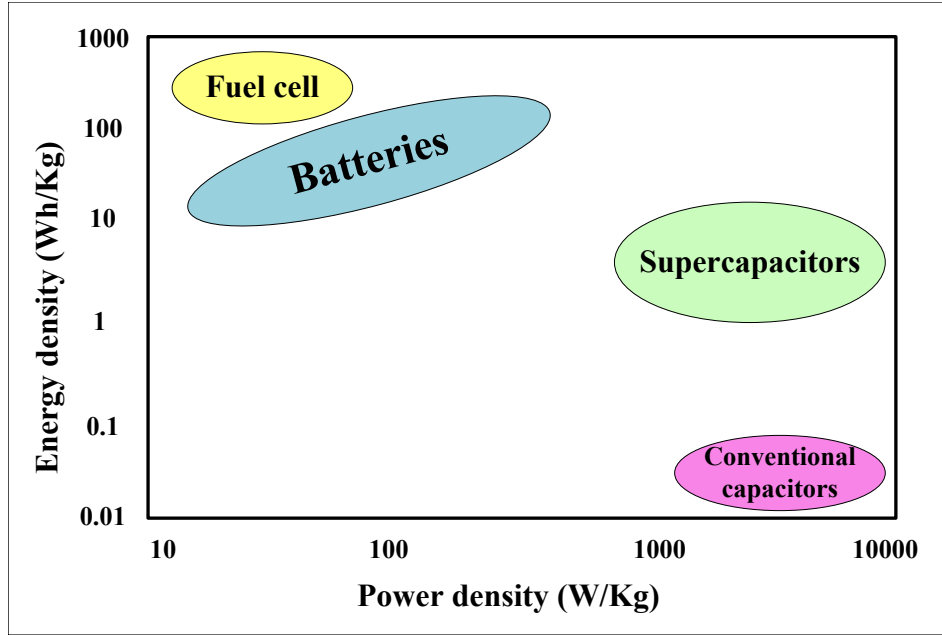


Figure 1.1: Characteristics of energy sources - Ragones plot

1.3 Characteristics of Hybrid Sources

Characteristics of sources are significant for the lifespan, performance, and comfort of EV users. Understanding the major issues lithium-ion batteries face due to the varying driving and environmental conditions, the relevant characteristics of hybrid sources are discussed in the below subsections. Figure 1.1 shows the Ragones plot which briefs the energy and power density of each sources. Each sources in the hybrid system must handle the drawbacks or shortcomings of other. Table 1.1 shows the parameters of each source (Lithium-ion battery, Supercapacitor (SC), Superconducting magnetic energy storage (SMES), Compressed Air Energy Storage (CAES), Fuel cell (FC), Flywheel energy storage (FES)) and the details characteristics, response, energy and power capability of each source.

1.3.1 Lithium-ion battery

Li-ion batteries are modeled as equivalent circuit models (ECM) and electrochemical models [Wang et al., 2021]. A second-order RC ECM implements the dynamics of a Li-ion battery, considering the computational complexities and accuracy [Tremblay et al., 2007]. Series and parallel cell arrangements develop the battery with energy density, voltage, and current ratings needed for the EV by the cell-to-module combinations [Amine et al., 2020].

To evaluate battery degradation, which is a significant aspect of EV batteries, an aging model of Li-ion batteries is implemented based on Arrhenius Law [John et al., 2011]. The lithium-ion battery's parameters are shown in Table 1.1. The higher energy density of Li-ion batteries enables EV makers to choose it as the primary source of BEV. The least-square fit method was used to calibrate the

Table 1.1: Characteristics of source systems that can be utilized in EV, HEV

Parameters	Li-ion battery	SC	SMES	CAES	FC	FES
Rated power (MW)	0-0.1	0-0.4	0.1-10	100-300	0-50	0-0.25
Typical discharge time	mins-hours	ms - mins	ms - 10 s	1-2 days	s-days	s-hr
Power density (W/kg)	10-100	1000-10000	500-2000	NA	500W/L	400-1600
Energy density (Wh/kg)	10-100	0.1-20	0.5-5	30-60	500-3000	5-150
Response time	ms	ms	ms	mins	ms-mins	ms-s
Lifetime (years)	10	15	NA	20-40	25	20
Cycle lifetime (years)	600-1200	10 ⁵ -10 ⁶	NA	NA	10 ³ -10 ⁴	10 ⁴ -10 ⁷

aging model equations based on the experimental data, and the capacity loss is shown in equation 1.1 [Ziyou et al., 2015]:

$$B_{Q_{loss}(k)} = 0.0032. \exp\left(\frac{(-15162 + 1516. C_{rate}(k))}{R. (T + 273)}\right). Ah(k)^z; \quad (1.1)$$

where $B_{Q_{loss}}$ is the capacity loss of the Li-ion battery, R is the gas constant (8.314472 J/(mol·K)), T is the absolute temperature (298.15 K), Ah is the ampere hour throughput. Instantaneous capacity loss ($B_{\delta Q_{loss}}$) is evaluated with Equation 1.2 to derive the battery degradation cost (Equation 1.3)

$$B_{\delta Q_{loss}(k)} = 9.78x10^{-4} \cdot \left(\frac{Abs(I_{B,k}) \cdot T_s \cdot \exp\left(\frac{(-15162+1516.C_{rate,k})}{(0.849.R.T)}\right) \cdot Q_{loss,(k-1)}^{-0.1779}}{3600} \right) \quad (1.2)$$

where I_B is the battery current, T_s is the sampling time = 1s, C_{rate} is the charge-discharge rate (I_B/B_C).

$$BDC = \frac{B_C \cdot V_B \cdot Price_{BAT} \cdot B_{\delta Q_{loss}(k)}}{(1000) \cdot (0.2)} (INR) \quad (1.3)$$

where B_C is the battery capacity, V_B is the battery rated voltage, $Price_{BAT}$ is the battery price in India per kWh = INR. 12,000/-.

1.3.2 Supercapcitor

SC's higher power density and response time play a significant role in electric vehicle applications. R_{int} capacity model with mathematical equations (open-circuit voltage, internal resistance (R_{Sc}) and capacitance (C_{Sc})) is adopted to show the SC response and dynamics behavior considering accuracy and less complexity of the model [Abdul et al., 2022]. Since the life cycles of SC are very high (approx. 500,000 cycles), most of the research works that involve SC in EV applications lack analysis on SC degradation and capacity loss. The proposed work performs the comparison of battery and SC degradation under similar driving scenarios. An

Arrhenius law with the SC model is employed for the analysis, which shows the impact of using SC during fluctuating and peak loads. Temperature, voltage, and current accelerates the SC degradation and are employed in the model [Kreczanik et al., 2014]. The degradation of SC is evaluated in the model using equations 1.4, 1.5, 1.6 [Abdul et al., 2022] [P K Singha et al., 2021].

$$SC_{deg} = \frac{1}{t_0} \cdot \int_{t_{ini}}^{t_{end}} \frac{\exp\left(\frac{V(t)}{V(0)} + \left(\frac{\theta(t)}{\theta(0)}\right) + \left(\frac{I_{SCRMS}}{I_{SCRMS0}}\right)\right)}{t_{end} - t_{ini}} dt \quad (1.4)$$

where SC_{deg} represents the speed of degradation in $\% s^{-1}$, θ is the SC temperature, I_{SCRMS} is the SC RMS current and $I_{SCRMS0} = (30/(\ln(2)))$ A.

$$C_{deg} = \sum_{n=1}^n (0.2 \cdot C_0) \frac{1}{t_0} \cdot \int_{(i-1)T}^{iT} \exp\left(\frac{V(t)}{V(0)} + \left(\frac{\theta(t)}{\theta(0)}\right) + \left(\frac{I_{SCRMS}}{I_{SCRMS0}}\right)\right) dt \quad (1.5)$$

where C_{deg} represents the loss in capacitance (End of life if C_{deg} is higher than 20%),

$$R_{deg} = \sum_{n=1}^n (R_0) \frac{1}{t_0} \cdot \int_{(i-1)T}^{iT} \exp\left(\frac{V(t)}{V(0)} + \left(\frac{\theta(t)}{\theta(0)}\right) + \left(\frac{I_{SCRMS}}{I_{SCRMS0}}\right)\right) dt \quad (1.6)$$

where R_{deg} represents the increase in (equivalent series resistance) ESR, and End of life (EOL) of SC occurs during a decrease of 20% in the capacitance and an increase of 100% in the ESR),

1.3.3 Solar Photovoltaic

The technology that converts solar energy to electrical energy under the photovoltaic effect of semiconductors constitutes PV power generation. A PV array is a group of PV modules connected in series and parallel [Djamila et al., 2014]. Equation 1.7 shows the nonlinear V-I characteristics of the photovoltaic cell:

$$I_{PV} = n_p \cdot I_{PH} - n_p \cdot I_{RS} \cdot \left[\exp\left(\frac{(V_{PV} + I_{PV} \cdot R_S)}{(V_{TH} \cdot n_s)} - 1\right) \right] - \frac{(V_{PV} + I_{PV} \cdot R_S)}{R_{SH}} \quad (1.7)$$

where V_{PV} and I_{PV} represent the output PV voltage and current of the module, n_p and n_s are the number of parallel and series connected panels. I_{PH} is the photo-current, I_{RS} is the module reverse saturation current, V_{TH} is the diode thermal voltage and R_S , R_{SH} are the series and shunt resistance respectively. The highly fluctuating nature of PV irradiance and ambient temperature affects power generation and stability in supporting an energy system. The MPPT algorithm extracts maximum power during such high fluctuations. Equation (1.8) shows

the PV peak power (W_P), load energy calculations of the HSEV, and Monthly battery energy consumption (BEC_M) (Eq.1.8) shows the impact of PV energy in EV [Solar, 2020].

$$W_P = \frac{I_r \cdot A_{PV} \cdot \eta_{PV}}{100}; LEC_{Day} = EC_{DC} \cdot N_{Dc}; BEC_M = TEC_M - E_{PVM} \quad (1.8)$$

where I_r is peak irradiance, A_{PV} is area of PV panels, η_{PV} is PV conversion efficiency, LEC_{Day} is daily load energy consumption, EC_{DC} is energy consumption under single driving cycle, N_{Dc} is number of driving cycles in a day, TEC_M is total monthly load energy consumption and E_{PVM} is monthly PV energy consumption.

1.3.4 Future significance of PV and SC

As per the implementation of the Paris Agreement sustainable development goals, the position of PV power in transportation systems will be extreme. All nations are planning strategies to reduce the global peak of greenhouse gases to achieve zero emissions by 2050 [GE0, 2020]. Further research in the improvement of PV module conversion efficiency and reduction in PV cell cost can enhance the EV energy efficiency to a large extent [Elia et al., 2021]. Table 1.2 compares the size and performance parameters of the battery, SC, and PV cells and details the research improvements undergoing in respective energy sources [Abdul et al., 2022]; [P K Singha et al., 2021]; [PV-NREL, 2022]. However, cells with an energy density higher than 100 Wh/kg are under development in research to utilize SC as an efficient energy storage device in electrified transportation. Higher energy-dense SC is achieved by Aowei Technology's UCK42V6800C [Supercapacitor-AOWEI, 2022] [Wanlu et al., 2022]. IEC 62576-2009 standards certify and confirm the test procedure and performance of the SC cell. The cycle life of SC is approximately 100 times more when compared to a battery. Moreover, SC is less deteriorated to high C-rate operations, and its charging speed is higher compared to a battery [Supercapacitor-AOWEI, 2022]. The major disadvantage of using SC in large-scale energy applications is the cost. However, cheaper SC technologies (2500 USD/kWh) are developed as per the NREL data, which makes it economical in the long run (10-20 years of usage). Roy et al. conducted an economic comparison (calendar and cyclic cost) of battery and SC systems for wave energy harvesting, which identified that an SC-based system is less costly than a Li-ion battery system [P K Singha et al., 2021]. Abdul et al. summarize SC and Li-ion battery capital costs and depicts that SC's energy capital cost (cost/kWh) shows a reduced trend. Moreover, the power capital cost (cost/kW) is significantly lower for SC when compared to the battery due to its higher power density. [Abdul et al., 2022].

Future improvements in SC can enable it to be the main source considering its long life cycle, lower maintenance, high power density, and lower charging time. Researchers are working to improve the energy density of SC by synthesizing the electrodes with different chemical compositions [Abdul et al., 2022] [Ying et al., 2020] [Wanlu et al., 2022]. The discharge and charge response characteristics of the

Table 1.2: Comparison of EV sources

Parameters	Li-ion battery cell	SC cell	PV cell
Energy density (Wh/kg)	10-100	1-100	10-100
Power density (W/kg)	1,000	10,000	20
Mass (kg)	0.5	0.125	0.4
Efficiency (%)	70-80	85-98	15-50
Charge time	1-5 h	0.3-30 s	na
Discharge time	0.3-3 h	0.3-30 s	na
Operating temperature (°C)	-20°C to 45°C	-40°C to 70°C	-40°C to 85°C
Projected cycle life	2,000	5,00,000	na
Projected lifetime (years)	3-5	10-20	25-30
Energy capital cost INR./kWh	15,000	2,02,500	na
Power capital cost INR./kW	20,000–45,000	10–20	32,000

battery and SC with ratings are mentioned in Table 1.2. The charging time of SC compared with lithium-ion batteries under similar conditions is low due to its high power density and faster response time. SC can handle higher and sudden charging currents from the high-rated charging stations with lower deterioration. This can significantly reduce the charging time of the EVs [Abdul et al., 2022] [Ying et al., 2020]. As the focus of the work does not consider the charging station analysis, only a brief of available charging stations for battery and SC are only discussed. Gemamex Motion Co. implements a charging station for the battery and SC with a maximum of 200A DC through the CCS2 interface and 550 A DC through the pantograph, respectively [Charging Stations-Gemamex., 2022]. Moreover, the advanced charging station scenarios in office buildings focus on intelligent models to control the EV fleet charging to minimize electricity usage and maximize self-consumption. Such intelligent algorithms handle the fluctuations in PV, EV energy demands, and user behavior [Brida et al., 2021].

Another aspect of concern is the conversion efficiency of PV cells. As per NREL research, the increment of a PV cell with a conversion efficiency year by year to land at 47.1 % (Four-junction) is under research, showing the significance of PV and its emergence in the transportation/grid energy sector [PV-NREL, 2022]. Reduction in the cost of PV cells from 2010-2022 (INR.68 to INR. 25 per Watts) indicates the role of RES in a sustainable mode of transportation [Ranganath and Debasis, 2021]. Similarly, battery prices fell from 1100 USD in 2010 to 132 USD in 2022, hinting that energy source prices declined with increased production, market, and improved technologies. However, due to the shortage of lithium and the high requirement for Li-ion battery manufacturing for EVs, the cost share of cathode materials increased by 6.7 % in one-year [Lithium ion Battery cost, 2022].

Considering such factors, SC manufacturing research and the market is achieving their peak in the coming 5-10 years. Hence by 2035, a fall in SC's initial price and improving energy density can ensure the SC-based vehicles in the market with less maintenance and replacements, thus eliminating the dumping of e-wastes from EVs. It also ensures the fastest recharging, like ICE vehicle fuel filling, and an accelerated complete EV adoption.

1.4 Motivation for the Work

Hybrid sources are employed in electric vehicles as Lithium-ion batteries are severely deteriorating due to varying driving and environmental conditions. Incorporating green and renewable energy sources in EVs is a tremendous vision focusing on net zero emissions by 2050. Hybrid source energy management is essential, which manages the power allocation among each source based on the fluctuations in driving and environmental conditions. Moreover, optimal source operations are ensured with energy management strategies. The exhaustive literature survey on energy management systems and strategies with power converter topologies, modeling, analysis, and algorithms for hybrid sources in electric vehicle applications need to investigate, and present the findings.

1.5 Problem Statement

To design and develop hybrid source systems incorporating renewable energy sources is a crucial step in the electrified transportation sector. Moreover, implementation of an efficient energy management strategy for the optimal power allocation among each source in a hybrid source system for Electric Vehicles without any complex modeling and data compilation.

1.6 Outline of the Thesis

The whole thesis is organized into six chapters as follows,

Chapter 1: A brief introduction to the energy economy and the impact of electrified transportation. Major issues of battery electric vehicles with an overview of introducing the hybrid source models and its energy management strategies in electric vehicles are discussed in this chapter.

Chapter 2: An extensive literature survey of the hybrid source energy management strategies along with various DC-DC converter topologies, identified research gaps and research objectives are discussed in this chapter.

Chapter 3: Absolute energy sharing based energy management strategy using fuzzy controller with an optimal energy sharing scheme are discussed in this chapter. Moreover, a techno-economic assessment is performed by comparing the proposed control scheme with existing EMSs and BEVs.

Chapter 4: The hybrid combination of high-efficiency PV panels coupled with high energy dense Supercapcitor for the Hybrid Source Electric Vehicle model with an improved Energy management algorithm (EMA) is discussed in this chapter with a Techno-economic analysis at different locations.

Chapter 5: This chapter concludes the contributions of the proposed research work and also discusses the scope for possible future works which can enhance the energy economy, longevity, and efficiency of the green mode of transportation.

Chapter 2

Literature Review on Hybrid Sources in Electric Vehicles

Contents

2.1	Introduction	11
2.2	Hybrid Energy Source System	13
2.3	DC-DC Converter Topologies	14
2.3.1	Passive topology	15
2.3.2	Semi-active topology	16
2.3.3	Full-active topology	17
2.4	Hybrid Energy Management Strategies	20
2.4.1	Rule-based EMS	22
2.4.2	Optimization based EMS	26
2.4.3	Learning-based EMS	34
2.5	Identified Research Gaps	39
2.6	Objectives	39

The current chapter presents an extensive literature survey on the background of the research work, including an overview of features and drawbacks of existing electric vehicles, hybrid source electric vehicles, their topologies, and energy management strategies. Finally, the research gaps are summarized, and the main objectives of this research work addressing those identified gaps are given in this chapter.

2.1 Introduction

The current situation of fossil fuels considering their cost, increase in demand, comprehensive utilization, harmful effects on the environment, and non-availability of

resources, initiated the usage of an alternative solution that can resolve these issues [Boulanger et al., 2011]. This led to the development of a clean, reliable, and highly efficient solution that has attracted researchers' attention to improve the transportation, energy, and environment sectors [Chan et al., 2009]. Development of innovations in electrifying transportation is explored with electric vehicle (EV), hybrid electric vehicle (HEV), and plugin electric vehicle (PHEV), which has been raised as an environmentally friendly and effective solution. More than 40% of the energy is lost in conventional ICE vehicles as heat via exhaust, causing severe environmental pollution [Tie and Tan, 2013]. EVs convert more than 70% of energy for their operation and accessories, which reduces wastage of energy and assures clean power with lower emission [Zhu et al., 2018]. The US, China, India, and a few European countries have imposed different policies to improve the popularity of EVs [Martinez et al., 2017] [Dhar et al., 2017]. This shows that the recent trends in EV usage have increased by 60% from the last decade [Global EV, 2020]. The attraction toward EVs have improved significantly with different types of charging structures (Level I, Level II, DC fast charging), EVs interconnection grid (V2G), vehicle-to-infrastructure (V2I), and vehicle-to-vehicle (V2V) applications [Capasso and Veneri, 2015] [Rahbari et al., 2017] [Fazelpour et al., 2014].

EV, PHEV, and HEV have different powertrain configurations based on their structure. The significant designs include series, parallel, series-parallel, and hybrid [Wu et al., 2015]. The ICE and electric motor are employed in different patterns depending on the vehicle's application, considering cost and performance. An optimal power train is selected for vehicles and is followed by fixing the system's main components: energy storage system [Hemmati and Saboori, 2016], electric motors [Singh et al., 2019] [Vishnu and Kashyap, 2020] power electronic interface [Gao, 2005]. Energy management strategies (EMS) are another essential aspect of EV technology. EMS's role is highly crucial since it ensures fuel and energy economy, motor performance to meet the required power demand [Xi et al., 2014] [Song et al., 2014a]. All these individual factors are essential for the design and development of the EV. Each aspect must be highly effective and optimal to solve IC Engine vehicle issues and compete with its different variants, attracting new transportation innovations. EV mainly uses batteries as the source to power the EV motor to meet the driving demands. However, the driving power demand conditions vary at different routes, primarily based on traffic, driver's behavior, etc. Thus, battery vehicles can undergo severe issues due to such load changes [Lu et al., 2013], which can even deplete the performance and life of the vehicle and battery. One of the significant issues is the range anxiety of battery electric vehicles (BEV), which adversely affects EV's popularity. Other problems include battery lifetime, battery capacity reduction, less availability of charging stations, and a considerable charging time of EVs [Sun and Xiong, 2015] [Dougal et al., 2002] [Ahmadi et al., 2014]. These aspects are the main focus of researchers towards EV research.

Further gaps are analyzed in this review that considers the performance of EV batteries and its impacts on battery life. Highly fluctuating (frequent charge-

discharge cycles) and high current (C-rate) power demands are typical in vehicle driving profiles which highly affect the battery life and reduces its capacity [Udin et al., 2016]. This leads to the replacement or frequent maintenance of EV batteries which will be an extra burden for the users since the battery is the most expensive part of EV (40%-50% of total EV cost) [EV Battery, 2020]. Varying driving profiles, driver behaviors, traffic conditions, road types, etc., highly affect battery capacity and life. This also causes a reduction in mileage and capacity after a certain period of use [Zhang et al., 2020] [Vukajlović et al., 2020] [Hao et al., 2020]. Improvement in vehicle performance without affecting its battery life and capacity considering all such parameters develops an effective EMS. These factors motivate the research and highlight the necessity of the work. Thus, research gaps include vehicle performance considering the issues in acceleration, hilly areas, etc. The battery life and range of EVs is still a critical issue since it affects EV users in terms of financial and anxiety aspects, respectively [Lu et al., 2013]. Influencing factors that affect energy consumption, battery life, performance, and range of EVs are classified as. 1. Vehicle-related (velocity, acceleration, braking energy). 2. Driver-related (driving patterns/ behaviors, route planning). 3. Environmental-related factors (temperature, wind, road terrain). Such aspects are not considered in existing research works. These factors highly affect the C-rate, depth of discharge (DoD), and internal resistance of the battery [Zhang et al., 2020]. It eventually reduces the vehicle's battery capacity, range, and performance. Battery life depletion and mileage vary for different users, their driving styles, and the type of roads [Vukajlović et al., 2020] [Hao et al., 2020]. The utilization of hybrid sources with different characteristics handles the issue of range anxiety of an EV. Figure 1.1 shows the energy and power densities of different storage devices [Xie et al., 2018a]. This plot proves the application of various sources based on their energy and power densities. The battery has a high energy density and can smoothly drive continuous power demand for a longer time. Since the battery has low power density, it cannot handle sudden power demand on urban roads during peak time [Lu et al., 2013]. This reduces the battery life and even fails to develop the required torque in the EV motor, which reduces vehicle performance. A single power source cannot meet such power demand during acceleration, braking, hill climbing, etc. Hence, deploying multiple power sources is significant to power EVs.

2.2 Hybrid Energy Source System

Energy sources are highly significant in the present energy scenerio. Energy sources utilized for powering EVs are categorized as mechanical, electrical, and chemical. A hybrid energy source system (HESS) employs two or more multiple sources coupled together to ensure the vehicle's efficient performance by managing the demands at any driving condition [Xiong et al., 2018b] [Kouchachvili et al., 2018] [Fathabadi, 2018]. All these types have different performance characteristics and are chosen based on the driving demand requirements. It is clearly explained in Table 1.1 and shows that the response time of the compressed energy storage

system (CES), battery, and fuel cell are slower when compared to the fast response of SC, flywheel, and superconducting magnetic energy storage (SMES) [Sellali et al., 2019a]. Hence, each source is used to help others diminish their drawbacks and improve the system’s efficiency. Different topologies are used for the Hybrid Power Source System (HPSS) assigned to the couple to power EV: battery, SC, fuel cell, SMES, and CES to power EV. By analyzing Ragone’s plot (Figure 1.1) and Table 1.1, it is clear that a significant focus is required on the SC characteristics since it suits to combine with battery to develop a hybrid source system for EV [Xie et al., 2018a].

Range is improved with a single full charge since different power sources such as supercapacitor (SC) [Kouchachvili et al., 2018] [Song et al., 2014b] fuel cell, [Fathabadi, 2018], renewable energy sources (solar, wind, etc.) [Jing et al., 2018] are combined with battery form hybrid topologies for powering EV. Energy management strategy (EMS) utilizes advantages of each source and avoids its disadvantages while meeting the power demand [Akar et al., 2017]. SC is used as an auxiliary source with the battery since SC achieves high power density. SC can easily handle sudden changes in power and acceleration and even consume regenerative power during braking. This improves the vehicle’s performance and protects the battery from exposure to sudden current variations [Song et al., 2014b] [Akar et al., 2017]. Fuel cells are suitable to deliver constant power and can be used to cruise vehicles with battery and SC. Thus, battery SoC and lifetime are highly improved [Fathabadi, 2018]. The implementation of fuel cell setup can increase the weight and cost of the vehicle to a large extent. Such drawbacks allow fuel cell vehicles to limit their development only to heavy-duty vehicles and not passenger vehicles. Utilizing renewable energy sources and other sources can improve the overall system’s energy efficiency [Jing et al., 2018]. Power from renewable energy sources charges the EV battery. The range of EVs is extended to a high rate, and battery life is improved.

DC-DC converter topologies and EMS of EV are two major aspects that improve the efficiency of EV [Geetha and Subramani,]. EMS with higher SC utilization considering its SoC, can improve energy efficiency and extend EV battery life [Alobeidli and Khadkikar, 2018]. The major topologies utilized for battery and SC includes (a) passive (b) semi-active (c) full active type DC-DC converters [Cao and Emadi, 2012] [Song et al., 2015b]. Full active topology serves the hybrid source integration with EV motor and proves to be the efficient structure among all three types, but converter complexity is very high. Even though its ability to utilize SC with the protection of battery from peak current demand makes it more attractive [Trovao et al., 2013].

2.3 DC-DC Converter Topologies

Hybrid source systems are used in EVs to power their motor to meet the required driving demand. Different sources can be coupled to power the EVs since a single source is not recommended to meet the EV driving demand, including sudden

power fluctuations and high C-rate operations. It causes a reduction in battery life and accelerates its aging [Lu et al., 2013]. Different types of sources can be integrated to power the EVs to form hybrid power sources. Battery and fuel cells constitute the chemical energy storage systems. SC and SMES are electrical energy storage systems, and mechanical energy storage systems include flywheel and compressed air energy storage systems [Xiong et al., 2018b, Kouchachvili et al., 2018, Fathabadi, 2018, Song et al., 2014b, Li et al., 2015]. EV powered using battery and SC hybrid sources is discussed with their importance [Kouchachvili et al., 2018]. It briefly about the topologies used in the energy management of EVs. The major topologies are as follows: (a) passive (b) semi-active, (c) full active with a bidirectional DC-DC converter to perform power conversion from bus to source during braking and reverse during driving conditions [Song et al., 2015b] [Trovao et al., 2013]. Each topology, conversion efficiency, cost, and adaptability are analyzed in this section. Figure 2.1 shows the structure of topologies used for battery-SC coupled hybrid source systems. Different DC-DC converters for hybrid sources are classified based on their converter structure and detailed in the figure.

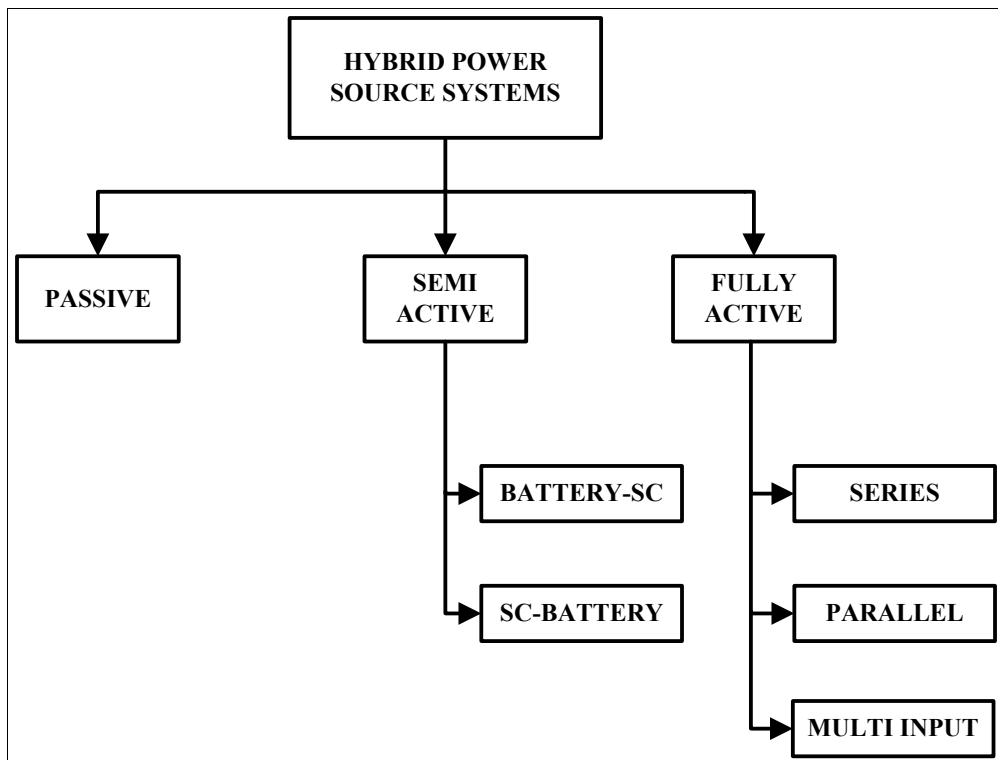


Figure 2.1: Topology classification of hybrid sources for powering EV.

2.3.1 Passive topology

The passive topology is shown in Figure 2.2. Hybrid battery-SC passive topology is the cheapest topology since it is directly connected to the DC bus. The DC-DC converter is not included in this topology, and power is distributed among the battery and SC based on internal resistances [Cao and Emadi, 2012]. HPSS is

not controlling the power flow between the battery and SC, battery ratings are higher to meet the DC bus ratings, and battery current undergoes high-frequency currents and peaks during accelerations. During braking and deceleration, the battery sometimes gets overcharged due to the direct connection with the DC bus. SC utilization is least managed, and thus battery stresses are higher when compared with other topologies [Hu et al., 2016]. SC and battery advantages are not appropriately exploited. Therefore, it is used very rarely in EV energy management systems.

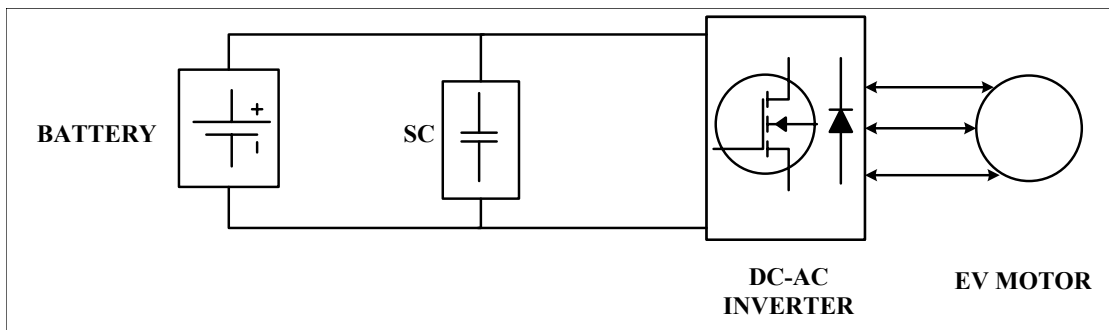
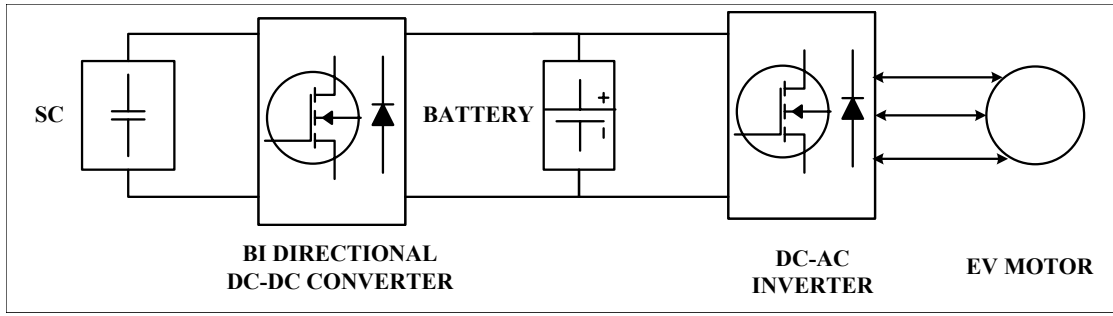


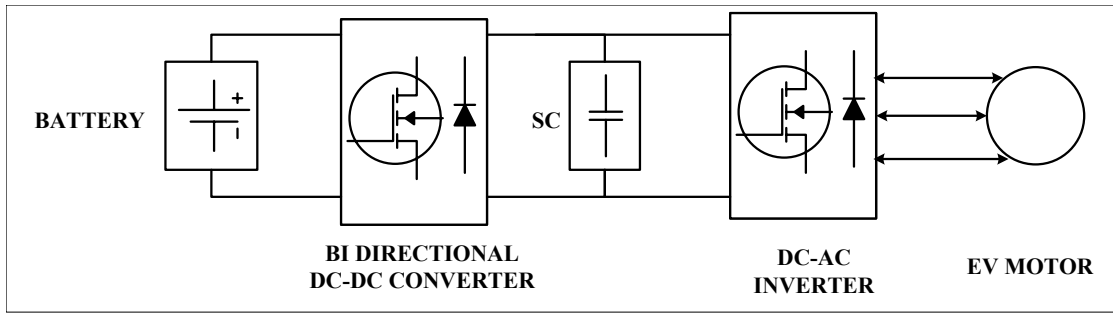
Figure 2.2: Schematic of the passive topology of hybrid sources in electric vehicles.

2.3.2 Semi-active topology

A bi-directional DC-DC converter couples the battery and SC with a DC bus. Semi-active topology is of two types. SC is connected to the DC bus with a DC-DC converter, and the battery is connected directly (SC-battery topology, Figure 2.3 (a)). The other is that a DC-DC converter connects the battery with the DC bus, and SC is connected directly to the DC bus (Battery-SC topology, Figure 2.3 (b)) [Song et al., 2015b]. Figure 2.3 shows the schematic structure of both semi-active topologies. DC bus is directly connected with the battery in SC-battery topology; hence, bus voltage fluctuation is crucial to ensure battery safety. High fluctuations affect battery lifetime. Defects of this structure are briefed, and the performance of Battery-SC topology is analyzed [Trovao et al., 2013]. DC bus fluctuations are allowed to a specified range since the battery is not directly connected to the DC bus. DC-DC bidirectional buck-boost converter improves the utilization of SC since it can handle high-frequency power demands, which protect the battery [Min HT, 2017]. Experimentation results in Reference [Min HT, 2017] prove that energy efficiency is improved, and consumption is reduced by 7% in SC-battery topology compared to the other one. SC is effectively used to reduce battery stress in such a topology. Battery ratings are scaled down in the battery-SC topology since the DC-DC converter processes the required power that the battery can handle considering their SoC.



(a)

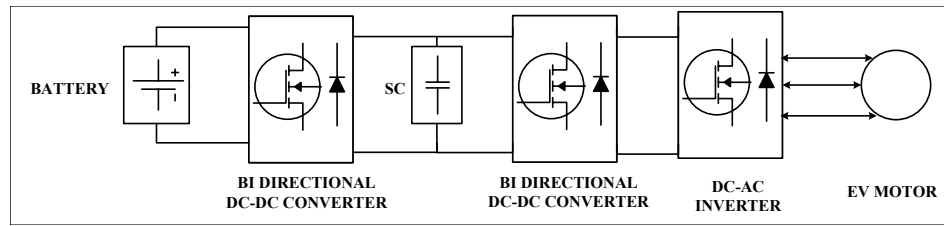


(b)

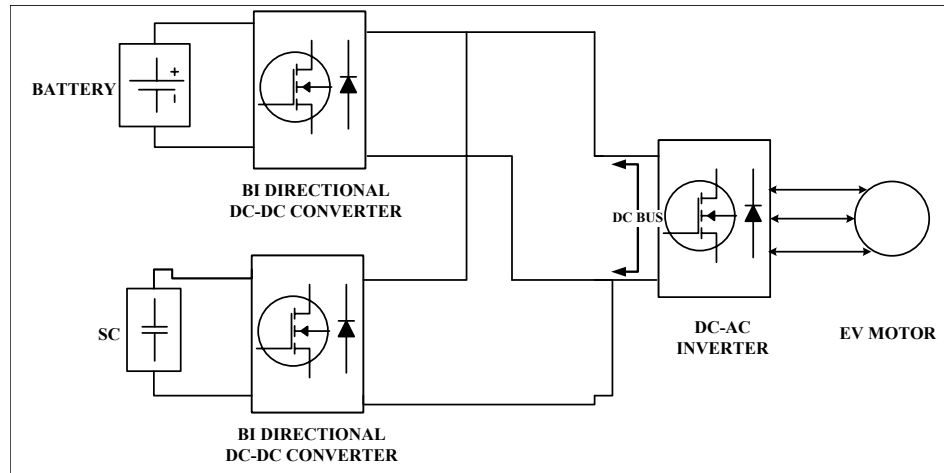
Figure 2.3: Schematic of the semi-active converter topology of HPSS (a) SC-battery (b) Battery-SC.

2.3.3 Full-active topology

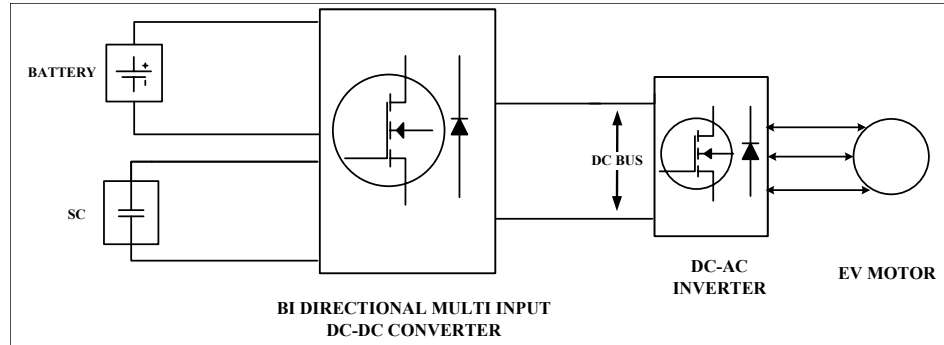
Full active topology uses DC-DC conversion for both battery and SC power. This helps the HPSS to support each other during lower SoC conditions. Figure 2.4 shows the schematic of full active topology with battery and SC. Three different structures of the same are described. Series complete active (Figure 2.4 (a)) topology in which both SC and battery are connected to DC bus with separate DC-DC converters. A converter is between the battery and SC and another is between SC and DC bus. This helps the system to make the battery voltage, and DC bus voltage stable with reduced fluctuations, and separate control is done considering the SoC of each source [Song et al., 2015b]. Figure 2.4 (b) shows the structure of parallel full active topology, which is the effective structure in which different sources are controlled separately and are connected in parallel with the DC bus, which develops DC bus voltage with fewer fluctuations [Trovao et al., 2013]. A multi-input type structure of full active topology is shown in Figure 2.4 (c). This arrangement allows the magnitude of both SC and battery voltage less than DC bus voltage and can even reduce the fluctuations [Cao and Emadi, 2012]. But the control scheme of this type is elaborate and can increase the losses.



(a)



(b)



(c)

Figure 2.4: Schematic of the fully-active converter topology of HPSS (a) series (b) parallel (c) multi-input type.

The full active type topology is highly stable, and converter efficiency is high since both sources are decoupled and controlled separately. The summary of different topologies based on significant characteristics is mentioned in Table 2.1. It is essential to note the DC bus fluctuations depicted in the table for passive and SC/battery semi-active topologies. The voltage fluctuations should be allowed in a minimal range since the battery is directly connected to the DC bus, and continuously fluctuating voltage can affect the lifetime of the battery. Even though DC bus voltage fluctuations can be entitled to a wide range in full active topology. It is highly stable and improves the EV motor's performance. This is achieved in

full dynamic topology since both sources are decoupled from the DC bus. Overall, the section’s discussion deals with the topologies utilized to power the EV using hybrid sources. The review majorly focuses on the battery-SC hybrid combination to power the EV. The existing topologies can undergo a similar structure for fuel cell-based EVs (FCEVs) with a unidirectional DC-DC converter connected with the fuel cell side and a bidirectional converter with the battery or SC side. The topologies discussed in this section with previous literature further have some drawbacks. Modifications on such converter structures result in an improvement in energy efficiency and the lifetime of sources. Moreover, charge and discharge between the battery and SC can be implemented considering the conditions of power demand and driving conditions. Those aspects need to be considered to achieve improved performance of the overall EV system. The topology enables reduced voltage ratings for the sources since they are individually controlled by the topology. It ensures the best performance among all the different topologies. Even though, certain drawbacks exist in power loss, cost, and the number of components for this topology. Considering the advantages in maximum utilization of each source and its ease in controlling separately strictly based on the EMS algorithm makes it a suitable option for hybrid sources in electric vehicles.

Table 2.1: Analysis of different topologies of coupling battery-SC hybrid system

Characteristics	Passive	Battery/SC	SC/Battery	Full active
Efficiency of converter	very low	medium	medium	high
Charge-Discharge performance of battery	very low	high	medium	high
Charge-Discharge performance of SC	very low	medium	medium	high
Allowable DC bus voltage fluctuations	no	medium-range	short-range	wide-range
Usage of semi-conductor switches	very low	medium	medium	high
Complexity and cost	low	medium	medium	high

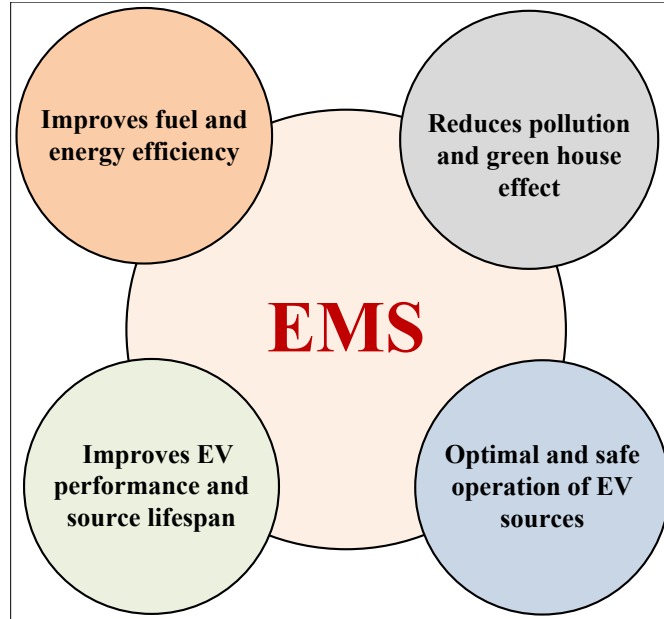


Figure 2.5: Primary targets of EMS in EV, HEV, PHEV.

2.4 Hybrid Energy Management Strategies

As mentioned in the previous section, EVs utilizing a battery and SC as a hybrid source improves lifetime, energy utilization, etc. This is an excellent alternative source system for EV since the improvement in efficiency and lifetime of sources plays a significant role in EV's overall performance. Improved coordination among these sources to meet the power demand is the key role of an energy management system. In other words, EMS needs more attention where power of both sources are efficiently allocated, considering the charge states and other driving conditions.

Improvement in energy consumption, reduced emissions and efficient power flow among different source systems are highly dependent on the selected topology and the type of EMS used in EVs. EV, HEV, PHEV utilizes a strategy to control the power flow among the different power trains and sources. The design depends on the type of conditions that vehicles need to overcome. Different topologies of the hybrid sources in EV are discussed in the previous section. The main aims that can be considered for developing an EMS are mentioned in Figure 2.5. Significant aspects that need attention during the control of EMS include fuel consumption improvement and less emission in the case of HEV, PHEV, and consideration of the state of charge of all sources during all modes of operation, lifetime improvement, and safety sources for pure EV. Researchers use various driving profiles for analysis and testing purposes (NEDC, US06, IUDC, and HWDC) [US-EPA, 2019]. The ICE and power sources used in HEV and PHEV effectively split the power demand for different driving profiles is the crucial function performed by EMS achieves the aspects mentioned above to improve overall energy and cost-efficiency. However, real driving conditions are not exactly similar to these profiles and varies its power

requirement and energy consumption based on different factors related to the vehicle, driver, and environmental conditions. EMS plays a vital role in pure EV powered with a hybrid source system. Different power sources have variations in their current handling capability, time response, power, and energy density. Thus, EMS in pure EV focuses on achieving control by considering different characteristics of power sources used in the EVs. Typically, battery-based EVs are supported by SC, Fuel cell, SMES, and FCEV coupled along with battery and SC [Xiong et al., 2018b] [Kouchachvili et al., 2018] [Fathabadi, 2018] [Song et al., 2014b] [Li et al., 2015] [Li et al., 2016].

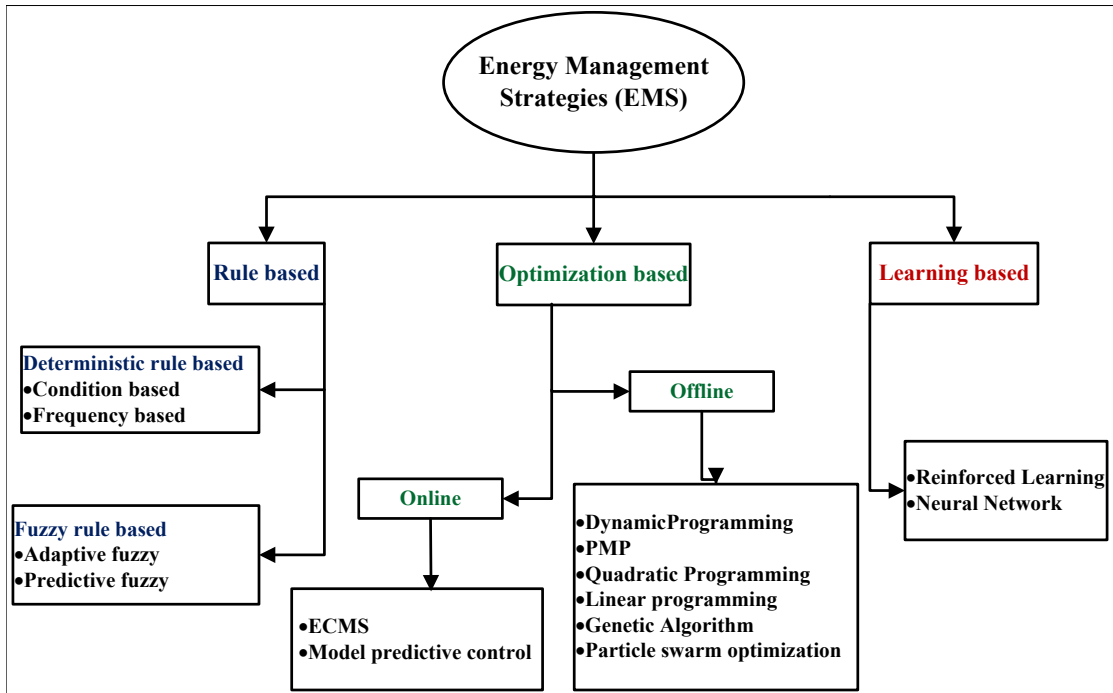


Figure 2.6: Classification of EMS employed in hybrid source EVs.

Over the last decade, a lot of research is continuing to improve the EMS of EVs. This work is focused on vehicles powered by pure electric sources. General classifications on EMSs for pure EV are of three types: Rule-based, Optimization-based and Learning-based. The detailed classification of EMSs is depicted in Figure 2.6. A battery- SC hybrid combination of power sources is considered to explain the strategies. SC, with its high-power density and fast response, is utilized during acceleration and for storing regenerative energy from the vehicle during braking. The battery meets the average power demand, which is nearly constant during EV cruising. SoC of sources is a significant factor in deciding the amount of energy that each source can manage. Overcharging and deep discharging of the source can accelerate aging by reducing capacity and performance [Lu et al., 2013] [Uddin et al., 2016]. Thus, EMS should be designed with various modes of operation, considering the SoC condition of power sources. SC also effectively meets the high frequency charging and discharging during the city driving cycle, where the traffic condition is conjoined [Uddin et al., 2016]. High-frequency operations can

affect the battery lifetime [Tran et al., 2020]. The behavior of the driver is also an essential factor for high-level EMS. Rule-based EMS is further classified into deterministic and fuzzy logic-based strategies [Tran et al., 2020] [Marzougui et al., 2017] [Florescu et al., 2015]. Optimization-based EMS is classified into offline and online modes. Offline modes consist of DP, PSO, Pontryagin’s minimization principle (PMP), and GA [Song et al., 2015a] [Wieczorek and Lewandowski, 2017] [Chen et al., 2016]. Online modes include ECMS and model predictive control (MPC), respectively [Golchoubian and Azad, 2017] [Li et al., 2017a]. They require a model of the whole system, which is very complicated. Learning-based EMS reduces the complexity of the strategies but needs high quality and many data sets for the control, which is a measure of its accuracy. It utilizes historical data for the learning process. It is an effective EMS and shows its scope with online data-based approaches such as artificial intelligence and machine learning techniques [Zhang et al., 2021]. The combination of multiple EMS can improve fuel economy and energy efficiency. Table 2.2 briefs the different types of EMS with their merits and demerits. The importance of each strategy can be clearly identified in the table.

2.4.1 Rule-based EMS

Rule-based (RB) EMSs operate with human experiences and instincts. The main advantage of this method is that knowledge of the driving cycle is not required to handle. It is feasible and straightforward for real-time implementations. Calibration is necessary to update the control parameters for a specified range of any driving profile. Since this EMS is based on the rules designed, its major drawback is applying the same algorithm to different power trains and source architectures. Other methods can be combined with a rule-based approach to improve the efficiency of the overall EV system. Deterministic and fuzzy logic-based controls are the different subsystems of rule-based EMS. Their simplicity in real-time implementations make it a better competitor among EMS’s. Figure 2.7 shows the algorithm for a normal battery-SC HPSS for powering the EVs with rule-based EMS [Tran et al., 2020]. This gives the basic idea of the strategies of complete rule-based EMS. SoC of SC is considered in the explained rule-based approach, which can assure the source’s safety. SC gets charged as per the assigned rule in the algorithm, and maximum utilization of SC can achieve reduced stresses to the battery to meet the desired driving profiles.

2.4.1.1 Deterministic-based energy management strategy

The EMS develops different rules based on previous experience of the behavior of the system. The primary task of the EMS is to distribute the demand power among the other powertrains (HEV, PHEV) and various sources in HPSS based EV. The rules for power allocation among various sources are defined based on previous situations. Frequency-based decoupling control is used to split the power among the sources. Low-frequency power is handled by a battery in the case of a battery-SC hybrid system in EV [Kouchachvili et al., 2018], and the fuel cell

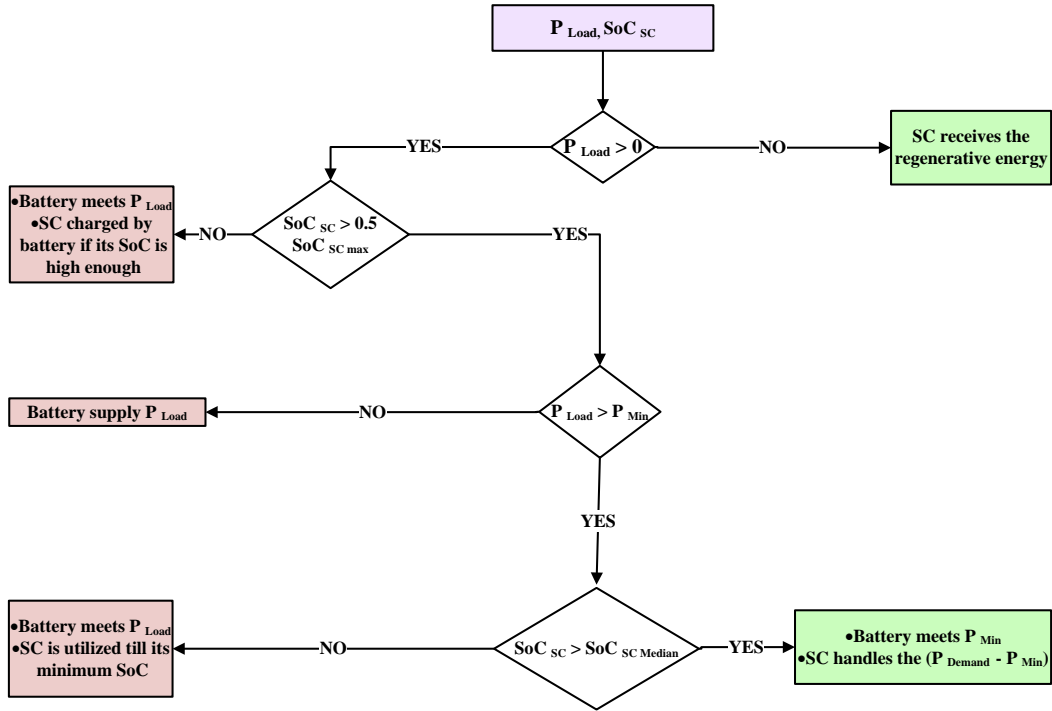


Figure 2.7: Algorithm for battery-SC hybrid source system using Rule-based EMS.

manages this with an improved life cycle in fuel cell EVs [Fathabadi, 2018].30 High frequency and peak power are allocated to SC, which has faster dynamics and compensates for such power demands. Figure 2.7 explains the deterministic rule-based algorithm derived from the previous experience and shows the battery-SC hybrid system’s energy management. The SoC of an SC is considered in the rules to decide the ratio of power splitting. When an SC SoC is lower than its minimum value and power demand is high, power is met by the battery to support the SC. In these works, the frequency of the filter which splits the power demands among sources is constant. [Kouchachvili et al., 2018] [Fathabadi, 2018]. This reduces the adaptability of the EV control system.

Similarly, other cases are also defined in the algorithm, which guarantees the protection of sources. But the optimal solution cannot be determined with this EMS. Rule-based strategy combined with filter control improves the power splitting among sources. The filter splits the high and low-frequency power demands to allocate for sources. Generally, a low-pass filter performs this task to divide the power considering the power characteristics of the battery and SC. A battery manages low-frequency power demand and high-frequency component is taken care by SC. A rule-based system, along with a filter, can improve efficiency [Blanes et al., 2013]. The limitation of this strategy is observed in the adaptability and flexibility of the overall system since the filter frequency is fixed, and there is a chance to affect the safety of the sources. A rule-based strategy is proposed by Song et al. [Song et al., 2015a] for pure EV in which tuned DP parameters are utilized to achieve optimal solutions. Sellali et al. [Sellali et al., 2019b] developed a

fuzzy-based EMS combined with a rule-based strategy with experimental study and discussion on the combined strategy’s effectiveness. ECMS-based work is performed by Hemi et al. [Hemi et al., 2013] with a rule-based strategy, and the improvement in results is briefed. Results prove that integrated methods can improve the system’s efficiency compared to rule-based EMS. The combination of rule-based and optimization-based EMS improves the optimality of the solution. Thus, it can attain both real-time implementation and high optimal solution, and the energy efficiency of the hybrid source system in EV can be improved greatly. However, drawbacks of these work can be identified in the performance of the vehicle. Such a strategy does not assure performance as the charge availability of SC is not considered in the control strategy during the overall drive. The EMS must focus on scheduling of SC charge-discharge profile considering the status of the acceleration profile of the vehicle. This is highly effective in terms of energy economy and battery life [Vukajlović et al., 2020] [Madhusudhanan and Na, 2020] [Hegde et al., 2020]. Parameters that affect EV battery life and capacity (such as driving profiles, driver’s behaviors, road terrain, load conditions, etc.) must be considered in the strategy to enhance the power allocation among the sources [Vukajlović et al., 2020] [Hao et al., 2020]. Easiness of operating in real-time and its simplicity in control strategy are the major merit points of this control strategy. However, adaptivity is an essential factor for EV energy management since its load demand varies at each instant. Control parameters need an update based on the load demands, source charge, and vehicle driving conditions.

2.4.1.2 Fuzzy logic-based energy management strategy

Fuzzy logic controller (FLC) is basically bound by a set of fuzzy rules, input and output. Human knowledge and reasoning on a solution for the problem are derived from condition rules. It includes input membership functions, fuzzy quantization, fuzzy rule set, defuzzification, and output membership functions. Fuzzy rules decide the accuracy of the control. Tuning is done very easily in the FLC. Rules are designed based on the experience of the user. The fuzzy controller handles problems occurring in nonlinear, time-varying problems in EV energy management. Trov ao et al proposed a fuzzy-based energy and power split management algorithm for a battery SC-based hybrid-powered pure electric three-wheeler (3W) [Trovão et al., 2017]. This work depicts FLC’s importance in EVs energy management and compares the work with the battery-only system. Reduction in battery RMS current by 12% eventually increases lifetime and reduces battery cost. HIL real-time simulations confirm the improvement in energy consumption of the proposed FLC system. Battery RMS current reduction can improve the life cycle of 3W batteries. The performance of the vehicle to achieve required acceleration during overtaking, hill climbing, and utilization of braking energy during deceleration are not considered in this work. This gap is addressed in our study and highlights the importance of SC utilization considering any driving profile and behaviors to enhance EV performance without compromising battery life cycle and capacity [Zhang et al., 2020] [Jafari et al., 2018]. A fuzzy super twisting control is implemented by Sellali et al. for a battery-SC powered EV. Different

modes are introduced in FLC to achieve the controller’s highly accurate performance, considering the state of voltage in SC [Sellali et al., 2019a]. The controller neglects the requirement of additional controllers to regulate the DC bus and SC voltage. The defined fuzzy rules decide the reference powers of both sources and guarantee better power for EMS in EVs. The strategy discussed by Sellali et al. lacks the power demand conditions for varying driver behaviors, temperature, and road terrains, which affects the life cycle of the battery [Vukajlović et al., 2020]. Figure 2.8 shows the FLC-based schematic control diagram for EMS in EV.

Optimal results are not developed with the conventional type. FLC is divided into optimized fuzzy, adaptive fuzzy, and forecasting FLC. Optimization is utilized with the FLC in the first type, thus achieving improved optimal solutions utilizing various optimization techniques. Controller parameters are optimized and tuned in FLC through an optimization algorithm to attain the control objectives (SoC improvement, battery life improvement, etc.). FLC is improved by introducing an optimization algorithm to optimize both the membership functions and fuzzy rules using PSO, [Chenghui et al., 2007] GA [Eckert et al., 2020], and DP [Song et al., 2015a]. Optimization improves the fuzzy control strategy, but optimizing battery life with varying driving conditions and behaviors are not addressed. This affects the life and capacity of EV battery [Song et al., 2015a] [Eckert et al., 2020] [Chenghui et al., 2007].

Adaptive algorithms are introduced into fuzzy strategy with a motive to overcome the demerit in self-adaption. Power split among the battery and SC in a hybrid source-powered EV is discussed. Yin et al proposed an adaptive fuzzy-based EMS that effectively splits the power demand in EV for city and highway driving profiles. The control strategy ensures better performance compared to the conventional schemes with reduced battery current variation [Yin et al., 2016]. Adaptive fuzzy-based EMS enhances system reliability and performance. However, the control strategy lacks the behavior of the system on the degradation of EV batteries due to the effects of varying driver behaviors. Hussain et al. proposed two adaptive controllers for the energy management of battery SC powered EV [Hussain et al., 2019]. Adaptive FLC performs the optimal power sharing among the sources considering the SoC of SC. The second adaptive control is performed by FLC to achieve an adaptive PI control for protecting the SC from deep discharging and overcharging. Predictive FLC utilizes future states of the vehicle, generating real-time control signals for optimal power sharing. But it limits its prediction accuracy due to the non-inclusion of aspects of driver behavior and road conditions in the strategy. These parameters highly reduce the battery capacity [Jafari et al., 2018]. Wang et al. proposed a strategy using a Markov chain for power prediction, which is essential for the system with a fully EV powered with battery and SC [Wang et al., 2019]. The Markov chain improved the demand power when implemented along with fuzzy logic due to high prediction accuracy. Various parameters that affect the EV performance and battery life are not highlighted in the power prediction using Markov chain [Jiquan et al., 2018]. This issue limits the reliability and flexibility of the EV.

Usually, most FLC is used as a joint control strategy to combine with other EMS to improve the optimal operating conditions and to adapt different driving behaviors of EV. Gao et al improved the traditional FLC by implementing optimization results for a pure EV utilizing battery - SC hybrid system [Gao et al., 2016]. At the same time, Dusmez et al modified a similar EV with a wavelet transform (WT) and improved the adaptivity of the control system [Dusmez and Khaligh, 2014]. SC utilization can improve the performance of hybrid source systems. SoC of SC plays an essential role in the optimal control in this direction. Both works utilizes SC to reduce the stress on battery but failed to discuss the effect of driver behaviors and road terrain on the energy consumption of EV batteries. The control strategy must consider battery capacity loss in the control algorithm to avoid anxiety issues [Vukajlović et al., 2020]. He et al. proposed a FLC-based management to allocate power among sources considering SC SoC with varying driving conditions [He et al., 2013]. Zhou et al. depicted an adaptive membership function based on FLC, which operates on the previous information [Zhou et al., 2014]. This work achieves an update of the fuzzy control function, and improvement in energy management is analyzed. This improves the adaptability of the system, but it does not consider the driving style, road conditions, temperature, and load states, etc., which causes severe damage to the battery performance. Machine learning is utilized in optimization with more improved results. Murphey et al. used a machine learning algorithm for optimizing the hybrid source system for EV [Murphey et al., 2011]. This increases the computation cost and makes the system more complex without any significant improvement in battery life due to insufficient datasets. The fuzzy control strategy is highly adaptive and reliable since it can update the control parameters using optimization. Prediction-based fuzzy algorithms are seeking high interest in the present scenario, and it can be easily implemented in online applications. Driving conditions need to be predicted, and the interval based on the update of control parameters improves the control horizon and makes the system more reliable.

2.4.2 Optimization based EMS

It optimizes the solution by minimizing a cost function that improves system efficiency and performance. EMS in EV used to find the optimal control values satisfying all the constraints (SoC of sources, power limit, etc.) refers to optimization-based EMS control strategies. This scheme aims to minimize the cost function (Fuel consumption in HEV, energy efficiency, maintenance of source SoC in EV, power loss, hydrogen consumption in fuel cell EV) and achieve an optimal solution that controls the system. Based on its level of control and applications, it can be divided into offline and online strategies.

2.4.2.1 Offline optimization based EMS

This optimization strategy requires knowledge of previous conditions and needs different driving cycles for processing its control. They are not utilized in online applications due to the requirements of EV driving cycles. It is used to get a

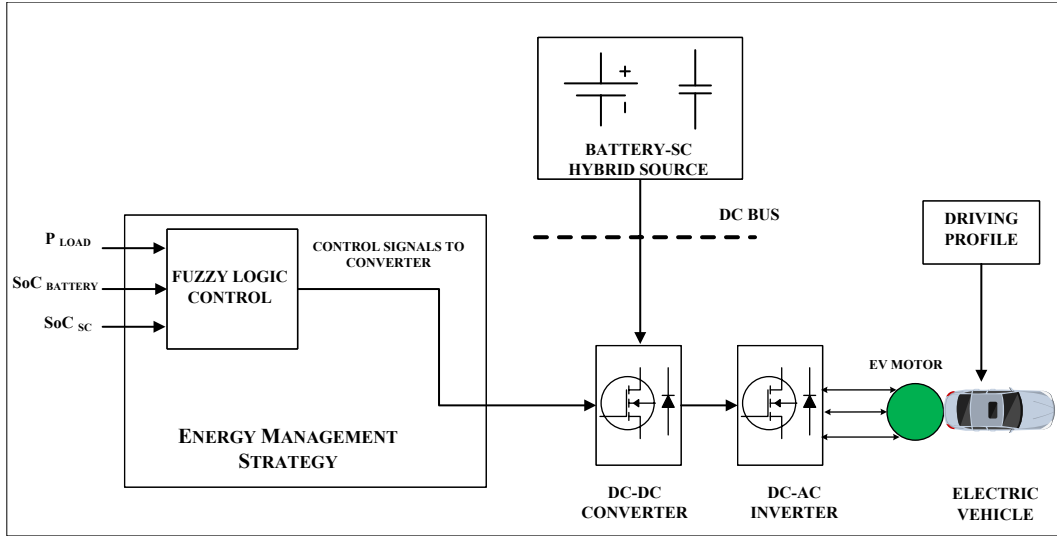


Figure 2.8: Fuzzy logic control (FLC) based EMS for battery-SC hybrid source powered EV.

benchmark to compare with other online strategies. Modified optimization strategies are used in online applications. Optimization problems for different types of vehicles differ based on their powertrain architecture and converter configurations for hybrid sources. For series HEV, optimization can be done to solve a problem to minimize the energy consumed. In contrast, in parallel HEV, it can be done to reduce fuel utilization and reduction in emission of gases. Major optimization objectives focus on reducing energy losses, peak or RMS battery current, and maintaining the SoC of sources. Different constraints that guarantee the system's safety must also be satisfied. Algorithms for optimization are the next important aspect following the problems and limitations. Researchers perform different algorithms to solve the EMS of EVs using optimization. They are grouped into direct, indirect, gradient-based, and derivative-free. They are divided based on their process to optimize the specific problem. Discretization of the problem and solving it as a static optimization is done directly (DP). Optimization based on the calculus of variations is termed under indirect type (PMP). Several derivative-free algorithms (GA, PSO) are utilized in problems where derivative information is unavailable or difficult to develop. The algorithm uses a stochastic search to produce the optimal global solution. Dynamic programming DP requires knowledge of the EV driving cycle and is mostly used to solve EMS problems. It can be generalized and termed deterministic dynamic programming (DDP). The optimization problem is divided into minor issues by discretizing the overall time. This is the logic behind DDP. The cost function is minimized in each discrete sample time utilizing DP techniques. The DDP applications are explained and performed by Masih- Tehrani et al. to improve energy management performance for pure EV with hybrid sources [Masih-Tehrani et al., 2013]. Consideration of varying driving behaviors, traffic, and load conditions, which is a vital factor that determining battery life, is missing in the work and can be highlighted as a drawback of the system. Sundstrom and Stefanopoulou, in their work, performed DDP-based EMS

for fuel cell battery EV minimized the hydrogen usage and maintained battery SoC at specified levels but not focusing on the battery energy consumption during varying conditions of the driving environment [Sundstrom and Stefanopoulou, 2006]. This highly affects the range and battery performance. Santucci et al. applied DDP in pure EV with hybrid sources (battery-SC) and improved battery life [Santucci et al., 2014]. The effects of battery performance at low temperatures are discussed by Song et al. and proposed a DP-based HESS management control for EV [Ziyou et al., 2015]. The battery degradation model is utilized to identify the temperature effects at different discharge levels and optimizes the HESS system with optimal solutions. The solution to reduce the effects that accelerate the battery life depletion is not mentioned and limits the real ability of the strategy.

Significant challenges faced by DDP include (a) driving cycle requirement (b) high computational cost (c) not suited for real-time implementations. The popularity of DDP is not widespread in EMS of EV since it is not achieving an optimal solution for all driving cycles. The time consumption of DDP is also high and unable to implement a feedback solution directly. This challenge is overcome in stochastic DP (SDP) based work proposed by Romaus et al. and depicts the energy management for nickel-metal hydride (NiMH) or lithium-ion (Li-ion) batteries-based hybrid power source fed pure EV [Romaus et al., 2010]. The optimization is achieved, considering the stochastic influences of traffic and drivers. Drawback on the performance of EV is a concern; frequent sudden load demands can also reduce battery life. Lin et al. proposed a DP utilizing Markov chain as a driving profile demand and turned as stochastic DP (SDP) [Lin et al., 2004]. Random driving profiles are selected to optimize the EMS to improve the reliability of the optimization strategy. This method also faces several drawbacks. An optimal solution for the problem cannot be developed for different Markov chain models, which are not mentioned. Time consumption and cost of tuning parameters are very high in SDP. DP-based strategies are not used in online applications since they require prior driving cycle information to achieve optimal solutions. It lacks the adaptivity in control strategy during real-time application. Additional adaptive tuning algorithms can increase the complexity of the system.

Pontryagin’s minimum principle (PMP): It is an indirect algorithm that is processed with a calculus of variations. Global optimization problems are solved using PMP, which Lev Pontryagin derives. The problem’s optimal solutions are provided using PMP consisting only of necessary conditions, and the Hamilton equation provides sufficient conditions. Several small Hamilton minimization problems are developed, which is reduced from constrained global optimization problems and are the essence of PMP. The initial costate of all Hamilton problems are identified with the iterative process using a predetermined driving cycle. Since different driving profiles are available, the initial costate also differs. Due to all this data, the computational cost of PMP is high. It is not well suited to real-time applications. Adaptive and accurate adjustments of costate value can improve the performance of PMP strategy. Nguyen et al. depict the optimal

control behavior of PMP-based strategy to control the power flow among battery-SC EV [Nguyen et al., 2014] . This strategy gains attraction since it's suitable for real-time applications. Optimal solutions are easily achieved by employing a feedback loop and reducing time consumption. However, Nguyen et al. proposed a PMP-based EMS for a battery-SC powered EV. The work focuses on developing a real-time PMP strategy without utilizing any additional mechanism for the costate variable [Nguyen et al., 2017]. Simulations presented in the method show improvement in battery life. This lacks improvement in EV performance since it focuses on improving the lifetime of EV batteries. The ability of EVs to achieve improved acceleration performance is also a factor considering the popularity of EVs. PMP provides an optimal solution near to DP strategy. Recently researchers are modifying the PMP to utilize in real-time applications. Bernard et al. implemented a PMP global optimization strategy to improve the power allocation of fuel cells and the battery-SC hybrid system in an FCEV, which also focused on reducing hydrogen consumption [Bernard et al., 2006]. However, the control strategy does not discuss the battery life cycle depletion, which is a drawback of the system. PMP and Markov chain joint control strategy utilized by Hemi et al. shows the solution derived for EMS in FC-SC hybrid vehicles [Hemi et al., 2015]. The method improves HESS's real-time efficiency since the Markov chain improves the global optimization horizon with different driving profiles. Nguyen et al. proposed a PMP-based adaptive real-time strategy for a HESS (battery-SC) powered EV [Nguyen et al., 2019]. PMP is simplified to utilize the proposed system in real-time and avoids additional adaptive mechanisms. Battery RMS current is reduced by 50% when compared with the conventional methods. The utilization of SC can be further improved to enhance energy efficiency and reduce battery stress. Jiang et al. proposed a 2D Pontrygin's minimum principle and discussed a motive to reduce energy consumption [Jiang et al., 2019]. It is utilized to achieve an optimal fuel cell/battery/SC hybrid power source vehicle strategy. Knowledge of the future driving cycle is acquired by combining intelligent transportation, GPS, and GIS with the PMP strategy to correct the initial costate. This can handle the initial costate effects on SoC variations.

Genetic algorithm (GA): In a system where the derivative is not available, it is challenging to solve the problem. Hence a derivative-free algorithm (DFA) is developed, which provides a global solution. One significant type of DFA is GA. It is a search method based on evolution related to genetics developed in 1975 by Holland. The vital phases of GA constitute reproduction, crossover information, and mutation. Different types of optimization problems solved using GA include nonlinear, multi-model, and intermittent time-based problems. Tashakori Abkenar et al. proposed a power management strategy for all-electric ships powered with FC and battery as the sources [Tashakori Abkenar et al., 2017]. A GA is utilized to regulate the FC output voltage within a specific range and achieve high performance at different ship operating conditions. Apart from that, it also guarantees reduced hydrogen consumption and also avoids sudden power fluctuation of FC. However, a study on the battery life cycle is not considered and this affects its life during frequent sudden power demands [Vukajlović et al., 2020]. Addition of

SC as an auxiliary source can further improve overall energy efficiency as SC can handle higher C-rate requirements. Correa et al. developed a GA-based EMS for battery-SC-powered EV [Correa et al., 2017]. It achieves improvement in energy efficiency with optimal sizing of sources without affecting the range of EVs. But the availability of SC during varying driving scenarios to support the battery is a huge concern. SC energy must be utilized based on the varying driving conditions which can improve the battery life. Guang et al. proposed an EMS for an FC-SC powered EV utilizing improved GA [Guang et al., 2017]. An FLC-based strategy is implemented in the work, and GA acts to optimize the parameters of membership functions to minimize the voltage and current variation of FC. Improvement in the lifetime of the FC stack can be guaranteed since SC carries sudden power fluctuations. Multi-objective optimization for minimizing the size of hybrid sources and maximizing the range of the EV is implemented using GA. This work does not guarantee improvements in the battery life cycle. Parameters that affect the battery life cycle and safety of sources are not highlighted which is a major drawback of the work. The work proposed by Eckert et al. combines GA with FLC for a dual hybrid energy source system (battery-SC) powered EV [Eckert et al., 2020]. Results prove the importance of optimizing the HESS size and improving the driving range. The control strategy lacks the parameters to improve the performance of the vehicle.

Particle swarm optimization (PSO): is also a derivative-free algorithm and is utilized to optimize the problems where it is impractical to get the derivative. The operation of PSO is similar to the movement of an organism in a group. All the members are in connection with each other. They can update their individual best position achieved and conclude with an optimal solution by selecting the group's best solution. The swarm particles move in the direction of the updated place which is the best location. It is like an ant colony. This relation is exploited to achieve an optimized solution. Hegazy et al. detailed the PSO-based algorithm for optimal power flow among fuel cell-based hybrid EV with battery and SC as the secondary source [Hegazy et al., 2012]. Battery stresses and their effects on capacity fading are not explored in the strategy. This increases the battery degradation cost and affects the safety of sources. A Particle The swarm-Nelder-Mead optimization algorithm is coupled with a rule-based strategy which optimizes the control parameters of the rule-based control as depicted by Mesbahi et al. [Mesbahi et al., 2017] Battery power stress and the life cycle is improved with the proposed strategy and compared with the rule-based and battery-powered system. However, achieving the availability of SC energy during all acceleration intervals is not assured in the strategy. This affects the vehicle's performance during an unknown driver's behavior, driving profile, or road conditions. Lin et al. achieved better fuel economy and improved battery energy efficiency for a PHEV using PSO. The neural network is implemented to train the optimized results from PSO [Lin et al., 2010]. Driving behaviors, road traffic, road conditions, and temperature are not utilized effectively in the control strategy and may accelerate the battery life cycle depletion. Energy consumption and ampere hour throughput for similar driving routes vary considering these factors. PSO-based strategy is utilized for

optimization of HESS sizing for SC and fuel cell in FC-SC-based EV [Hegazy and Van Mierlo, 2010].

2.4.2.2 Online optimization based EMS

The strategy behaves as local optimization since it does not utilize knowledge about driving cycles as optimization-based offline systems require. Thus, online-type algorithms are not ensuring optimal solutions for EMS problems in real-time. Global optimization problems are not suited for real-time applications due to the low memory and computational time of the real-time environment and are formulated as online strategies. Significant types of such methods are ECMS and MPC, which are commonly used.

Equivalent consumption minimization strategy: PMP is formulated into ECMS and is utilized in a two-stage energy management for a fuel cell-based vehicle by Geng et al. [Rodatz et al., 2005] The focus of this work is to improve the fuel cell life, and the minimization principle effectively performs the task. The drawback of the work is a compromise on battery life to improve the fuel cell life. Reduction in battery performance can be observed with the control strategy. Rodatz et al. proposed a real-time ECMS strategy to control the distribution of power flow among FCSC- based EV [Pei and Leamy, 2013]. The strategy's focus is to minimize the consumption of hydrogen fuel for any stage of the driving scenario. The availability of SC to act throughout the driving cycle is not ensured and can affect the fuel cell life. ECMS is a local problem of the PMP by reducing fuel consumption. The equivalent fuel factor is identified by ECMS develops the actual energy consumption required for recharging batteries and regenerative energy. The equivalence factor (EF) behaves precisely like a costate in PMP and holds similar functions to manage. Many studies have been developed to estimate the EF, which comprises a detailed analysis of the SoC of the battery, charge or discharge current, and driving cycle information. There are two types of estimation that are highly used for this purpose: (a) offline using optimization methods mentioned in the previous section and (b) online by updating the EF in each step. Information on a complete driving profile is required to develop the optimal EF in offline estimation methods. This can be created using different algorithms. Optimization-based algorithms are well known in this DP [Pei and Leamy, 2013], GA [Sinoquet et al., 2011]. Recalibration is essential for each driving cycle to get an optimal value. EF needs to get updated based on certain factors in an online estimation method which is already mentioned in the section. Battery SoC change occurs continuously; the EF optimal value from offline estimation is added with a correction term for the SoC deviation, which is an important aspect. However, factors other than the driving cycle need to be utilized in the offline estimation to improve the flexibility of the control strategy. Temperature effects on capacity fading are higher and accelerate the battery degradation [Hao et al., 2020]. For an FCEV, the reduction of hydrogen fuel usage is a vital improvement. ECMS is developed to reduce hydrogen usage. Battery and SC are utilized to reduce hydrogen consumption during sudden peak demands, which cannot be handled by fuel cells. This ECMS-

based work is discussed by García et al. employs fuel cells to manage constant energy demands and battery SC to handle peak power demands to improve fuel economy [García et al., 2013]. Control strategy does not explain the effect of unknown driving behavior and profile on the battery life cycle. Li et al. proposed an ECMS-based EMS for fuel cell EV [Li et al., 2017a]. The strategy is explained with efficient power management among the hybrid sources, which guarantees a reduction in fuel cell degradation. Li et al. also studied a novel (Quadratic program) QP-based ECMS scheme for fuel cell-battery-SC-based vehicles. The increase in the lifetime of sources and reduction in hydrogen fuel consumption is considered as the main aim of the work, and it achieves those when compared with a rule base control strategy and hybrid ECMS strategy [Li et al., 2018a]. Verifying the influence of driving style, road, and environmental conditions, etc on battery capacity and life cycle serves as a major factor to improve the overall performance and efficiency of EVs which is a drawback of the work. Fu et al. worked on a similar kind of EV powered by battery-FC-SC [Fu et al., 2019]. An ECMS combined with a low pass filter-based strategy is utilized for efficient power allocation among the sources. The low pass filter-based EMS keeps the SoC of SC under desired limits and ensures SC handles peak powers, reduce the stress on battery and FC, and achieves higher SC utilization. Meanwhile, the ECMS scheme is implemented to split the power between the battery and FC considering the improvement in the lifetime of sources and reducing hydrogen consumption. ECMS performance improvement is observed by Li et al. analyzed ECMS and it shows a reduction in hydrogen consumption compared with a rule-based strategy [Li et al., 2019]. It proves the real-time control ability of ECMS in a fuel cell-based SC-battery hybrid source vehicle.

Model predictive control (MPC): The issues of DP algorithms in terms of inability to online implementation due to its requirement for knowledge on future driving cycles, road profiles, and vehicle states. A new predictive-based control strategy is utilized to tackle those issues in global optimization-based DP and called MPC. It is a receding horizon control with the development of a model of a whole system that undergoes online optimization to improve real-time applications. It mainly operates on three schedules: (a) Optimal input calculation inside a horizon, satisfying the constraints. (b) Implementing the inputs to the plant. (c) Shifting of the entire prediction horizon and again performing from first step. In a hybrid source-based energy management system, an update of real-time control parameters is essential; thus, MPC is famous in the EMS of EV. Prediction accuracy and optimization are the two primary tasks of MPC. Unlike global optimization, which is an infinite horizon based optimization, MPC solves optimal control problems in each predicted horizon, and control parameters are obtained on rolling of the horizon. Prediction-based control strategy in HPSS which predicts the vehicle’s driving conditions have improved the efficiency and performance of real-time optimization control of the overall system. Vehicle communication technologies are utilized to achieve maximum prediction accuracy.

Adaptive MPC (AMPC) is utilized to formulate the cost function as a stan-

dard DP algorithm [Zhang et al., 2017]. MPC toolbox in MATLAB is used for power prediction and proposes a control algorithm to allocate the power among HESSs [Hredzak et al., 2014]. It is essential to represent the system using a complex nonlinear system to show the control algorithm’s effectiveness and accuracy [Laldin et al., 2013]. Computational complexity of complex models is high and is tested by Golchoubian and Azad [Golchoubian and Azad, 2017] utilizing battery-SC HESS based EV. Nonlinear MPC is derived and compared to the HESS performance with RB strategy and linear MPC. This work proves the improvement and importance of the scenario. However, it considers constant values for battery and SC resistances, efficiencies of the motor, and the DC/DC converter, which affects the performance of the control strategy. Also, the computational cost is high and it lacks considerations on battery life cycle improvement for varying driving profiles and behaviors. MPC is highly complex, and its effectiveness in control makes it more popular. Hredzak et al. developed a low-order MPC model that can separately control different HESS sources and multiple models of such type to improve the performance with reduced complexity [Hredzak et al., 2015]. Prediction accuracy of the model is less and SC is not utilized effectively since it only aims to reduce the complexity. Many researchers have reduced the complex model to a nonlinear one that minimizes the computational cost and improves the prediction accuracy of MPC [Gomozov et al., 2017]. This utilizes a non-uniform sampling time to ensure improved performance. Nonuniform sampling time provides improved results in reducing peak battery power and maximum utilization of SC when compared to long and short prediction horizons. But sudden and unexpected driving behaviors due to traffic variations and driver behavior reduces the control performance and even affect the battery life. Thus, the importance of predicting the real driving pattern comes into the picture. Liu et al. proposed an MPC based EMS for EV powered from the battery-SC hybrid source. The strategy enhances the service life of the battery [Liu et al., 2016]. This highlights the improvement in life but SC availability to meet sudden accelerations and recuperate energy during braking is not guaranteed for varying driver behavior which increases the stress on batteries. Li et al. explain the predictive model for vehicle dynamics and hybrid sources (battery-SC), which initiates the MPC strategy and ensures a reduction in battery power variation and maintaining SC SoC within the desired range [Li et al., 2018b]. Power performance and battery lifetime are improved with the combined adaptive and MPC scheme. However, the inclusion of states such as road profile, driving styles, driving behaviors, and optimized sizing of sources in the control strategy can further improve the performance and EV battery lifetime. Syahbana and Trilaksono proposed an EMS for battery-FC-SC hybrid power sources [Syahbana and Trilaksono, 2019]. The EV operates with the power demand by sharing power among each source. Filter-based strategy is combined with MPC and achieves an effective switching strategy with minimum switching losses. The potential of HESS might not be fully utilized because the prediction horizon was not updated with the varying conditions. Filter frequency is not adaptive to varying driving conditions and behaviors which develops severe effects on the battery life cycle. A varying predictive horizon is explained by Xie et

al. to improve the velocity prediction accuracies. DP algorithm is utilized to solve the MPC optimization [Xie et al., 2017]. Similar works with the DP algorithm are proposed by Sun et al and Xie et al respectively [Sun et al., 2015] [Xie et al., 2018b]. All these works face issues due to the huge calculation burden of the DP algorithm is inevitable and impedes the online application of the strategy.

He et al. in their work proposed an EMS based on MPC for a fuel cell-based hybrid system [He et al., 2020]. FC’s power variations and temperature changes are considered in MPC to meet the objective function of reducing hydrogen fuel usage and improving the SoC profile of the battery. Since the MPC problem is formulated under constraints on power fluctuations to reduce hydrogen consumption and achieve higher fuel cell service life. This smoothens the fuel cell power profile but sometimes exposes batteries with larger power output due to the speed of change or variations in load power. Wang et al. explain that the (AMPC) with cost function is selected to enhance the battery life span and system efficiency [Wang et al., 2020]. Energy loss, current battery rate, and SC energy are set as the cost function and show better results than PI and MPC methods. This shows an improved strategy compared to other MPC strategies. The inclusion of additional factors (varying driving behaviors, road conditions, and load conditions) to this model may reduce the effect on battery capacity fading and degradation which further enhances the adaptability of the control strategy.

2.4.3 Learning-based EMS

Real-time implementations are essential in EMS control for EVs, and thus learning algorithms are attaining popularity. Learning-based algorithms utilize data analysis for acquiring real-time details of vehicle conditions, driving patterns, etc. Model accuracy is highly critical with MPC-based control, as depicted in the previous section. The size and structure of data are crucial in deciding the performance of these algorithms; hence, the complexity and time consumption are high for developing an exact database. This algorithm can efficiently operate with different driving profiles by its control laws, which are highly adaptive due to the massive data loaded into the algorithm. Machine learning methods can handle such large datasets with high performance. Model-based approaches are also utilized for tuning the parameters. The tuning is done with optimization, and thus, the system can behave with improved performance for different driving profiles, threshold values, and driver’s driving attitudes and styles. Other types of learning-based algorithms are discussed in EMS for EV, classified as their type of knowledge, including reinforcement learning, and neural network learning.

2.4.3.1 Reinforcement learning

The significant components of reinforced learning are an agent and environment, and the learning agent does the interaction with the environment. The learning agent receives an observation at each interval, and it shows the states. Action is selected by the learning agent and provided to the ground. A new state is

achieved corresponding to the selected action and feedback is given to the agent in the form of a reward. Agent receives instant rewards with each state change, and control is developed to map the present state to optimal action up to that state. Based on the control policy agent acquires the decision at each step. Finally, the cumulative reward within the time is learned after the required training. The total prize is maximized by considering the best series of selected actions based on the learning agent’s optimal policy. An RL-based algorithm is developed to reduce the hydrogen consumption in work proposed by Hsu et al. which is used to FCEV with battery [Hsu et al., 2016]. An RL-based EMS learns optimal policy without any predictions, which is based on the input data. Zou et al. discusses learning based EMS for an HEV [Zou et al., 2016]. Reinforced learning is utilized in those works and shows better optimal solutions. Li et al. adopted an RL method to define the optimal control logic with an Actor-Critic way [Li et al., 2017b]. An RL-based nested structure is implemented by Lin et al which is operated with two loops. The inner loop reduces the operating cost, and battery SoH improvement is made with the outer circle [Lin et al., 2015].

A deep network combined with an RL to form deep reinforcement learning (DRL). Hu et al. developed an EMS for a PHEV which utilizes a deep system with a fixed target [Du et al., 2022]. The proposed DRL receives an action from the driving state. Producing continuous movement is the critical problem faced by both RL and DRL, which is satisfied in all the recent works discussed in this section. A real-time EMS that exploits RL for the HESS in an HEV is proposed by Liu et al. [Liu et al., 2015] Simulation results of both RL and DP strategies are compared and prove the performance of the RL-based real-time EMS. Battery lifetime and temperature variations in HESS are considered to be forgetting factors for the EMS based on the RL strategy discussed by Xiong et al. for a PHEV [Xiong et al., 2018a]. Compared to a rule-based approach, the RL-based algorithm results showed a reduction of 16.8% in energy loss. Learning of varying driving profiles, road terrains, temperature effects and driver behavior using RL strategy can develop higher flexibility to the EV source system. This adaptively varies the policy by identifying the behavior or pattern of load conditions to guarantee a higher range of EV with an improved battery life in the long run. Sun et al. proposed multi-EMS combined to improve FC’s fuel efficiency and extend battery and SC life span [Sun et al., 2020]. An adaptive fuzzy filter strategy is applied to reduce the complexity of controlling all sources and an ECMS to optimize a multiobjective problem. Finally, the Q-learning algorithm splits the power demand among the authorities. Shen et al. developed a partially observable Markov decision process-based EMS combined with a convex optimization algorithm for action selection [Shen et al., 2020]. The FC-battery hybrid source powers are allocated based on the selected driving schedule and prove reduced computational time and energy efficiency improvement. Lee et al. proposed a Q learning-based energy management for an HEV that learns the driving conditions and updates the policy adaptively [Lee et al., 2020]. This is achievable by developing a separate control structure for power train and driving environment models. Velocity and energy consumption predictions are depicted by Hegde et al and are well-suited

for EMS application of EV. Data are identified utilizing sensor technologies and V2X infrastructures [Hegde et al., 2020]. Moreover, factors such as temperature, drive behavior, and instant road and traffic conditions can be utilized to highlight the performance enhancement of control strategy at any input conditions. Recent strategies are mainly focused on learning-based control due to its effective power allocation capability. It can learn the model based on the driving conditions and behaviors to update the control policies instantly.

2.4.3.2 Neural network

The process that is modeled and resembles its characteristics like thinking and computing a human brain and developed like neurons of the brain is called neural network learning. Nodes are the objects in a neural network that are analogous to real brain neurons. It consists of multiple inputs and outputs, like synapses in real neurons. Interconnecting different neurons form structures, and these networks are utilized to model other behaviors. NN learning can be improved by undergoing enough optimal training and massive datasets. NN's learning is repeated learning and modifying the weights of neurons in many instances. Changing the values is done by the learning process and distributed to achieve a stable range. The amount and quality of training data decide the optimality of NN [Koziel and Yang, 2011]. Major characteristics that are highlights of NN are (a) a high degree of the nonlinear global role, (b) a high degree of parallelism, (c) fault tolerance and memory, (d) adaptive and learning ability.

Moreno et al proposed a NN based EMS experimental implementation for a lead-acid battery-SC hybrid source EV. Introducing SC in the vehicle improves the range by 5.3%, and the NN scheme increased it to 8.9% [Moreno et al., 2006]. However, it is not a highly optimized control strategy as it lacks optimized results for training. Optimal solutions can further improve the prediction accuracies of the control strategy. ANN-based EMS also utilizes optimization algorithms to train the optimized data results and improve the optimality. A DP-based optimization algorithm is developed for the EMS of battery-SC EV by Shen et al. which exploits neural networks for training the EMS. NN-based real-time controllers are developed for certain driving profiles offline, the effect on control strategy might be affected due to any changes in driving profiles due to the uncertainties in traffic, driver behavior, etc [Shen and Khaligh, 2015]. Also, the availability of SC is not assured during the whole trip, which can eventually enable batteries toward frequent higher C-rates. This affects the life cycle and capacity of the battery [Vukajlović et al., 2020]. Zhou et al proposed a nonlinear autoregressive neural network (NARNN) to predict FC-battery EV's driving cycle [Zhou et al., 2017]. Future velocity states of the vehicle are expected for short or medium time range with this strategy. Predicted driving data can be utilized for effective online energy management. The drawback of this strategy can be highlighted by considering its accuracy in velocity prediction for different driving cycles. This can be improved by introducing input data sets of different classes which are related to vehicle, driver, environments that have a major impact on EVs. Alobeidli and

Khadkikar described a new EMS strategy for a battery- SC-based vehicle, which focuses on regulating the SC energy at acceleration and allowing SC to meet the whole range of EVs, making SC available for an extended period [Alobeidli and Khadkikar, 2018]. Two-stage ANN is implemented where the first stage sustains the SC energy and the second stage regulates the depletion rate considering battery SoC. It reduces the energy losses by 20% when compared with the RB approach. External factors related to the environment, driver, and vehicle that accelerate battery capacity and deplete its life cycle are not discussed and are a drawback of this model. Zhang et al. utilized the NN strategy for driving pattern recognition in a fuzzy optimal EMS for FC-SC vehicles. Pattern recognition improves the response and accuracy of a fuzzy-based control scheme [Zhang et al., 2019]. NN-based EMS for multi-source EVs with battery, SC, and fuel cells as the power sources are derived. Yavasoglu et al proposed the NN model to derive an optimal solution to the multi-objective energy management problem and compare it with the other optimization methods [Yavasoglu et al.,].

Table 2.2: Summary of EMS in EV with significant merits and demerits

Type of algorithm	EMS	Merits	Demerits	Application mode(References)
Rule-based	Deterministic	Simple, robust	Online calibration not accurate	Online application [Kouchachvili et al., 2018] [Fathabadi, 2018] [Trovao et al., 2013]
	Fuzzy logic control	Adaptive and predictive	Requires adaptive corrections for different profiles	Online application [Sellali et al., 2019a] [Masih-Tehrani et al., 2013] [Nguyen et al., 2014]
Optimization-based (Offline)	DP	Global optimal solutions, multi-object and non-linear problem solving	Complex computation, future driving information is essential	Offline application only [Tashakori Abkenar et al., 2017] [Correa et al., 2017] [Guang et al., 2017] [Song et al., 2015a]
	PMP	Highly optimal control with a global trajectory	Approximation of modeling is necessary to reduce the computational cost	Typically suitable offline application [Li et al., 2018a] [Li et al., 2019] [Hredzak et al., 2015] [Liu et al., 2016]
	QP	Computation is faster	Derivative information is essential and is complex	Offline application only [He et al., 2020] [Zhang et al., 2017] [Hsu et al., 2016]
	GA	Driver behaviour can be included to improve the solution, derivative-free processing.	Computation is involved, not recommended for multi-objective and non-linear problems	Offline application only [Ziyou et al., 2015] [Li et al., 2017b] [Liu et al., 2015] [Sun et al., 2020]
Optimization-based (Online)	ECMS	Online and real-time implementations	Highly sensitive to driving profiles	Online applications [Blanes et al., 2013] [Sellali et al., 2019b] [Chenghui et al., 2007] [Hussain et al., 2019] [Wang et al., 2019] [Dusmez and Khaligh, 2014]
	MPC	High accuracy online applications, Improved adaptivity and predictivity	Accurate prediction of the driving cycle and highly sensitive to it, The necessity of high accuracy model	Online application [Golchoubian and Azad, 2017] [Lin et al., 2004] [Bernard et al., 2006] [Jiang et al., 2019] [Lin et al., 2010] [He et al., 2013] [Hegazy and Van Mierlo, 2010]
Learning-based	NN	Low computational cost and high adaptivity	Extensive and high-quality training data required	Online application [Alobeidli and Khadkikar, 2018] [Xiong et al., 2018a] [Shen et al., 2020] [Koziel and Yang, 2011] [Zhou et al., 2017]
	RL	Real-time and efficient online control, system modeling is not required	High computational time	Online application [Pei and Leamy, 2013] [Sinoquet et al., 2011] [Fu et al., 2019] [Gomozov et al., 2017] [Sun et al., 2015]

2.5 Identified Research Gaps

After the thorough literature survey, some vital problems are identified which can be rectified and thus improve the overall performance of electric vehicles. The varying driving and environmental conditions affect the BEVs to a large extent by accelerating battery depletion, increasing the chances of battery replacement, and frequent maintenance requirements. From the literature survey, it is observed that the Hybrid source systems in EVs handle such issues of batteries. However, in the hybrid source EMS with battery and SCs, the availability of SC is not ensured by existing strategies in the literature. The battery is forced to handle high (high C-rate) frequency/sudden load currents. Moreover, the higher DC bus voltage fluctuations affect the electric vehicle motor drive efficiency and increase losses. Therefore, it is worth investigating and developing new hybrid source systems, the optimal EMSs, and investigating the techno-economic assessments of EMSs in hybrid source EVs.

2.6 Objectives

The main objective of this research is to develop various models of hybrid sources in electric vehicles and to design and develop optimal energy management strategies. In this regard, the following objectives are set:

1. Allocation of low frequency power demands towards the battery, ensuring maximum utilization of supercapacitor irrespective of driving conditions.
2. Minimization of DC bus voltage fluctuations with varying load current demands in a real driving scenario.
3. Techno-economic assessment that includes performance and economic parameters of proposed Energy management strategy with existing strategies.
4. Implementation of EMS in new hybrid energy vehicle and investigating its major significance and feasibility at different locations.

Chapter 3

Proposed Intelligent Energy Management Strategy for Hybrid Electric Vehicle

Contents

3.1	Introduction	41
3.2	Electric Vehicle Modeling	42
3.2.1	Dynamics of electric vehicle	43
3.3	Proposed Hybrid Source Model	45
3.4	Proposed Energy Management Strategy	52
3.4.1	Technical evaluation	58
3.4.2	Economy evaluation	62
3.5	Simulation Results	63
3.5.1	Impact of PV power	65
3.5.2	Techno-economic analysis	69
3.6	Summary	74

3.1 Introduction

The literature survey in Chapter 2 shows that the optimum power allocation in the hybrid system significantly improves vehicle performance. The EMS controls the system's overall performance with reduced fuel and energy consumption [Vukajlović et al., 2020] [Niu et al., 2022], which improves battery longevity, driving range, Etc. The proposed work focuses on the EMS of the hybrid sources. A combination of Battery, SC, and PV are utilized as Hybrid sources in the proposed HSEV. Table 3.2 shows the parameters of each source, and the details

power-sharing description of each source follows in this section. The overall block diagram is shown in Figure 3.1. EV power demand generation system includes an EV model which derives the load power demand based on varying test driving profiles. The multi-input fully active bidirectional buck-boost converter interconnects the DC bus with Battery, SC, and the DC-DC boost converter connects the Solar PV with an MPPT control algorithm constituting the Hybrid source electric vehicle (HSEV). EMS optimizes the battery's energy consumption by optimizing the energy management in the system, considering the driving and environmental conditions, and is carried out by Fuzzy based absolute energy sharing algorithm (AESAs). The regulation of assigned power from each source is handled by the double loop controllers (inner current and outer voltage). Both EMS and converter controllers combines to form Energy management system (Figure 3.1). Furthermore, the ratings, weight, life, and other technical (Section 3.4.1) and economic (Section 3.4.2) parameters of the battery compared with BEV and existing EMSs.

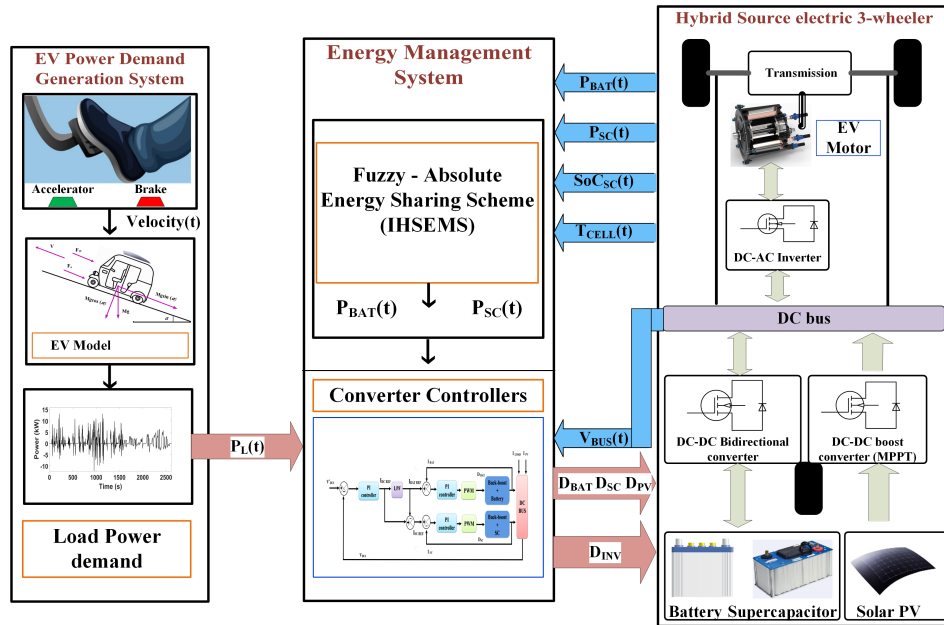


Figure 3.1: Overall block diagram of hybrid source system in electric 3W.

In this chapter, the EV mathematical modeling is detailed, which generates the varying load power demand based on the real-world driving conditions, the proposed hybrid source EV power train with its Intelligent Hybrid Source Energy Management Strategy (IHSEMS) which includes the Absolute Energy Sharing Algorithm (AESAs) is briefly discussed, and a comparative techno-economic assessment is conducted with the simulation result analysis.

3.2 Electric Vehicle Modeling

The driving-related issues which are mainly based on driver behavior, route selections, road type, etc. Further discussions can be more connected once the

relationship between electric vehicles and such aspects is clear. This section discusses the mathematical model of electric vehicles under longitudinal motion. All the resistive forces which oppose the vehicle motion are discussed in detail (included in Appendix A) to implement the EV model, which generates the required power demand.

Table 3.1: Design parameters of electric vehicle.

Sl No	Parameters	Symbols	Values
1	Vehicle category		L5M auto
2	Seating capacity		Driver + 3 seaters
3	Kerb weight	M_0	450 kg
4	Gross weight (with full capacity)	M_T	800 kg
5	Gradeability	α	10°
6	Average velocity	V	40 km/hr
7	Frontal area	A_F	2 m^2
8	Rolling coefficient	f_r	0.01
9	Drag coefficient	C_D	0.5
10	Air density	ρ	1.225 kg/m^3
11	Roof area	A_R	5 m^2
12	Acceleration due to gravity	g	9.81 m/s^2
13	Efficiency of hybrid system (%)	η_{HESS}	95
14	Transmission efficiency (%)	η_T	90
15	Motor drive efficiency (%)	η_M	85

3.2.1 Dynamics of electric vehicle

The longitudinal vehicle motion and its modeling with the dynamic equation is shown in Figure. 3.2. Table 3.1 shows the parameters considered for the electric three-wheeler to calculate load demand [Trovão et al., 2017] [NPTEL:, 2018]. The hybrid source has supplied the required load demand estimated using a dynamic equation. The load demand during traction (P_{L1}) and braking (P_{L2}) intervals are depicted in Eq. 3.1 – 3.2, respectively [Niu et al., 2022]. The P_{LT} (Eq. 3.3) is the total load power demand, includes different resistive forces such as rolling resistance (friction on tire), aerodynamic drag (air resistance on the vehicle), and Grade (opposes the motion during a road slope). These combined forces oppose the vehicle motion during the drive and support it during braking. Moreover, the motor power overcomes the resistive force and accelerates the vehicle with the desired velocity.

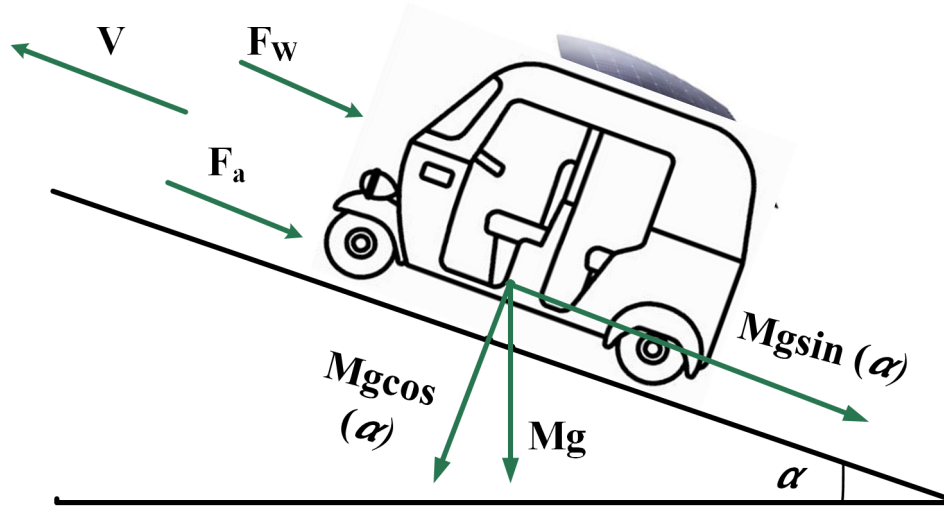


Figure 3.2: Dynamics of electric 3W vehicle.

$$P_{L1} = \frac{(M \cdot g \cdot f_r \cdot \cos(\alpha) + \frac{1}{2} \cdot \rho \cdot A_f \cdot C_D \cdot V^2 + M \cdot g \cdot \sin(\alpha) + \lambda \cdot M \cdot \frac{dV}{dt}) \cdot V}{\eta_{HESS} \cdot \eta_T \cdot \eta_M} \quad (3.1)$$

$$P_{L2} = (M \cdot g \cdot f_r \cdot \cos(\alpha) + \frac{1}{2} \cdot \rho \cdot A_f \cdot C_D \cdot V^2 + M \cdot g \cdot \sin(\alpha) + \lambda \cdot M \cdot \frac{dV}{dt}) \cdot V \cdot \eta_R \quad (3.2)$$

$$P_{LT} = P_{L1} + P_{L2} \quad (3.3)$$

where M is the gross weight of the vehicle, g is the acceleration due to gravity, f_r the rolling resistance coefficient, α the gradeability, ρ the air density, A_f the frontal area of the vehicle, C_D the drag coefficient, V the velocity of the vehicle, λ the rotational inertia constant η_R is the regenerative braking efficiency, η_{HESS} is the hybrid system efficiency, η_T is the transmission efficiency, and η_M is the motor drive efficiency.

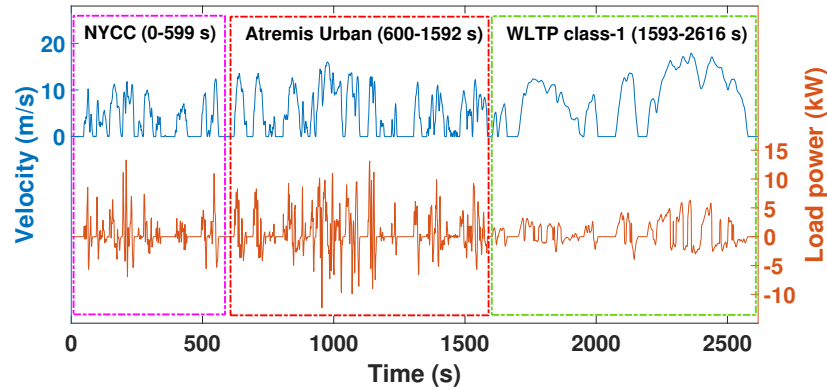


Figure 3.3: Velocity profile of NYCC, Artemis Urban, and WLTP class-1.

Standard driving profiles are employed to mimic the actual driving conditions in the EV model. A combination of three standard driving profiles performs as the best test bench for any EV - NYCC (Newyork city cycle), Artemis Urban, and WLTP-1 (Worldwide Harmonized Light Vehicles Test Procedure). Figure. 3.3 shows the combined driving profiles (CDP), where NYCC and Artemis Urban cycles fluctuate highly, and the WLTP class-1 cycle has fewer fluctuations [USEP-Agency, 2022]. This varying driving condition of CDP highlights the importance of EMS.

3.3 Proposed Hybrid Source Model

The multi-input fully active bidirectional buck-boost converter interconnects the DC bus with Battery, SC, and the DC-DC boost converter connects the Solar PV with an MPPT control algorithm, as shown in Figure. 3.4. EMS optimizes the energy consumption of each source employing AESA and ensure optimal battery operation. Furthermore, the other technical (Section 3.4.1) and economic (Section 3.4.2) parameters of the proposed hybrid source system are compared and analysed with BEVs and existing EMSs.

Table 3.2: Parameters of hybrid sources

Sl no	Components	Parameters	Symbol	Values
1	Lithium-ion battery	Cell type		3.2V, 2.6 Ah, LFP cell
2		Battery capacity	C_B	5.4 kWh
3		Rated voltage	V_B	36 V
4		Specific energy	e_B	151Wh/kg
5		Battery inductance	L_{BAT}	80 μ H
5	Supercapacitor	Module ratings		32 V, 250 F
6		Maximum current	I_{SCmax}	1900 A
7		Specific energy	e_{SC}	3.65 Wh/kg
8		SC inductance	L_{SC}	64 μ H
9		DC bus capacitance	C_{BUS}	23 mF
10	Solar PV	PV array power		965.6 W
11		Voltage at maximum power	V_{PV}	34 V
12		Current at maximum power	I_{PV}	28.4 A
13		Total panel area	A_{PV}	4.8 m ²

Lithium-ion cells are arranged in series and parallel to achieve high energy density and ensure normal battery pack operation. An open circuit voltage (OCV) - internal resistance equivalent circuit battery model is considered in the further analysis [Kouchachvili et al., 2018] [Nguyen et al., 2021]. The equation for battery cells and pack is mentioned in Eq. 3.4, [Pedro et al., 2019]. Lithium-ion batteries are the primary source of the proposed EV. Table 3.2 shows the parameters of

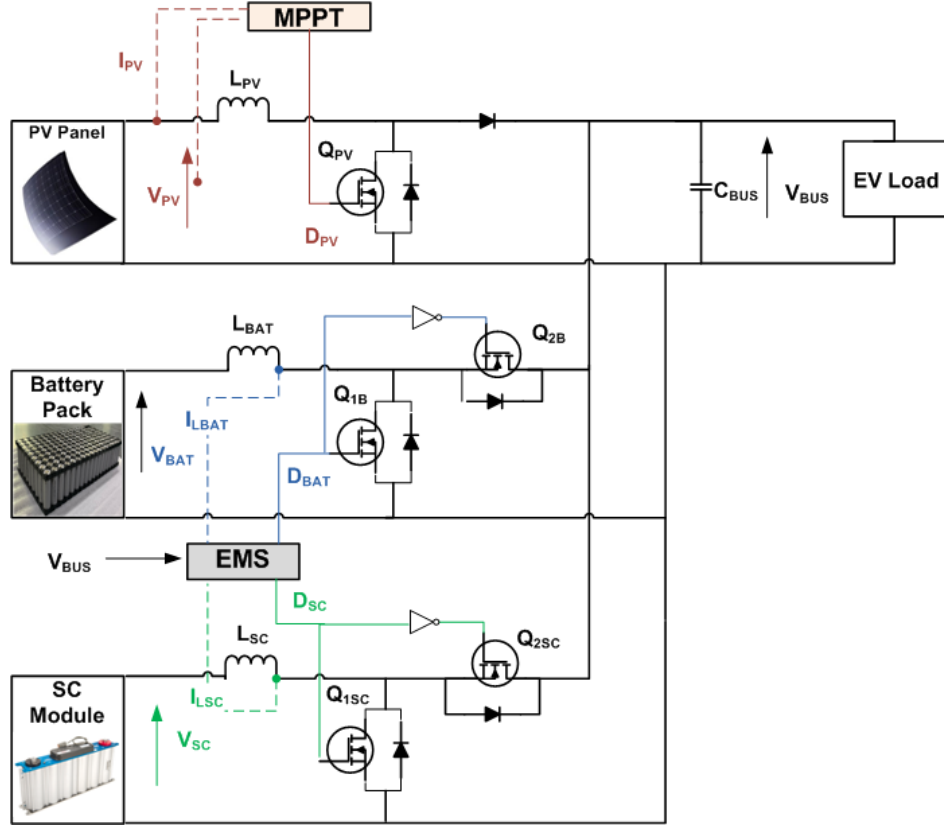


Figure 3.4: Circuit diagram of proposed EMS of hybrid source electric vehicle.

the lithium-ion battery pack. The battery function in the hybrid EV system is to provide a long driving range. Due to their high energy density, batteries can support the vehicle during average power demands.

$$B_C = n_{pBc} \cdot C_{Bc}; R_B = n_{sBc} \cdot R_{Bc} / M_B; V_B = n_{sBc} \cdot V_{Bc} \quad (3.4)$$

where n_{pBc} and n_{sBc} represent the number of batteries cells in parallel and series, B_C and C_{Bc} are the nominal capacity, R_B and R_{Bc} are the internal resistances, v_B and V_{Bc} are the voltage of the battery pack and battery cell respectively.

The high power density of SC plays a significant role in electric vehicle applications. SC module is designed mainly to reduce the stress of the primary source in the hybrid system (i.e., battery) by handling the sudden peak power demands and absorbing the regenerative braking energy. The proposed work combines a 12-series configuration of MAXWELL 3000F, 2.7 V cell to form the SC module. The parameters of the SC module are related to the SC cells as mentioned in Eq. 3.5, [Sun et al., 2017]. The behavior of the SC pack can be represented by a first-order electrical element, which constitutes an open-circuit voltage (OCV), internal resistance (R_{Sc}), and capacitance (C_{Sc}). The capacitance in parallel with an internal resistance represents leakage of SC model [Mellincovsky et al., 2014] [Raman et al., 2021]. Parameters of SC are shown in Table 3.2. Due to the long life cycle (1,000,000 cycles), the degradation of SC is considered to be very low in the analysis. [Vukajlović et al., 2020].

$$C_{SC} = n_{pSC} \cdot C_{Sc} / n_{sSC}; R_{SC} = n_{sSC} \cdot R_{Sc} / n_{pSC}; V_{SC} = n_{sSC} \cdot V_{Sc} \quad (3.5)$$

where n_{pSC} and n_{sSC} represent the number of SC cells in parallel and series, C_{SC} and C_{Sc} are the nominal capacity, V_{SC} and V_{Sc} are the nominal voltage and R_{SC} and R_{Sc} are the internal resistances of the SC module and SC cell respectively.

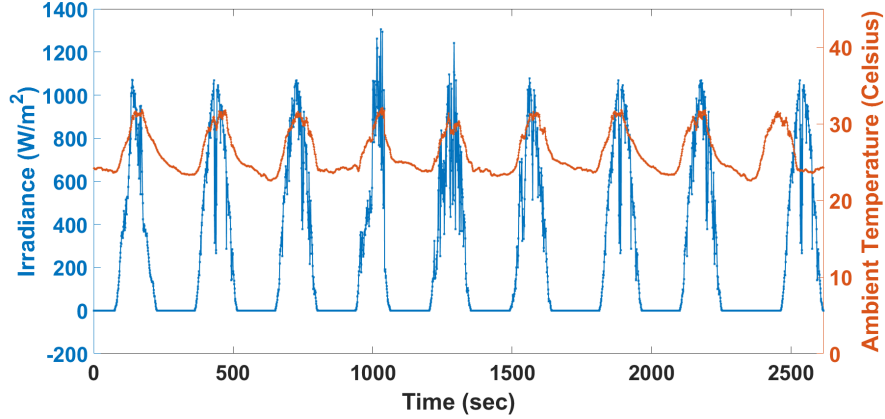


Figure 3.5: Irradiance (blue), ambient temperature (red)(March).

Figure. 3.5 shows the high fluctuating irradiance and ambient temperature environmental conditions to exhibit the system's response. Solar energy is highly recommended for electric vehicles to improve energy efficiency. Photovoltaic (PV) panels are employed to trap the solar energy. A PV array is a group of PV modules connected in series and parallel. Table 3.2 shows the parameters of PV panels employed in this work. The area of solar panels is selected based on the vehicle roof area as listed in Table 3.1 [Sunrunmotors, 2022]. The Maximum Power Point Tracking (MPPT) algorithm extracts maximum power during irradiance and temperature fluctuation. PV supports the primary source battery to meet the required energy demand which improves the energy efficiency. The output current of the PV module is depicted in Eq 3.6. The PV peak power and load energy calculations of the HSEV are as follows in Eq.(3.7) [Solar, 2020]. The impact of PV power is reflected in BEC_M (Eq.3.7), which shows the reduction in battery energy consumption per month with the inclusion of PV panels over the vehicle.

$$I_{PV} = n_p \cdot I_{PH} - n_p \cdot I_{RS} \cdot \left[\exp \left(\frac{V_{PV} + I_{PV} \cdot R_S}{V_{TH} \cdot n_s} \right) - 1 \right] - \frac{(V_{PV} + I_{PV} \cdot R_S)}{R_{SH}} \quad (3.6)$$

where V_{PV} and I_{PV} represent the output PV voltage and current of the module, n_p and n_s are the number of parallel and series connected panels. I_{PH} is the photo-current, I_{RS} is the module reverse saturation current, V_{TH} is the diode thermal voltage and R_S , R_{SH} are the series and shunt resistance respectively.

$$W_P = \frac{I_r \cdot A \cdot \eta_{PV}}{100}; LEC_{Day} = EC_{Dc} \cdot N_{Dc}; BEC_M = TEC_M - E_{PVM} \quad (3.7)$$

where W_P is the Installed peak PV panel power, η_{PV} is the PV conversion efficiency. LEC_{Day} represents the Load energy consumption per day, EC_{Dc} is the energy consumption per driving cycle, N_{Dc} is the number of driving cycles needed to complete the total expected drive per day. BEC_M , TEC_M , and E_{PVM} are the battery energy consumption, total energy consumption, and PV energy consumption per month, respectively.

MPPT algorithm maximizes the power by modifying the duty cycles of switches in the DC-DC converter to achieve maximum power points at each irradiance levels. Various algorithms are already existing. In proposed system a Perturb and Observe (P&O) MPPT algorithm is used to generate the switching pulses for PV boost converter [Zineb et al., 2021]. The flow chart of the P & O algorithm are shown in figure 3.6 where the duty ratio, D keeps varied at difference is present P(k) and previous output power (P(k-1)). Voltage and current of PV boost converter is monitored and the algorithm is developed based on algorithm in 3.6 and the equation 3.8.

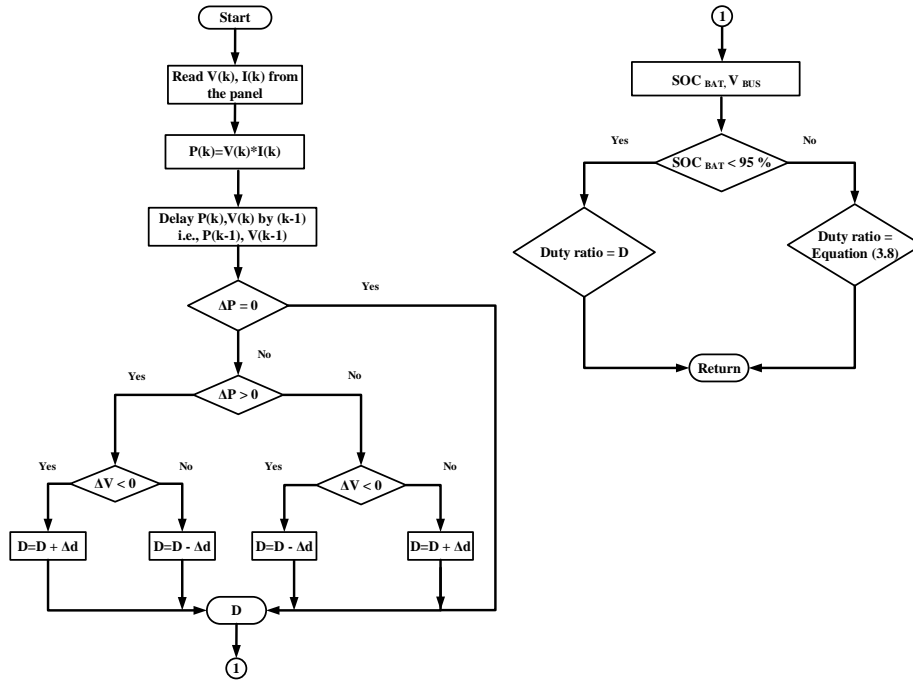


Figure 3.6: Perturb and Observe (P & O) MPPT algorithm.

$$Duty\ ratio = (V_{BUSREF} - V_{BUSREF}) \cdot (K_{Ppv} + \frac{K_{Ipv}}{s}) \quad (3.8)$$

where K_{Ppv} and K_{Ipv} are the proportional and integral gains for the PV duty ratio controller, Δd is the perturbation step-size.

The modes of operations of each converters of respective sources in figure 3.4 are detailed with their equations in the section. The battery side buck-boost converter operates in two modes, namely battery discharge, and charge modes. The discharge mode of the converter is the boost converter operation. Switch Q_{1B} , Q_{2B} are controlled with the PWM signals derived from the EMS of the system based on the fluctuations in load current and SoC of the battery. Table 3.2, and Table 3.3 shows the design parameters of battery and respective DC-DC converter. The discharge mode model of the battery side converter circuit is derived as Equation 3.9.

$$\frac{di_{BAT}}{dt} = \frac{-R_{BAT}}{L_{BAT}}.i_{BAT} + \frac{1}{L_{BAT}}.V_{BAT} - \frac{(1 - D_{1B})}{L_{BAT}}.V_{DC} \quad (3.9)$$

where R_{BAT} and L_{BAT} are converter resistance and inductance, D_{1B} is the duty cycle of switch Q_{1B} , V_{BAT} , I_{BAT} are the battery voltage and current. Charge mode of battery side converter operation is expressed with Equation 3.10.

$$\frac{di_{BAT}}{dt} = \frac{-R_{BAT}}{L_{BAT}}.i_{BAT} + \frac{1}{L_{BAT}}.V_{BAT} - \frac{(D_3)}{L_{BAT}}.V_{DC} \quad (3.10)$$

where D_{2B} is the duty cycle of switch Q_{2B} , combination of both the modes of battery operation can be expressed as:

$$\frac{di_{BAT}}{dt} = \frac{-R_{BAT}}{L_{BAT}}.i_{BAT} + \frac{1}{L_{BAT}}.V_{BAT} - \frac{(D_{23})}{L_{BAT}}.V_{DC} \quad (3.11)$$

where

$$D_{12B} = \begin{cases} 1 - D_{1B}, & \text{if Discharge mode} \\ D_{2B}, & \text{Charge mode} \end{cases}$$

Supercapacitor side DC-DC buck-boost converter also undergoes in two modes of operation similar to battery side converter. Proposed EMS controls the switch Q_{1SC} and Q_{2SC} considering the charge levels of SC and load current. Table 3.2 and Table 3.3 shows the design parameters of SC and respective DC-DC converter. Discharge and charge modes of operations can be combined into a single equation 3.12, which is equivalent to Equation 3.11 of battery side converter.

$$\frac{di_{SC}}{dt} = \frac{-R_{SC}}{L_{SC}}.i_{SC} + \frac{1}{L_{SC}}.V_{SC} - \frac{(D_{12SC})}{L_{SC}}.V_{DC} \quad (3.12)$$

where R_{SC} and L_{SC} are converter resistance and inductance, V_{SC} , I_{SC} are the supercapacitor voltage and current. D_{12SC} is the duty cycle combination of both the switches Q_{1SC} and Q_{2SC} .

$$D_{12SC} = \begin{cases} 1 - D_{1SC}, & \text{if Discharge mode} \\ D_{2SC}, & \text{Charge mode} \end{cases}$$

PV power is fluctuating and needs to be maintained at its maximum power for higher energy efficiency. This is achieved by a DC-DC boost converter with an MPPT algorithm. V_{PV} , I_{PV} are the PV panel voltage and current. D_{PV} is the duty cycle derived from the perturb and observe MPPT algorithm to control the boost converter. Two states of the boost operation can be evaluated (Q_{PV} ON and Q_{PV} OFF intervals). Table 3.2 and Table 3.3 shows the design parameters of PV and MPPT boost converter. The average model of the PV side DC-DC boost converter is shown by Equation 3.13.

$$\frac{di_{PV}}{dt} = \frac{-R_{PV}}{L_{PV}} \cdot i_{PV} + \frac{1}{L_{PV}} \cdot V_{PV} - \frac{(1 - D_{PV})}{L_{PV}} \cdot V_{DC} \quad (3.13)$$

Battery, super capacitor and PV sources are explained with their characters, advantages and mathematical equations in previous section. Converters design plays a crucial role in managing the power between the sources. The design of DC-DC converters for respective sources are explained below.

Design of battery side buck-boost converter

Inductor ripple current, $\Delta i_L = 10\%$ (I_L)

Considering $V_{in} = 40$ V

$$D_{40V} = V_{out} / (V_{in} + V_{out}) = 0.545$$

$$\text{Average inductor current, } I_L = (V_{out} \cdot I_{out}) / V_{in} = 270 \text{ A}$$

$$\Delta i_L = 10\% (I_L) = 0.1(270) = 27 \text{ A}$$

$$L_{40} = V_{in} \cdot D_{40V} / (\Delta i_L \cdot F_s) = 80.74 \text{ } \mu\text{H}$$

Similarly, $D_{24V} = 0.67$

$$I_L = 450 \text{ A}$$

$$\Delta i_L = 45 \text{ A}$$

$$L_{24} = 35.73 \text{ } \mu\text{H}$$

$L_{BAT} = 80 \text{ } \mu\text{H}$ to satisfy whole range of inputs.

Design of Supercapacitor side buck-boost converter

Inductor ripple current, $\Delta i_L = 7\%$ (I_L)

Considering $V_{in} = 32$ V

$$D_{32V} = V_{out} / (V_{in} + V_{out}) = 0.6$$

$$\text{Average inductor current, } I_L = (V_{out} \cdot I_{out}) / V_{in} = 438 \text{ A}$$

Table 3.3: Converter design parameters of hybrid sources

Sl no	Components	Parameter	Symbol	Values
Lithium-ion battery				
1		Input voltage	V_{in}	24 V – 40 V
2		Output voltage	V_{out}	48 V
3		Output current	I_{out}	225 A
4		Switching frequency	F_s	10 KHz
Supercapacitor				
6		Input voltage	V_{in}	16 V – 32 V
7		Output voltage	V_{out}	48 V
8		Output current	I_{out}	292 A
9		Switching frequency	F_s	10 KHz
Solar PV				
11		Input voltage	V_{in}	34 V
12		Output voltage	V_{out}	48 V
13		Output current	I_{out}	20.11 A
14		Switching frequency	F_s	5 KHz

$$\Delta i_L = 7 \% (I_L) = 0.07 (438) = 30 \text{ A}$$

$$L_{32} = V_{in} \cdot D_{40V} / (\Delta i_L \cdot F_s) = 64 \text{ } \mu\text{H}$$

$$\text{Similarly, } D_{16V} = 0.75$$

$$I_L = 876 \text{ A}$$

$$\Delta i_L = 61.32 \text{ A}$$

$$L_{24} = 19.56 \text{ } \mu\text{H}$$

$$L_{SC} = 64 \text{ } \mu\text{H to satisfy whole range of inputs.}$$

$$\text{Output voltage ripple, } \Delta V_{out} / V_{out} = 2 \%$$

$$C_{BUS} = (D_{max}) / (R \cdot (\Delta V_{out} / V_{out}) \cdot F_s) = 0.75 / (0.16 \cdot 0.02 \cdot 10000) = 23.43 \text{ mF}$$

Design of Solar PV side boost converter

$$\text{Inductor ripple current, } \Delta i_L = 20 \% (I_L)$$

$$\text{Considering } V_{in} = 34\text{V}$$

$$D_{PV} = 1 - (V_{in} / V_{out}) = 0.291$$

$$\text{Average inductor current, } I_L = (V_{out} \cdot I_{out}) / V_{in} = 28.40 \text{ A}$$

$$\Delta i_L = 20 \% (I_L) = 0.2(28.40) = 5.68 \text{ A}$$

$$L_{PV} = V_{in} \cdot D_{PV} / (\Delta i_L \cdot F_s) = 348 \text{ } \mu\text{H}$$

$$L_{PV} \text{ is } 352 \text{ } \mu\text{H to satisfy whole range of inputs.}$$

$$\text{Output voltage ripple, } \Delta V_{out} / V_{out} = 2 \%$$

$$C_{BUS} = (D_{max}) / (R \cdot (\Delta V_{out} / V_{out}) \cdot F_s) = 0.5 / (2.38 \cdot 0.02 \cdot 5000) = 2.1 \text{ mF}$$

3.4 Proposed Energy Management Strategy

This section examines the challenges in several EMSs approaches. A hybrid source system follows the deterministic rule-based strategy for easiness in real-time operation, which limits the source performance [Wang et al., 2022]. The vehicle needs an adaptive and flexible control strategy under varying driving conditions. If EMS does not consider the driving profile and source parameters into account may lead to an unstable system. This affects the battery's performance and life as mentioned in Section 3.4.1 on technical and 3.4.2 on economic aspects. The two standard EMSs, 1) SMC [S. Njoya Motapon and Al-Haddad, 2014] and 2) FDS [Cabrane et al., 2020], have been considered to illustrate the significance of the proposed EMS. The SMC includes eight states to control energy management using hysteresis switching, which delays the system's response during sudden load changes [S. Njoya Motapon and Al-Haddad, 2014]. The FDS performs the energy management by providing low-frequency load demands to the battery and high frequency to SC using a fixed frequency low pass filter, which reduces adaptivity and flexibility during varying driving conditions [Cabrane et al., 2020]. A more detailed comparison of EMSs has been given in Section 4.4.4.

The proposed EMS ensures each source's effective utilization by considering the impact of varying driving conditions. The energy generated from each source is used in the algorithm and allocated in an optimal ratio to meet load power demand. The main optimization parameter is the absolute energy of low and high-frequency components. Present research highlights the significance of the proposed absolute energy sharing scheme (as in Eq. 3.18-3.19). The variation in low and high-frequency absolute energy is monitored throughout the driving cycle. The control algorithm is assigned to modify the energy management ratio between the sources by optimizing the source absolute energies. An intelligent fuzzy logic strategy enables absolute energy sharing of sources as membership functions, therefore, named an Intelligent Hybrid Source Energy Management System (IHSEMS). The function of the proposed EMS is not limited to hybrid source energy management, moreover maintains SC_{SOC} , as mentioned in Section 3.5.2.1. The proposed EMS improves the EV's long-term economy by providing SC throughout the driving cycle and reducing battery capacity losses and stress.

The fuzzy control strategy makes the control process more realistic, especially suitable for controlling nonlinear systems [Wang et al., 2022]. An intelligent fuzzy logic control strategy improves the battery's range, performance, safety, and life cycle. The proposed control strategy focuses on monitoring the charging levels (source conditions), load current fluctuations (driving conditions), maximum current (C-rate), and Irradiance (environmental conditions) and outcomes an optimum cut-off frequency for the lowpass filter to ensure an effective power-sharing strategy. In EV, the load current is continuously varying. Fuzzy logic works to split the combined power P_C between the battery and SC while changing the

cut-off frequencies. The fuzzy system consists of four inputs and one output parameter, the Low-frequency absolute energy ($Abs E_{LF}$), High-frequency absolute energy ($Abs E_{HF}$), SC state of charge (SC_{SOC}), Battery cell temperature (T_C) and the cut-off frequency (F_{CUTOFF}), respectively. Further, the above fuzzy parameters are defined into three membership functions: Low, Medium, and High, as shown in the Figure. 3.7.

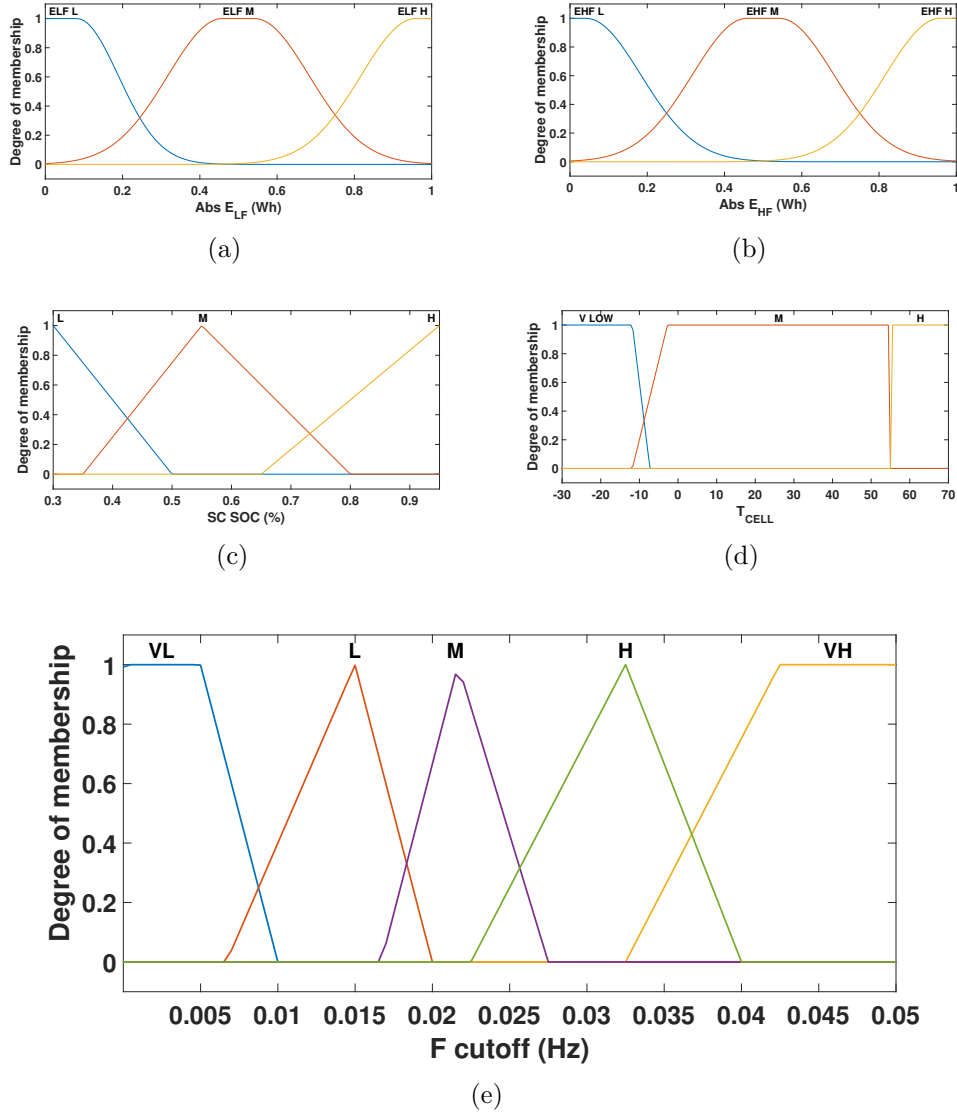


Figure 3.7: Input and output membership functions of fuzzy controller (a) Absolute low frequency energy (b) Absolute high frequency energy (c) SC SOC (d) Battery cell temperature (e) Cut-off frequency of LPF

IHSEMS allocates the load power among each source based on various driving conditions. Eq. (3.14) explains the total power the hybrid sources handle.

$$P_T = P_B + P_{SC} + P_{PV} = P_C + P_{PV} = P_{LT} \quad (3.14)$$

where P_T is the total power from hybrid sources. P_B , P_{SC} , and P_{PV} are battery, SC, and PV power, respectively. P_C is the combined power of the battery and SC. Eq. (3.15) shows the battery's and SC's combined power.

$$P_C = P_B + P_{SC} = P_{LT} - P_{PV} \quad (3.15)$$

The adaptive low pass filter (LPF) separates the load fluctuations into low and high reference currents. The battery and SC handle low (steady-state) and high (transient) frequency load current, respectively, as mentioned in Eq. (3.16). The total current supplied from hybrid sources is mentioned in Eq. (3.17).

$$I_{LF} = I_C \cdot \frac{(2 \cdot \pi \cdot f_c)}{(s + 2 \cdot \pi \cdot f_c)}; I_{HF} = I_C - I_{LF} \quad (3.16)$$

$$I_T = I_{LF} + I_{HF} + I_{PV} \quad (3.17)$$

where, I_{LF} , I_{HF} are low frequency and high-frequency current, f_c is the cut-off frequency of LPF. I_C is the total current demand. I_T is the sum of current from the battery, SC, and PV to meet the load current. Eq. (3.18) explains the absolute energy of low and high-frequency currents. $Abs(E_{LF})$ and $Abs(E_{HF})$ are the absolute energy generated by the battery and SC, respectively. A fuzzy controller limits the cut-off frequency, to satisfy an effective absolute energy-sharing between the sources. This sustains SC's participation (SC handles the high-frequency power) during sudden peaks, fluctuating power, and regenerative braking energy intervals. The absolute energy of the high-frequency component is higher than the low-frequency components of the load power Eq. (3.19). The flowchart of the absolute energy sharing algorithm (AESAs) is explained in Figure 3.8, where the cut-off frequency optimizes the energy sharing among each source, considering the fluctuations in driving and source conditions.

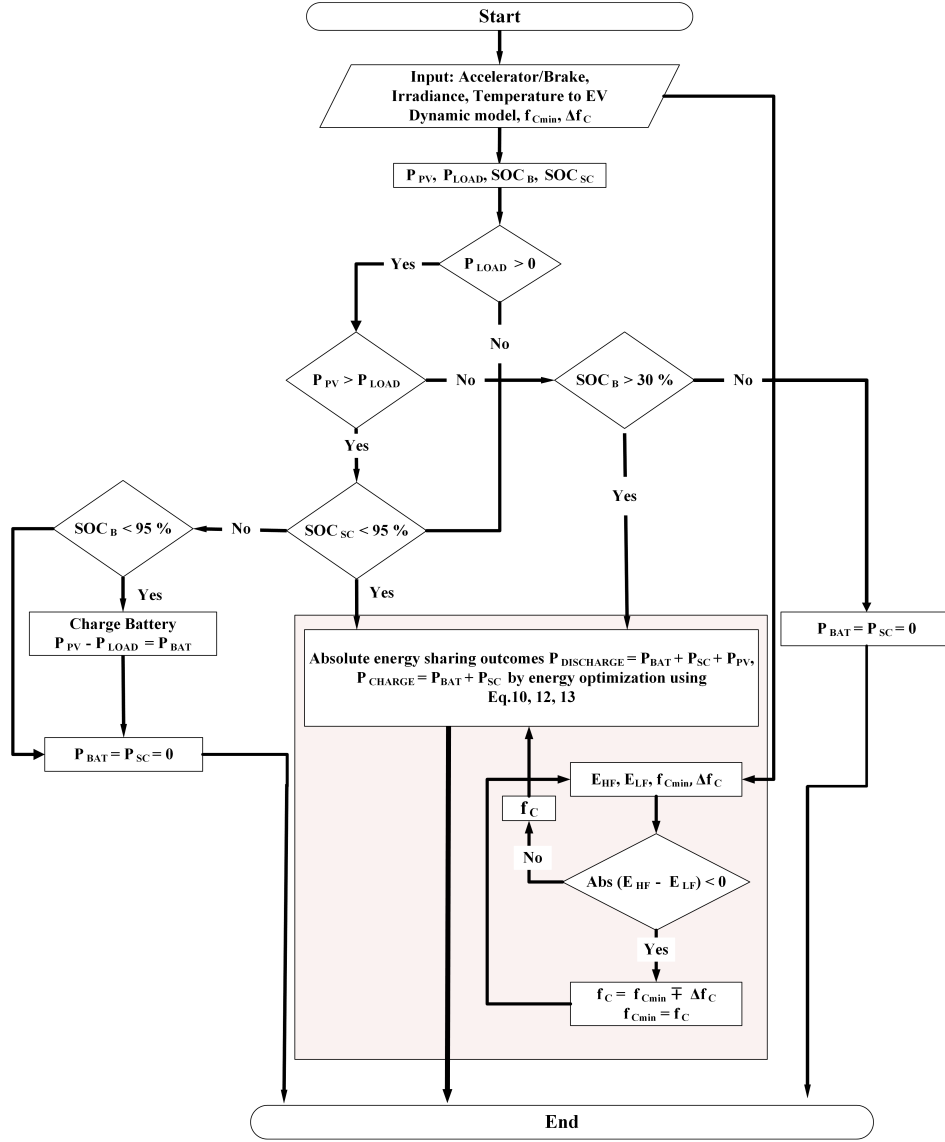


Figure 3.8: Flowchart of absolute energy sharing algorithm.

$$Abs(E_{LF}) = Abs\left(\int (P_{LF})dt\right); Abs(E_{HF}) = Abs\left(\int (P_{HF})dt\right) \quad (3.18)$$

$$Abs(E_{HF}) - Abs(E_{LF}) > 0 \quad (3.19)$$

where, P_{LF} and P_{HF} are the low and high-frequency load power components.

As shown in Figure 3.1, the controller consists of the outer voltage and inner current control loop for the battery and SC, which satisfies the battery's and SC's dynamics. The inner SC current loop operates faster than the outer voltage control loop to ensure the stability of the overall control system [Cabrane et al., 2020]. The outer voltage loop operates to stabilize constant DC bus voltage [P K Singha

et al., 2021]. IHSEMS generates the reference power for each source and utilizes a controller to generate the switching pulses required for the DC-DC converters. Thus IHSEMS ensures efficient power flow respective to absolute energy sharing. The PI controllers of each loop provide the desired phase margin at the required bandwidth for ensuring system stability based on frequency domain specifications [Cabrane et al., 2020]. The small-signal modelling (SSM) of the converter system generates PI values of each controller loop using the MATLAB SISO tool [Erickson and Maksimovic, 2007]. PI controllers reduce the error of reference versus actual source current. PWM derives the duty ratio for converters and generates the switching pulses for each converter D_{BAT} and D_{SC} .

The double loop voltage (outer) and current (inner) loop controller is designed for controlling the full active bidirectional buck-boost converter for both Battery and SC. The voltage controller maintains or stabilize the bus voltage at the DC bus. The inner current loop for both battery and SC regulates the actual currents to match the reference currents designed by the proposed EMS. The controller is designed based on the converter transfer functions which are derived using state space averaging techniques.

Voltage control transfer function (G_{vdx}) for the converter is designed as:

$$G_{vdx} = \frac{v_{ox}(s)}{d_x(s)} = \frac{(1 - D_x) \cdot V_O - I_{Lx} \cdot L_x \cdot s}{L_x \cdot C_{ox} \cdot s^2 + \frac{L_x}{R_L} \cdot s + (1 - D_x)^2} \quad (3.20)$$

The current control transfer function (G_{idx}) of the converter is designed as:

$$G_{idx} = \frac{i_{Lx}(s)}{d_x(s)} = \frac{C_{ox} \cdot V_O \cdot s + 2 \cdot (1 - D_x) \cdot I_{Lx}}{L_x \cdot C_{ox} \cdot s^2 + \frac{L_x}{R_L} \cdot s + (1 - D_x)^2} \quad (3.21)$$

Output impedance transfer function (G_{vix}) of the converter is designed as:

$$G_{vix} = \frac{v_{ox}(s)}{i_{Lx}(s)} = \frac{(1 - D_x) \cdot V_O - I_{Lx} \cdot L_x \cdot s}{C_{ox} \cdot V_O \cdot s + 2 \cdot (1 - D_x) \cdot I_{Lx}} \quad (3.22)$$

The controller block diagram is shown in figure 3.9. An accurate SSM model is essential for the controller design. An inner battery current loop with slower dynamics and a SC inner current loop with fast dynamics. The outer voltage loop is to stabilize the DC bus voltage constant. These criteria are considered in order to achieve a stable system operation and better transient response at various operating points. The controller parameter design is performed using MATLAB/SISO tool based on the frequency domain specifications. The bandwidth and phase

margin of each loop are selected based on that criteria to achieve a stable system and the design consideration with the PI gains for each loop are as shown in Table 3.4.

Inner current loop of battery controls the charge-discharge currents of battery side converter. Bandwidth of battery loop is selected lower than SC loop to considering the response characteristics of battery. Open loop transfer function of battery inner current loop is utilized to determine the compensation parameters. BW of 1.1 KHz at a phase margin of 60 degree is selected to determine the PI control parameters. Open loop and closed loop transfer function of SC inner current loop is as shown below. SSM representation with the transfer functions of the battery control loop is shown in figure 3.9. The input current controller equations ($G_{i_b D_B}$) are derived from Equation 3.21 and are shown as below:

$$G_{i_b D_B} = \frac{i_{LBAT}(s)}{d_{BAT}(s)} = \frac{(C_{BUS}) \cdot V_{BUS} \cdot s + 2 \cdot (1 - D_{BAT}) \cdot I_{LBAT}}{L_{BAT} \cdot C \cdot s^2 + \frac{L_{BAT}}{R} \cdot s + (1 - D_{BAT})^2} \quad (3.23)$$

Supercapacitor inner current control loop stabilizes the charging and discharging of SC considering the stable system operation. Bandwidth of SC loop is selected higher than other loops to ensure the immediate response of the control loop towards the system stability. Open loop transfer function of SC inner current loop is utilized to determine the compensation parameters. BW of 1.7 KHz at a phase margin of 60 degree is selected to determine the PI control parameters. Open loop and closed transfer function of SC inner current loop is as shown below. SSM representation with the transfer functions of the SC control loop is shown in figure 3.9. The input current controller equations ($G_{i_{SC} D_{SC}}$) are derived from Equation 3.21 and are shown as below:

$$G_{i_{SC} D_{SC}} = \frac{i_{LSC}(s)}{d_{SC}(s)} = \frac{(C_{BUS}) \cdot V_O \cdot s + 2 \cdot (1 - D_{SC}) \cdot I_{LSC}}{L_{SC} \cdot C \cdot s^2 + \frac{L_{SC}}{R} \cdot s + (1 - D_{SC})^2} \quad (3.24)$$

Bandwidth of outer voltage loop is lower than other loops to ensure the response of the system during sudden load changes. Open loop transfer function of outer voltage loop is utilized to determine its compensation parameters. BW of 100 Hz at a phase margin of 60 degree is selected to determine the PI control parameters. Open loop transfer function of outer voltage loop is as shown below. SSM representation with the transfer functions of outer control loop is shown in figure 3.9. The outer voltage loop controller generates the input reference current and EMS processes it to derive the battery and SC reference currents. The outer voltage controller loop equations (G_{vi}) are derived from Equation 3.22 and are shown as below:

$$G_{vi} = \frac{v_{BUS}(s)}{i_{BUS}(s)} = \frac{(1 - D_{SC}) \cdot V_O - I_{LSC} \cdot L_{SC} \cdot s}{C_{BUS} \cdot V_O \cdot s + 2 \cdot (1 - D_{BUS}) \cdot I_{LSC}} \quad (3.25)$$

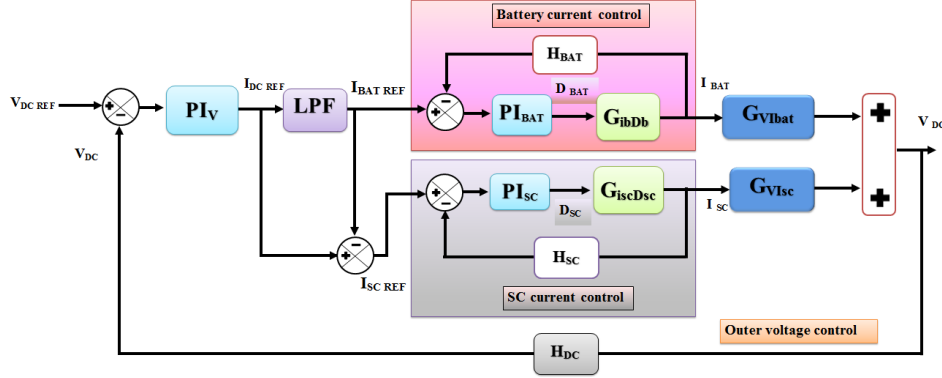


Figure 3.9: System controller block diagram.

Table 3.4: Controller parameters and specifications of hybrid source system.

Sl No	Parameters	Symbols	Values
1	SC inductance	L_{SC}	64 μ H
2	Bandwidth of inner current SC loop	BW_{SC}	10700 rad/sec
3	Phase margin of inner current SC loop	PM_{SC}	60 $^\circ$
4	Controller gains of SC current loop		$K_P = 0.013, K_I = 61.5$
5	Battery inductance	L_{BAT}	80 μ H
6	Bandwidth of inner current Battery loop	BW_{BAT}	6900 rad/sec
7	Phase margin of inner current Battery loop	PM_{BAT}	60 $^\circ$
8	Controller gains of Battery current loop		$K_P = 0.0098, K_I = 25.7$
9	DC bus capacitance	C_{BUS}	23 mF
10	Bandwidth of outer voltage loop	BW_V	630 rad/sec
11	Phase margin of outer voltage loop	PM_V	64.80 $^\circ$
12	Controller gains of outer voltage loop		$K_P = 12, K_I = 5380$

3.4.1 Technical evaluation

- (a) Battery peak power reduction (B_{PPR}) : The peak battery power demand (B_P) increases the battery C-rates (I_B/C_B) and reduces the life (Eq. 3.34) [Pedro et al., 2019] [Niu et al., 2022]. The percentage reduction in battery peak power is expressed as follows:

$$B_{PPR} (\%) = \frac{(B_P - B_{PEMS})}{B_P} \cdot 100 \quad (3.26)$$

where B_{PEMS} is the peak battery power with hybrid EMS. The EMS ensures optimal battery operation to enhance the longevity of the battery cells. Battery downsizing (reduction in battery size) can be possible by reducing the peak power demand by employing the suitable EMS [Samad et al., 2015].

- (b) Battery capacity reduction (B_{CR}) : Describes the percentage reduction in

battery capacity (B_C) [Samad et al., 2015].

$$B_{CR} (\%) = \left(\frac{B_C - B_{CEMS}}{B_C} \right) \cdot 100 \quad (3.27)$$

where B_{CEMS} is the battery capacity of Hybrid EMS. Reduction in battery capacity could be achieved by utilizing SC and PV as hybrid sources in HSEV to share the power demand.

- (c) Battery di/dt reduction (B_{IR}) : Rate of change of battery current (di/dt) and the percentage reduction are expressed in Eq. (3.28) and (3.29), respectively, which determines the stress on the battery.

$$di/dt (A/s) = \frac{I_{max} - I_{min}}{t_{max} - t_{min}} \quad (3.28)$$

$$B_{IR} (\%) = \left(\frac{di/dt_{BEV} - di/dt_{EMS}}{di/dt_{BEV}} \right) \cdot 100 \quad (3.29)$$

where I_{max} and I_{min} are the maximum and minimum battery current. T_{max} and T_{min} are the respective time instants of maximum and minimum battery current. di/dt_{BEV} and di/dt_{EMS} are the di/dt ratio of BEV and EMS, respectively. Battery internal stress directly depends on the C-rates, and the battery's current fluctuation rate [Rui et al., 2020]. Higher and sudden variations in battery current cause the development of Li^+ concentration more non-uniform and steeper gradients in the film [Jangid et al., 2019].

- (d) Battery RMS current reduction (B_{RIR}) : Battery RMS current reduction % can be calculated using Equation (3.30) and its reduction extends the battery life [Demircali and Koroglu, 2022]. RMS current is a vital factor that affects battery life and gives a rough estimation of the battery ohmic losses [Hussain et al., 2019]. The system's overall losses and efficiency highly depend on the RMS current. B_{RIR} by employing the suitable hybrid source in EV decelerates battery capacity degradation.

$$B_{RIR}(\%) = \left(\frac{B_{RI} - B_{RIEMS}}{B_{RI}} \right) \cdot 100 \quad (3.30)$$

where B_{RIR} is the battery RMS current reduction percentage, B_{RI} is the battery RMS current and B_{RIEMS} is the battery RMS current with EMS.

- (e) Battery capacity loss (B_{CL}) : Instantaneous battery capacity loss, the battery capacity loss, and the total capacity losses are evaluated from with Eq. (3.31), (3.32), and (3.33), respectively, [Song et al., 2018], [Niu et al., 2022].

$$B_{\delta Q_{loss}(k)} = 9.78x10^{-4} \cdot \left(\frac{Abs(I_{B,k}) \cdot T_s \cdot \exp\left(\frac{-15162+1516 \cdot C_{rate,k}}{(0.849 \cdot R \cdot T)}\right) \cdot Q_{loss,(k-1)}^{-0.1779}}{3600} \right) \quad (3.31)$$

$$B_{Q_{loss}} = F(C_{rrate} \cdot T \cdot A_h \cdot N \cdot DOD) = B(C_{rate}) \cdot \exp\left(\frac{-E_a(C_{rate})}{(R \cdot T)}\right) \cdot (A_h(N))^z \quad (3.32)$$

$$B_{Q_{loss}(k)} = 0.0032 \cdot \exp\left(\frac{-15162 + 1516 \cdot C_{rate}(k)}{R \cdot (T + 273)}\right) \cdot A_h(k)^z; \quad (3.33)$$

where I_B is the battery current, T_s is the sampling interval, $B_{\delta Q_{loss}}$ is the instantaneous battery capacity loss, $B_{Q_{loss}}$ is the battery capacity loss, R is the gas constant (J/mol K), T is the absolute temperature (K), A_h is the Ah-throughput, z is the power-law factor (0.828), C_{rate} the battery charge/discharge rate, DOD is the battery depth of discharge.

The capacity loss of a lithium-ion battery determines the life of the battery. Reduction in capacity from the initial capacity (100%) must be less than 20 % to achieve optimal battery operation for EV applications. A battery's end of life (EOL) is reached whenever the battery capacity reaches less than 80 % of its initial capacity [key,]. Arrhenius degradation model depicts the battery degradation [John et al., 2011]. The model explains how the battery temperature, Depth of Discharge (DOD), Current rate C_{rate} , RMS current and BIR (di/dt) highly deteriorate the battery life and increases the BDC Eq. (3.40) [Demircali and Koroglu, 2022] [Pedro et al., 2019].

- (f) Battery lifespan(B_{LS}) : The significant impact on battery life is due to the battery capacity loss, as expressed in Eq. (3.34) for a lithium-ion battery [Niu et al., 2022].

$$B_{LS} = \left(\frac{20\%}{Q_{lossD} \cdot D_{day} \cdot 365} \right) \quad (3.34)$$

where Q_{lossD} is the capacity loss at each distance, D_{day} is the average traveled distance per day. The highly fluctuating NYCC cycle was selected to analyze extreme battery degradation and life. However, the present analysis thoroughly studies EV battery LS for different hybrid EMSs versus BEVs under uniform environmental conditions. In a Li-ion battery, the capacity loss exceeds 20%, or the capacity goes below 80% of the nominal capacity is unsuitable for EV application. Battery lifespan improvement (BLSI) derives the battery life extension for the hybrid EMS compared to BEV.

- (g) DC bus voltage fluctuations(DC_{BVF}) : Eq.(3.35) expresses the percentage variation of the peak-to-peak DC bus voltage fluctuation [P K Singha et al., 2021] as follows:

$$DC_{BVF} (\%) = \left(\frac{V_{max} - V_{min}}{V_{bus}} \right).100 \quad (3.35)$$

where V_{bus} is the DC bus voltage. V_{max} and V_{min} are the maximum and minimum DC bus voltage. The difference gives the peak-to-peak value of the bus voltage. DC bus voltage fluctuations have severe impacts on the EV motor performance [Wen et al., 2012]. The difference between the maximum and minimum DC bus voltage gives the peak-to-peak value of the bus voltage. DC-DC converter with optimal EMS ensures a stabilized DC bus voltage.

- (h) Optimum battery size (B_{OS}) : The battery size provides a standard driving range to run a vehicle without PV irradiance for a day. The n_{sBc} and n_{pBc} are selected as 10 and 58, respectively, to meet the required average power demand and nominal voltage.

$$B_{OS}, n_{sBc}.n_{pBc} >= \frac{(\rho.A_f.C_D.V^2 + 2.M.g.f_r).D}{2.\eta_{HESS}.\eta_T.\eta_M.3600.C_{Bc}.V_{Bc} - (2.M_{Bc}.g.f_r)} \quad (3.36)$$

where D is the minimum EV driving range in km, M_{Bc} is the mass of the battery cell in kg.

The battery size of HSEV could be reduced by 26.72 % compared to BEV available in the market, as shown in Table 3.2. The derived battery size from Eq. (3.1) and expressed in Eq. (3.36) would provide the standard driving range even under adverse conditions. Also, the proposed vehicle can accommodate a PV panel. The output power ratings of PV are analyzed analytically in Section 3.5.1, considering different weather conditions.

- (i) Battery State of charge (B_{SOC}) : Charge levels in the battery are decided by the SOC. Improvement in energy economy is reflected in the battery SOC levels [Song et al., 2018].

$$B_{SOC} = B_{SOC0} - \int \frac{I_B}{B_C} \quad (3.37)$$

where B_{SOC0} is the initial battery SOC, I_B and B_C are the battery current and capacity.

- (j) SC State of charge (SC_{SOC}) : SC operates with higher efficiency at higher SOC. In order to achieve a better SC performance, SOC should not go below

40 % and over 100%. The relationship between SC_{SOC} and voltage is shown in Eq. (3.38) [Zhang et al., 2020].

$$SC_{SOC} = (U_{SC}/V_{SC})^2 \quad (3.38)$$

where U_{SC} and V_{SC} are the working voltage and nominal voltage of the SC module, respectively.

- (k) PV range (PVR) : As per the Indian electric 3W standard test case, the average driving range is 100 km per day [key, 2019]. PV energy per day directly impacts both the range and battery energy savings.

$$PV_{Range} = \frac{E_{PVday}}{ECR} \quad (3.39)$$

where ECR is the energy consumption rate in Wh/km, E_{PVday} is PV energy per day in Wh and PVR is the total PV range.

3.4.2 Economy evaluation

- (a) EV Battery degradation cost (BDC) : is the measure of battery replacement and maintenance cost from its capacity and instantaneous capacity loss (Eq. (3.31)) [Spotnitz, 2003] [Niu et al., 2022].

$$BDC = \frac{B_C \cdot V_B \cdot Price_{BAT} \cdot B_{\delta Q_{loss}(k)}}{(1000) \cdot (0.2)} (INR) \quad (3.40)$$

- (b) EV Electricity cost (EC) : is the cost associated with energy utilized (E_{source}) during the battery's charging. EC depends on the per unit cost (kWh), the battery size (Ah), and SOC(%) as expressed below [Jiahao et al., 2022]:

$$EC = \frac{E_{source} \cdot Price_{kWh}}{(1000)} (INR) \quad (3.41)$$

- (c) EV Total operation cost (TOC) : describes the cost associated with battery degradation with time and energy usage. The battery degradation cost (BDC) and electricity cost (EC) of EVs determine the total operation cost of the vehicle [Niu et al., 2022].

$$TOC = BDC + EC(INR) \quad (3.42)$$

where $Price_{BAT}$ is the per kWh battery price in India, $Price_{kWh}$ is the average price of electricity cost per kWh, B_C is the battery capacity, V_B is the battery voltage. $B_{\delta Q_{loss}}$ is evaluated from with Equation 3.31.

3.5 Simulation Results

The proposed energy management system (Section 3.4) of the HSEV disengages the battery from the effects of driving conditions 1) vehicle-related (acceleration, deceleration, braking), 2) driver-related (driving pattern, route planning), 3) environmental-related (temperature, irradiance, wind, road terrain) factors. Hence improves the battery’s longevity and avoids frequent battery replacement or maintenance [Akar et al., 2017].

Proposed IHSEMS are detailed in this section with the outcomes that manage the effective power allocation among the hybrid sources for varying CDP. Table 3.6 assesses a detailed comparison between the IHSEMS versus BEV, SMC, and FDS. In this work, an electric three-wheeler exhibits the significance and effectiveness of IHSEMS. Figure.3.3 shows an NYCC, Artemis Urban, WLTP class-1 CDP serves to test the IHSEMS since their driving conditions match with the three-wheeler’s average velocity. The average velocities and distances covered by each profile are 11.4 km/h and 1.90 km (NYCC), 17.7 km/hr and 4.874 km (Artemis Urban), 25 km/h and 8.091 km (WLTP class-1), respectively. The following initial conditions for the initial $B_{SOC0} = 50 \%$, and $SC_{SOC} = 86 \%$, are considered for test. The PV irradiance and temperature remain highly fluctuating to indicate the varying environmental conditions. The conversion efficiency of the PV panels is selected at 20 % as per the availability in the market. [Jia et al., 2021b, Shemin et al., 2022]. IHSEMS allocates the power among battery, supercapacitor, and solar PV and is implemented in MATLAB/Simulink environment. Moreover, the effects of variation in solar irradiance are mitigated by SC and regulate the bus voltage with reduced fluctuations, as discussed in the section 3.5.1. In sections 3.5.2.1, the technical and sections 3.5.2.2 economic parameters are detailed with the impact of driving conditions on EV [Zhang et al., 2020].

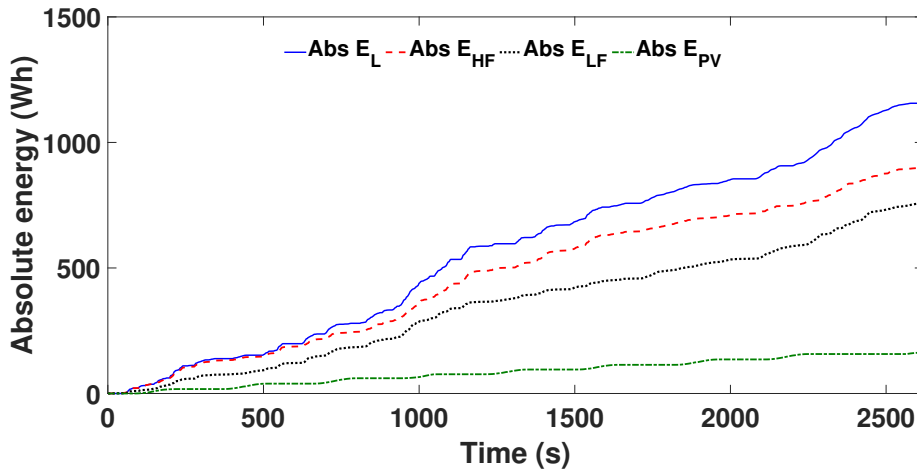


Figure 3.10: Absolute energy sharing profiles.

Figure.3.10 shows the absolute energy sharing of battery, SC, and PV energy towards the load energy demand. Energy sharing among each source ensures

that SC is available throughout the vehicle journey to handle the high-frequency load and regenerative energy. IHSEMS manages the energy, assigning SC with higher absolute energy and ensuring maximum utilization at any driving conditions considering the SOC. Hence the system adaptively varies the power allocation, such as low fluctuating highway drive and high fluctuating city drive. An absolute energy-sharing algorithm reflects the impact and ensures stress-free and optimal battery operation of the HSEV.

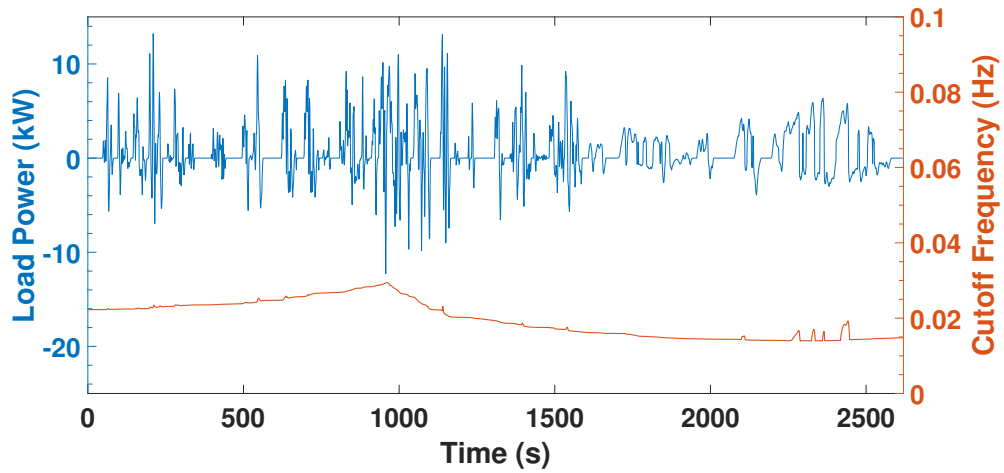


Figure 3.11: Cut off frequency derived for the CDP.

Figure.3.11 describes the load power versus cut-off frequency adaption. The cut-off frequency and load power for the CDP are analyzed to show the significance of the proposed IHSEMS. NYCC and Artemis Urban cycle show city driving cases with higher load fluctuations due to traffic conditions. Since the load fluctuations are higher during NYCC and Artemis Urban cycle, the cut-off frequency is optimized to ensure SC energy availability and the battery achieves optimal operation throughout the cycle. SC manages the sudden and peak load power demands in this driving interval and thus, in return, ensures a safe battery operation. The lower cut-off frequency during the WLTP class-1 cycle, where the fluctuation is low compared to the other two cycles. The battery can manage such low fluctuations with the selected cut-off frequency, and SC is used for the subsequent high-fluctuating driving intervals. Figure. 3.11 shows reduced cut-off frequency during the WLTP cycle to satisfy the energy optimization condition (Eq. 3.19) for varying driving conditions. The primary task of IHSEMS is to ensure an optimal power allocation among each source, as shown in Figure. 3.12 – 3.13. Figure. 3.12 shows the battery discharge power kept under 5 kW throughout the driving period. SC handles peak load power during $t=212$ s, 1140 s, which helps drop the battery C-rates. Most of the regenerative energy [time = 1130s – 1160s, 2275s – 2375s] absorbs by SC, which reduces the battery’s recurring charge and discharges to extend its life. Figure. 3.13 shows the energy sharing of the proposed IHSEMS where the SC energy is reserved for transient load conditions throughout the CDP based on the varying driving conditions. Moreover, the battery contributes more

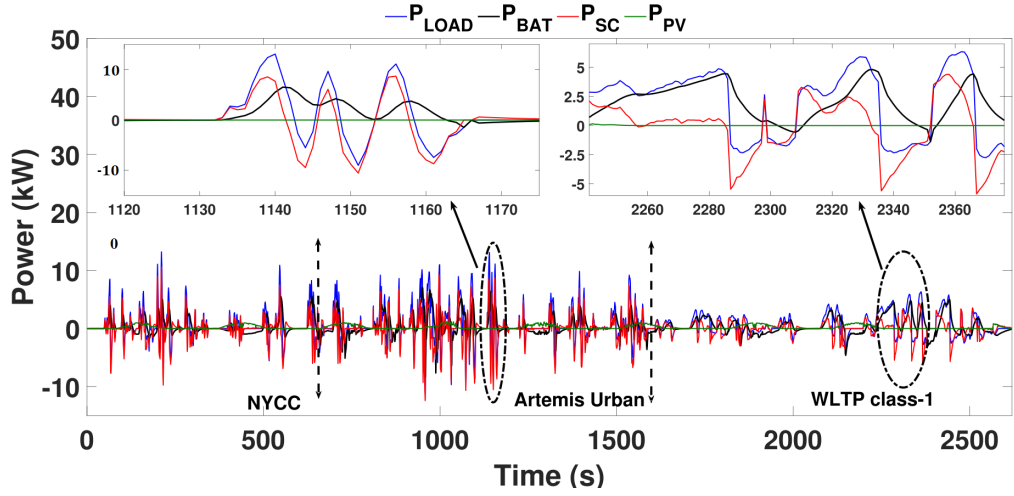


Figure 3.12: Comparison of battery, SC, PV and load power (BEV) with IHSEMS.

to smooth energy consumption during time interval $t=2200s - 2500s$ (under WLTP class-1) by assigning SC to handle even minor fluctuations in the load demand, as shown in Figure. 3.13. Overall, smooth battery energy consumption enables the stress-free operation of the battery during a sudden fall or rise in PV power.

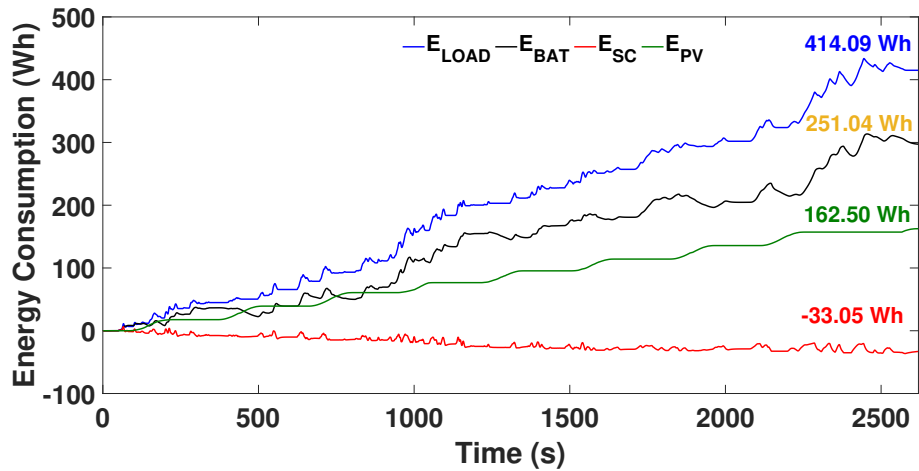
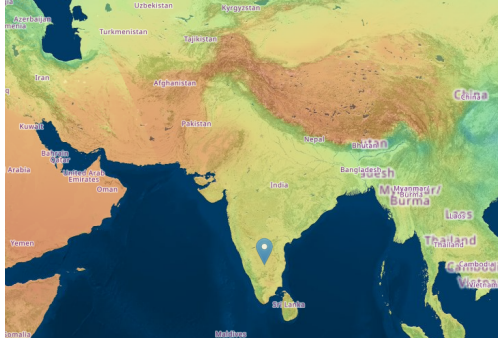


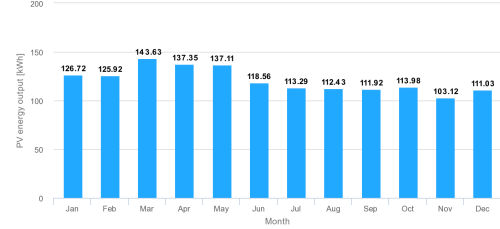
Figure 3.13: Comparison of source energy consumption of IHSEMS under CDP.

3.5.1 Impact of PV power

PV energy is chosen based on energy consumption from actual locations with real environmental conditions. Figure. 3.14(a) and 3.14(b) show the map of the selected location for the analysis (Bangalore-12.9716° N, 77.5946° E) and the monthly PV energy generation of Bangalore (India) throughout the year, respectively [European, 2022]. The PV energy generation considers an installed peak PV power [Wp] of 965.6 W (Eq. 3.7) for an area of 4.8 m² [Sunrunmotors, 2022], [European, 2022]. It is evident from Figure.3.14(b) that PV energy generation is



(a) Map of selected location for the analysis (Bangalore-12.9716° N, 77.5946° E).



(b) PV energy generation (kWh) at Bangalore, India throughout the year.

Figure 3.14: PV energy generation (kWh).

highest during March (143.63 kWh) and lowest during November (103.12 kWh). The yearly average PV energy production at Bangalore is 1455.07 kWh under a fixed panel arrangement. However, PV energy consumed by vehicles is significantly low due to the shading on roads and parking spaces which reduces the solar irradiance. Centeno et al., 2021 reported the annual average irradiance loss of 20% and 50% during driving and parking due to shadings, respectively [European, 2022]. Three cases with different PV irradiance and vehicle drive conditions are examined to show the significance of PV energy in HSEV. Scheduling of the daily NYCC driving cycle of electric 3W energy management is shown in Table 3.5. The daily standard 100 km driver's driving cycle needs to drive 53 times of NYCC driving cycle [Niu et al., 2022].

This section explores the varying environmental conditions like sudden irradiance change. PV power constantly fluctuates due to the varying Irradiance and temperature. An MPPT supports achieving maximum power at each irradiance level. An increase in Irradiance from 0 to 1000 W/m² at t = 221s and a decrease from 1000 to 0 W/m² at t = 257s verify sudden PV power variations. The power allocation of IHSEMS describe in Figure. 3.15(a) includes the load power, battery power, SC power, and PV power. IHSEMS takes care of the load demand at t = 221s, where PV irradiance and regenerative braking excess power at the bus. SC consumes this excess power at that instant by consuming more power (-ve rise shows the sudden increase in SC charge power) to avoid disturbances in battery power. At t = 257s, the PV irradiance suddenly reduces to zero, and traction operation demands dip power at the bus. SC delivers more power (+ve rise shows the sudden increase in SC discharge power) to avoid fluctuations in battery power. This strategy ensures a smooth battery operation during rising and falling PV irradiance and load variations. Similarly, Figure. 3.15(b) is with the same load fluctuation as discussed in Figure.3.15(a). However, the PV power is considered zero to analyze the impact of energy management during the same load fluctuations but with different environmental conditions. Under zero PV irradiance, SC is not taking additional charge or discharge currents which exists in the case of Figure. 3.15(a). Three different driving cases are considered based on the instant

of the driving time in a day and are as follows:

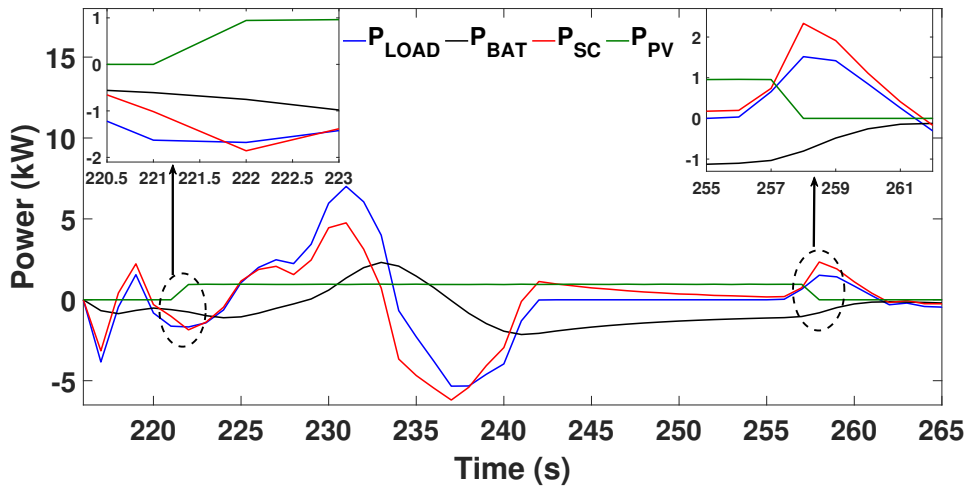
1. **Case-I:** Where a daily average PV Irradiance is available for charging
2. **Case-II:** Where half of a daily average PV Irradiance is available for charging
3. **Case-III:** Where zero daily average PV Irradiance is available for charging

In the first case, an average drive of a 3W is 100 km under a full sunshine hour (PV power = full). The driving schedule scenario and energy consumption of case 1 are shown in Table 3.5. 20 % additional energy consumption for varying driving profiles (driver/route/road terrain Etc.,) is considered in the analysis. In the second case, an average drive of a 3W is 100 km under a half sunshine hour (PV power = half). In the third case, an average drive of a 3W is 100 km during night time (PV power = 0).

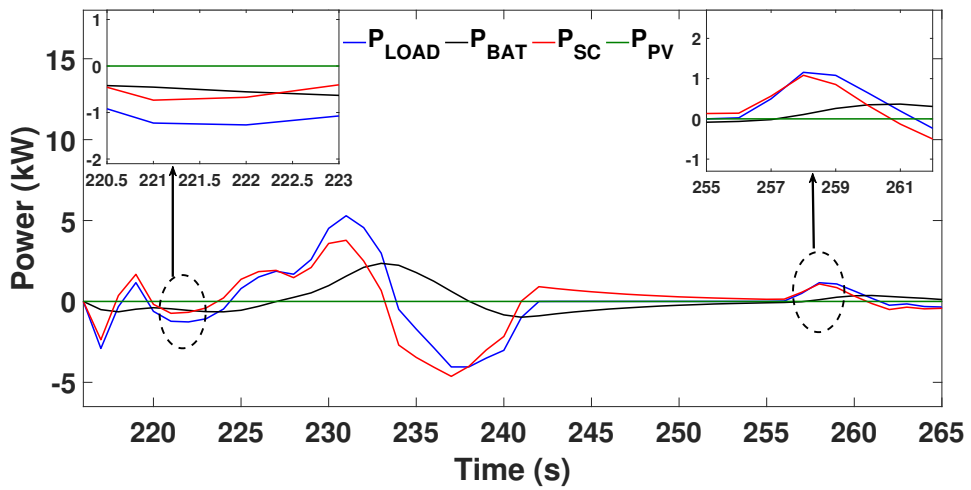
Table 3.5: Performance and economy analysis of EMSs.

Parameters	Case-I	Case-II	Case-III
Daily energy demand (Wh)	3,445	3,445	3,445
Monthly energy demand (Wh)	1,24,020	1,24,020	1,24,020
Monthly PV energy generation (Wh)	63,600	31,800	0
Monthly Battery energy consumption (Wh)	60,420	92,220	1,24,020
Daily 3W EV drive distance(km)	100	100	100
Daily PV range (km)	60	30	0

Table 3.5 summarizes different cases, and it is clear that when compared with a BEV, a Hybrid EV with PV, battery, and SC can achieve higher vehicle performance and energy efficiency with lower battery size. Further, case-II is selected for further analysis at half sunshine hour and a half outside. The half sunshine hour is due to shading obstacles during driving, parking, and variations in seasons may cause losses in Irradiance (nearly 60 – 70 % losses) [Shemin et al., 2022]. In order to match the actual scenario, all the environmental and driving conditions are considered in this thesis. In tropical countries where Irradiance is very high throughout the year, the battery charging from the grid could be reduced. Further, PV could manage the daily commute of the vehicle, and the battery could be used as an emergency source. PV saves charging time and shifts the attitude of EV users who are inhibited towards EVs due to the shortage of EV charging stations and high charging time. In the future, the position of PV power in transportation systems will be high because, according to the Paris Agreement, all countries will reduce the global peak of greenhouse gas emissions as soon as possible to achieve



(a) Power comparison with PV irradiance variations.



(b) Power comparison with zero PV irradiance.

Figure 3.15: Power allocation of IHSEMS for sudden variation in solar irradiance (a), zero PV power (b) under NYCC driving cycle.

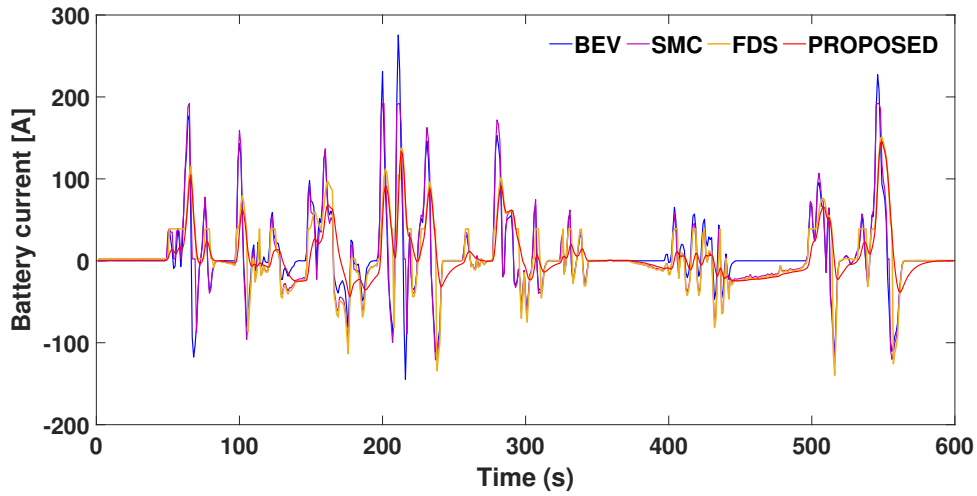
global climate change by 2050 [GE0, 2020]. Further, an increase in PV module conversion efficiency and a reduction in PV cell cost can improve the EV energy efficiency to a large extent [Elia et al., 2021].

3.5.2 Techno-economic analysis

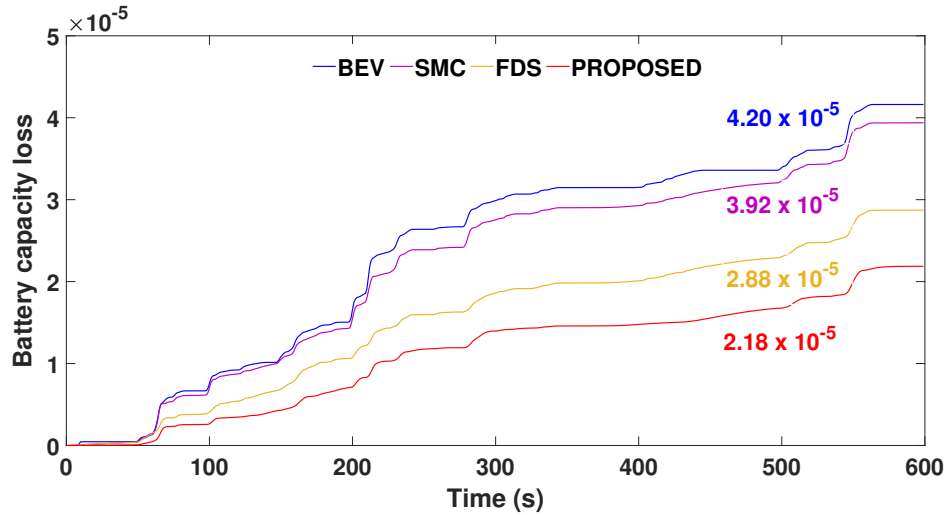
The comparison of technical parameters and economy analysis exhibits the significance of the hybrid sources EMSs strategy. Various EMSs strategies:

1. (1) IHSEMS,
2. (2) SMC [S. Njoya Motapon and Al-Haddad, 2014],
3. (3) FDS [Cabrane et al., 2020] and
4. (4) BEV

have evaluated for a fair and guaranteed comparison. The analysis also presents BEV configuration to highlight the superiority of Hybrid source EVs. An NYCC cycle shows the best urban driving profile, as shown in Figure 3.3. Therefore it was selected for technical and economic comparison of EMSs [Niu et al., 2022] in the below sections (3.5.2.1 and 3.5.2.2).



(a) Comparison of battery current.



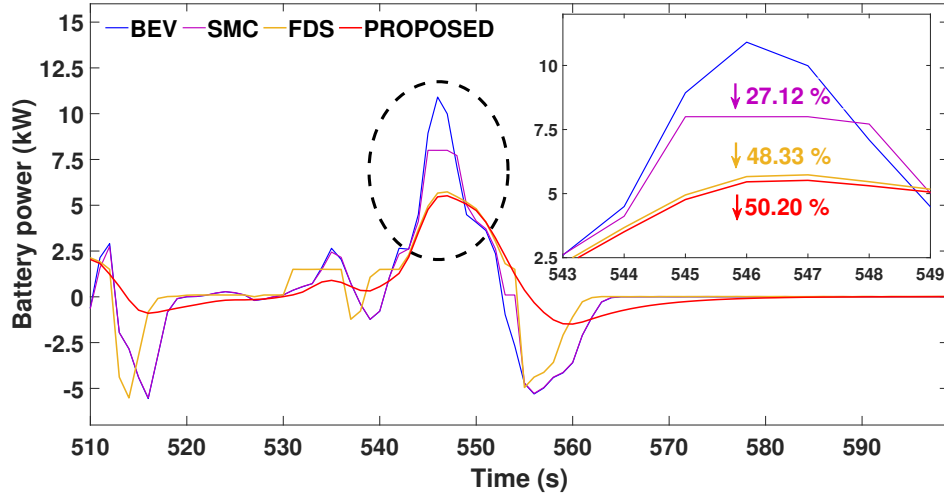
(b) Comparison of battery capacity loss.

Figure 3.16: Comparison of BEV, SMC, FDS, and IHSEMS in terms of battery current (a), battery capacity loss (b) under NYCC driving cycle.

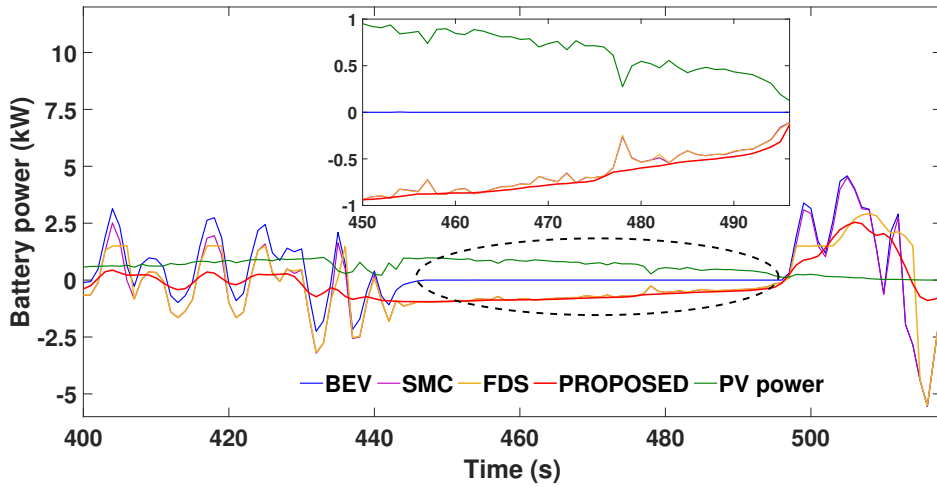
3.5.2.1 Technical performance comparison of EMSs

This subsection compares specific performance parameters of BEV, existing EMSs, and proposed EMS. Figure. 3.16 illustrates the battery current and capacity loss performance under the NYCC cycle for three different hybrid EMS. Battery-only (BEV) configuration is also analyzed to illustrate the significance of hybrid sources in EVs. It is clear from Figure. 3.16(a) that FDS and IHSEMS appear similar. However, FDS fails to reduce the average battery current at $t=300\text{s} - 350\text{s}$, $400\text{s} - 450\text{s}$, and $520\text{s} - 560\text{s}$, which eventually reflects in the battery degradation, and the IHSEMS performs better in reducing battery capacity loss than all strategies, as shown in Figure. 3.16(b). IHSEMS reduces frequent battery charging events and

thus achieves a decelerated battery degradation. Hence, the battery capacity loss is reduced by 48.10 % in comparison with the BEV under the NYCC cycle, where the capacity loss is evaluated with Eq. (3.31) and depicted in Section 3.4.1(e).



(a) Comparison of peak battery power for NYCC driving cycle (510 s – 599 s).



(b) Comparison of power fluctuations for NYCC driving cycle (400 s–520 s).

Figure 3.17: Comparison of BEV, SMC, FDS and proposed IHSEMS under NYCC driving cycle.

Figure. 3.17(a) and 3.17(b) illustrate two different time intervals for peak load power and sudden fluctuations in the battery power profile. The SC absorbs the transient conditions and prevents the battery from higher C-rates and fluctuations. During time interval 543s – 549 s in Figure. 3.17(a) IHSEMS, SMC, and FDS reduce the respective peak battery power by 50.20 %, 48.33 %, and 27.12 % compared to BEV as per Eq. (3.26). The effective control of C-rates in peak power instants has been found in the proposed strategy compared to the existing

EMS and BEVs. Similarly, as shown in Figure. 3.17(b) during interval $t = 400s - 440s$, the proposed strategy effectively reduces power fluctuations compared to the other EMSs. The BIR, as discussed in Section 3.4.1(c) and evaluated in Eq. (3.29), reduces to 76.2 % for IHSEMS compared to BEV. Hence, it is evident that battery stresses are minimized. Similarly, during $t=450s - 495s$, PV power fluctuations are higher and reflected in the battery power of SMC and FDS strategies. However, the proposed EMS removes the fluctuations, making the battery power profile much smoother and decelerating the battery's degradation. Moreover, RMS current reduction detailed in Section 3.4.1(d) and expressed in Eq.(3.30) shows the IHSEMS achieves a reduction by 46.60 % compared with BEV, 37.88 % compared with SMC, and 17.03 % compared with FDS.

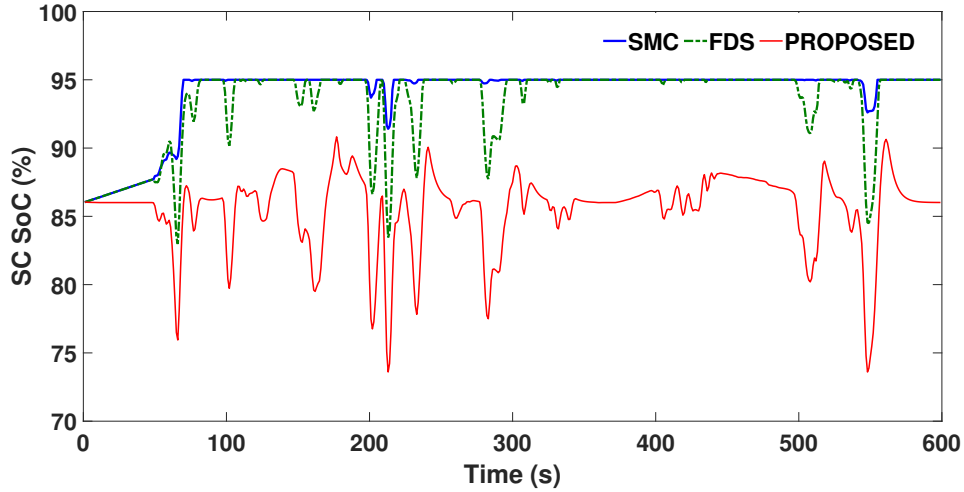


Figure 3.18: Comparison of SC_{SOC} with SMC, FDS, and IHSEMS under NYCC driving cycle.

The IHSEMS reduces the battery capacity loss and can plan the availability of SC. Figure. 3.18 shows the comparison of SOC of SC under the NYCC cycle for SMC, FDS, and IHSEMS. In NYCC (urban cycle), the IHSEMS initially controls SC to utilize maximum and later charges through the battery and braking energy, which was impossible through FDS and SMC EMSs. In the IHSEMS, the final value of SC_{SOC} maintains at 85 % for the smooth operation of (charging and discharging) future driving cycles. Since other EMSs charge SC to its maximum SOC, which increases the battery deterioration. Capacity loss of battery for the NYCC cycle is very low for IHSEMS compared with other EMSs and evaluated as discussed in Section 3.4.1(e). The performance parameters for BEV, SMC, FDS, and IHSEMS are explained in Table 3.6. Section 3.4.1(b) depicted the B_{CR} and evaluated as per Eq. (3.27) and is 26.72% for IHSEMS compared to BEV. The higher fluctuations in the NYCC driving profile provide an extreme environment for battery degradation and reduce the battery life span. To analyze the battery lifespan for BEV and hybrid EMSs, repeated NYCC cycles were tested and analyzed. Life span discussed in Section 3.4.1(f), and evaluated using Eq.(3.34)

shows that a battery life span improvement (BLSI) of 6.91 %, 45.50 %, and 92.68 % is achieved for the hybrid EMSs SMC, FDS, and proposed IHSEMS respectively compared to the BEV (Table 3.6).

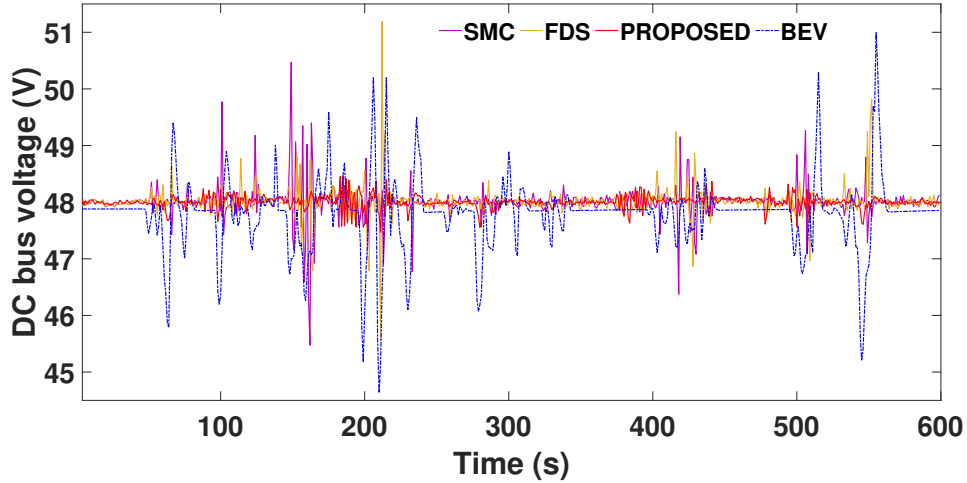


Figure 3.19: Comparison of DC_{BVF} bus voltage fluctuations with SMC, FDS and IHSEMS under NYCC driving cycle.

The bus voltage constantly fluctuates due to the sudden variations in EV load current. Section 3.4.1(g) describes the DC_{BVF} adversely affecting EV motor performance. However, the controller brings back the system stability with a fast response. Figure. 3.19 shows the comparison of DC_{BVF} with BEV, SMC, FDS, and IHSEMS under the NYCC cycle. DC_{BVF} of BEV is higher compared to SMC, FDS, and IHSEMS and is 13.19%, 10.90% and 5.20%, and 2.05 %, respectively and are tabulated in Table 3.6. Proposed EMS reduces the DC_{BVF} as evaluated using Eq.(3.35) by maximum utilization of SC during sudden load changes. The lower DC_{BVF} (nearly 2 %) in IHSEMS highly recommends an efficient motor drive system.

Table 3.6: Performance and economy analysis of EMSs.

Parameters	BEV	SMC	FDS	IHSEMS
Battery Peak Power (kW)	10.93	7.96	5.64	5.44
Battery capacity (kWh)	7.37	5.4	5.4	5.4
Battery di/dt (A/s)	113	98	61	26.8
Battery RMS current (A)	64	54.95	41.14	34.13
Battery Capacity Loss	4.20×10^{-5}	3.92×10^{-5}	2.88×10^{-5}	2.18×10^{-5}
Battery Life Span Improvement (%)	-	6.91 %	45.50 %	92.68%
DC bus voltage fluctuations (%)	13.19%	10.40%	5.20%	2.05%
Total Operational Cost (INR.)	18.54	12.942	9.50	7.25

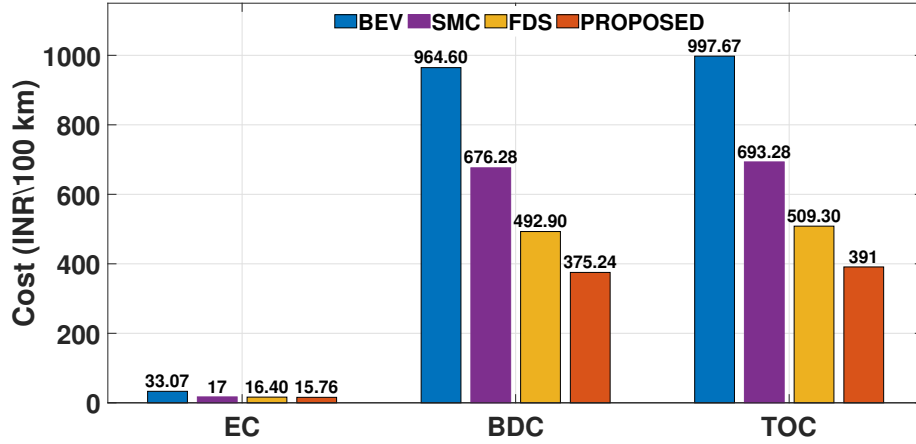


Figure 3.20: Comparison of DC_{BVF} bus voltage fluctuations with SMC, FDS and IHSEMS under NYCC driving cycle.

3.5.2.2 Economy analysis of EMSs

Battery's technical parameters reflect the impact on economic analysis discussed in Section 3.5.2.1. Section 3.4.2(c), (b), and (a) estimates the total operation cost (TOC), including the sum of Electricity cost (EC) and Battery Degradation Cost (BDC) of the EV. Figure. 3.20 illustrates the comparative results of EC, BDC, and TOC of the SMC, FDS, BEV, and IHSEMS for a 100 km drive. The proposed IHSEMS reduces the electricity cost by 52.4 % (INR. 17.31/100 km) compared to BEV. Moreover, BEV experiences a higher battery degradation cost and, in turn, a higher chance of replacement or maintenance. Comparison of economic analysis, in terms of TOC, is included in Table 3.6. Compared to the BEV, SMC, and FDS, the IHSEMS strategy reduces the total operation cost by 60 %, 43.9 %, and 23.68 %, respectively.

3.6 Summary

Globally, witness to a sustainable economy depends on the rapid development of renewable energy applications. In this context, a hybrid source with a renewable background plays a crucial position in the transportation sector. The present work highlights the importance of EMS for hybrid source EVs with the design and simulation modelling. The proposed IHSEMS allocates the load power to enhance the performance of the EV. The IHSEMS effectively manages the effects of varying driving conditions by employing an absolute energy-sharing algorithm (AESA). Incorporating solar and supercapacitors with existing BEVs improves battery life and energy efficiency. The SMC and FDS strategies are analyzed in the comparative study. Significant contributions and highlights of the proposed EMS are:

- The battery's stress reduces in IHSEMS by reducing RMS current 46.60 %,

37.88 %, and 17.03 % compared with BEV, SMC, and FDS methods.

- The battery peak power reduces in IHSEMS by 50.2 %, 30.74 %, and 3.71 % compared with BEV, SMC, and FDS methods.
- Compared to BEV, the battery capacity reduces in IHSEMS by 26.72 % (7.37 kWh to 5.4 kWh).
- The IHSEMS exhibits a reduction in battery peak power, RMS current, and continuous charge-discharge cycles, which improves the battery lifespan by 92.68 %, 80.22 %, and 32.40 % compared with BEV, SMC, and FDS EMSs, respectively.
- Economy analysis of IHSEMS shows a reduction of 60 %, 43.9 %, and 23.68 % in total operation cost compared to BEV, SMC, and FDS, respectively.

Moreover, using solar energy in electric vehicles enhances the economy of energy sustainability. Solar prices drop daily, providing insight into improving the technologies of solar-powered vehicles. Increased PV panel efficiency improves the energy economy of the transportation system.

Chapter 4

Proposed SC-PV Hybrid Electric Vehicle

Contents

4.1	Introduction	77
4.2	Proposed Hybrid Source Model	78
4.3	Proposed Energy Management Algorithm	78
4.4	Simulation Results	83
4.4.1	Cases of EV run under varying PV irradiance	83
4.4.2	Cases of EV run under varying driving locations	91
4.4.3	Cases of sudden load demand fluctuations in EV drive	99
4.4.4	Technical parametric analysis	101
4.5	Summary	103

4.1 Introduction

This chapter introduces an EV-integrated PV system with a high energy and power density supercapacitor for an EV-3W and analyzed using technical and economic parameters. One of the main aims is to develop an EMA that operates with the EV load demand, and the PV energy consumption during the drive from real-world data and to maximize EV self-sufficiency. The PV power fluctuations from solar irradiance and driving route variations (shading and obstacles) are not reflected in the DC bus using the Energy Management (EM) among the source and load. An Energy management algorithm (EMA) is proposed to control the electrical power flows between the PV, SC, and EV load. The proposed system and control strategy utilizes the SC effectively and manages it for short transient periods whenever PV irradiance is available. Also, EM modes ensure the protection of SC from overcharging and over-discharging. The investigated solution reduces the

power losses, protects the sources, minimizes the DC bus voltage fluctuation, and enhances the overall system performance.

This chapter details the significance of the proposed HSEV with the techno-economic comparison with BEV. Overall, a hybrid source-powered EV is designed to improve energy efficiency and enhance the goal of sustainable transportation.

4.2 Proposed Hybrid Source Model

Hybrid sources in EVs improve energy efficiency. However, the power flow among each source must be regulated to improve the source performance characteristics. This section deals with the discussion on performance and lifetime models of each source discussed in the literature. Moreover, EMA monitors and manages the effective power sharing among each source in the power train to enhance energy efficiency, EV performance, and battery longevity [Vukajlović et al., 2020] [Xie et al., 2018a]. The overall structure of the proposed HSEV plays a significant role, as shown in Figure 4.1. A parallel connection of Photovoltaic (PV) panels over the EV roof and Supercapacitor modules connected to the DC bus with DC-DC converters. DC-AC inverter interconnects the motor with the DC bus to provide traction by coupling towards the rear wheels via mechanical transmission.

4.3 Proposed Energy Management Algorithm

This section deals with the proposed energy management of the SC-PV hybrid system in the electric 3W. EMS's primary function is keeping the SC in safe operating conditions and monitoring and controlling SC charge-discharge profiles to meet the required EV load demand. The block diagram of the proposed EMS is shown in Figure 4.1, which performs both the functions mentioned earlier. The proposed HSEV EMS structure is divided into section 3.2.1) Power demand, 3.3) Hybrid source, and 3.4) the energy management system (Figure 4.1). The power demand profile consists of the driver (accelerator and brake) and load (EV motor power), and environmental condition (wind speed) as expressed in the mathematical equations (Eq. 3.1-3.2). A hybrid source supports the power demand profile, and the contributions of each source are detailed in section 3.3.

In addition, the proposed EMS optimizes the energy flow of the whole system by considering the fluctuations on the DC bus from variations in PV power and driving conditions. The EMS handles the power flow among PV and SC to meet the EV load demand, and regenerative braking energy is fed back to the SC from the motor. The proposed EMS assigns SC to absorb the power fluctuations due to the varying driving and environmental conditions to ensure smooth load currents. The sudden drop and fall in PV power cause a shortage or additional power at the DC bus, which may affect the operation of the motor drive. However, the proposed EMS ensures an optimal power flow throughout the drive by the maximum utilization of SC. The EMS utilizes fast response and high power density

of SC without affecting the lifespan. Moreover, the EMS controls the overcharging of SC from PV during parking. Figure 4.2 shows the algorithm of the proposed EMS in a hybrid SC-PV source system.

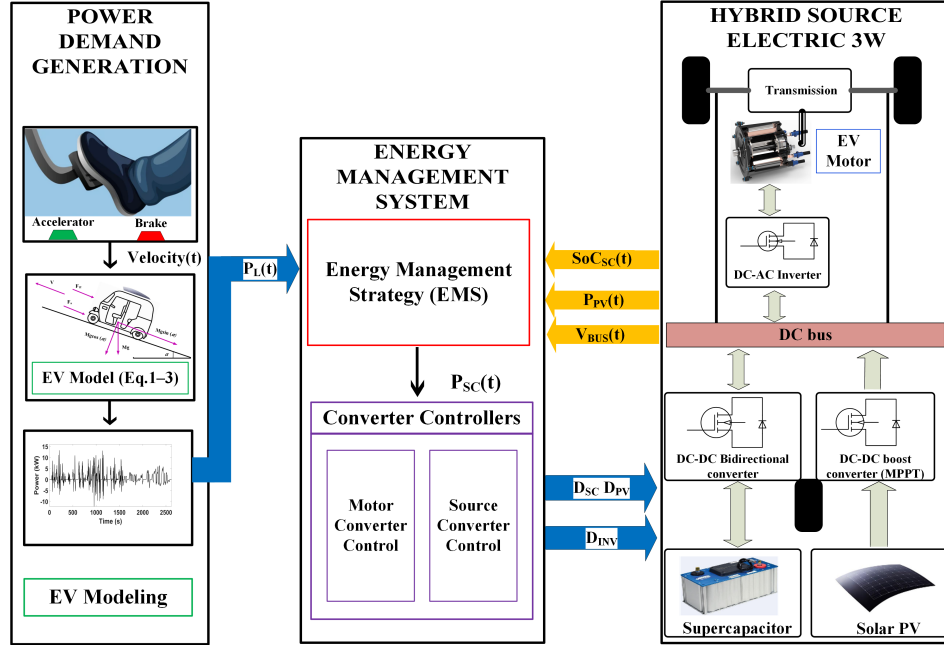


Figure 4.1: Complete schematic structure of hybrid source energy management in Electric-3W

The algorithm focuses on the availability, utilization of SC by reducing the peaks and fluctuations in EV demand. To achieve increased self-sufficiency in the EV, the load demand must be mostly satisfied by the PVs and SC (discharging, supplying the remaining required power). Therefore, the idea is to provide power to the EV load from the PVs (if available during sunlight) and/or the SC to support the peak demands. The PV power throughout the sunshine hour with a highly fluctuating profile is shown in Figure 3.5, which is considered in work to analyze the significance of the proposed EMS. Sudden variations in the PV power reflect the importance of eliminating the fluctuations without affecting the DC bus. EMS monitors the PV power and segregates the high-frequency components towards the SC by modifying the control strategy as discussed in the equation 4.3. The load power is managed by the high energy-dense SC and the proposed EMS allocates the energy sharing considering the PV power, source charge states, and driving conditions. Total power handled by the hybrid source in the EV during EV drive and parking are explained in Eq. (4.1) and Eq. (4.2).

$$P_T = P_{SC} + P_{PV} = P_L \quad (4.1)$$

where P_T , P_{SC} , P_{PV} , P_L represents the total power, SC power, PV power, and load power, respectively. During the parking time, the charging power P_C is the total power handled by the SC and is shown in Eq. (4.2).

$$P_C = P_{PV} \quad (4.2)$$

The flowchart in Figure 4.2, depicts the proposed EMS for the charging/discharging of the hybrid SC-PV source system. Two different modes are described as (1) Surplus Power Mode (SPM) and (2) Deficit Power Mode (DPM). The operation during which the generated PV power is higher than the required EV load power enables to charge the SC represents the SPM. SOC_{SC} is monitored under this mode to limit the over-charging of SC. However, DPM is the operation mode during which the PV power is lower than the required EV load power. Under this mode, SOC_{SC} is monitored to keep the SC under optimal operation and to avoid deep discharging. The flow chart depicts that the state of each mode decides the buck or boost operation of the SC bidirectional converter. Whenever the SPM mode is set (SPM=1), the converter is under buck mode of operation (charging), and when DPM mode=1, the converter is under boost operation (discharging). Similarly, considering the availability of SC, two additional sub-modes (Overcharge and Over-discharge) are defined concerning the safe operation of the EV. During SPM, if the SC is above 95 % sub-mode Overcharge (OC) = 1 (set) and there is no chance of charging in the SC, and this mode initiates the turn off of the PV boost converter switch and the buck mode switch in bidirectional DC-DC converter of the SC. Similarly, during DPM, if the SC is below 40 % sub-mode Over-discharge (OD) = 1 (set) and SC lacks the energy for further EV drive, and this mode initiates the turn off of the boost mode switch in the bidirectional DC-DC converter of the SC which denies the vehicle without recharging the SC. Both the sub-modes provide additional protection and ensure optimal operation of the SC. Table 4.1 shows the different modes of operation and respective SC reference currents.

Table 4.1: Operating modes and reference currents

Case	Conditions	Modes	Submodes	Reference currents
1	$P_{PV} > P_{load}$	SPM=1	OC=OD=0	I_{SCR}^* at $I_T^* > 0$
	$SOC_{SC} \geq SOC_{SCmax}$	DPM=0	OC=1, OD=0	0 at $I_T^* \leq 0$
2	$P_{PV} > P_{load}$	SPM=1	OC=0, OD=1	0 at $I_T^* > 0$
	$SOC_{SC} \leq SOC_{SCmin}$	DPM=0	OC=OD=0	I_{SCR}^* at $I_T^* \leq 0$
3	$P_{PV} \leq P_{load}$	SPM=0	OC=OD=0	I_{SCR}^* at $I_T^* > 0$
	$SOC_{SC} \geq SOC_{SCmax}$	DPM=1	OC=1, OD=0	0 at $I_T^* \leq 0$
4	$P_{PV} \leq P_{load}$	SPM=0	OC=0, OD=1	0 at $I_T^* > 0$
	$SOC_{SC} \leq SOC_{SCmin}$	DPM=1	OC=0, OD=0	I_{SCR}^* at $I_T^* \leq 0$

The EMS for the hybrid source system in EV is responsible for monitoring the generated PV power, the SC SOC, and the load power to manage the supplied/absorbed EV load power and increase EV performance. The closed-loop controller designs the regulation of voltage and current from the sources. A dual voltage and current loop regulate the DC bus voltage and SC currents, respectively. Figure

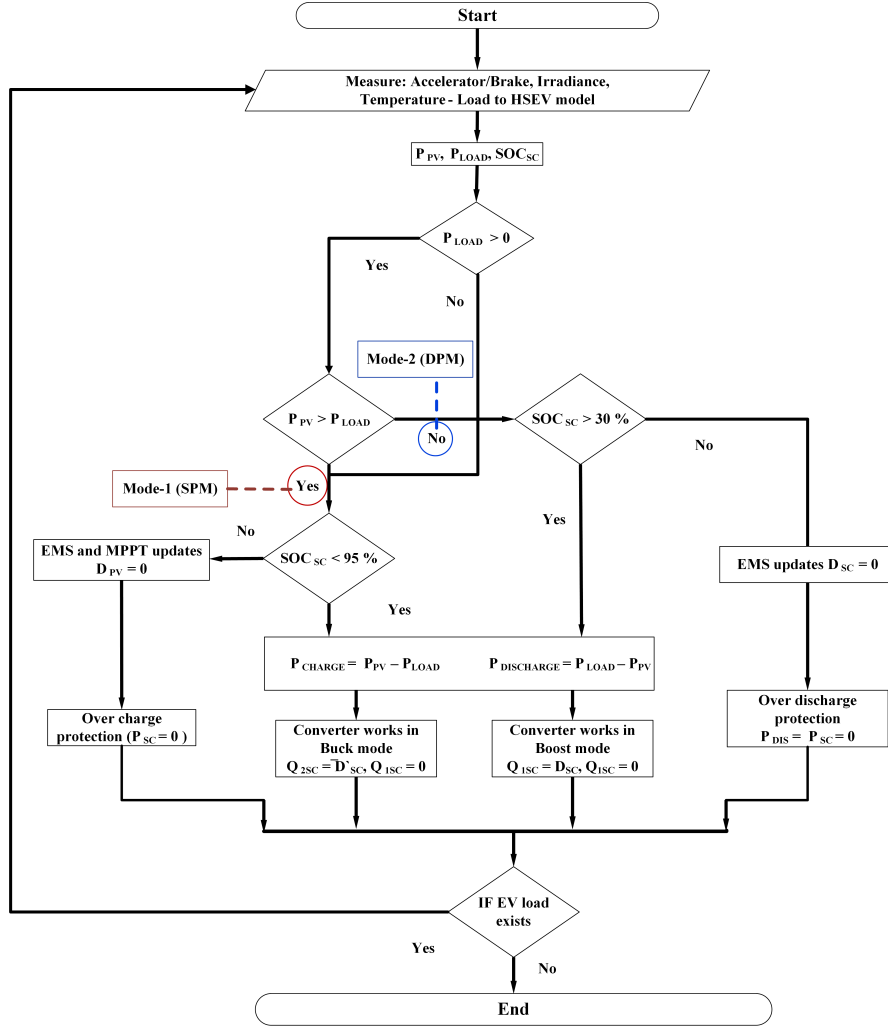


Figure 4.2: Algorithm of proposed energy management strategy for SC-PV hybrid system in EV(modify the algorithm further)

4.3, shows the control block diagram of the hybrid system. Bus voltage regulation is achieved by employing an outer voltage loop where the PI controller defines the total reference current required to stabilize the bus voltage and meets the load demand (Equation 4.3). The reference current for SC is evaluated from the difference of total reference current (I_T^*) and PV current, (I_{PV}) as in Eq. (4.3). SC reference current (I_{SCR}^*) is compared to the actual SC current (I_{SC}) (Equation 4.4). The remaining error current (e_{SC}) passes through a PI controller to generate the appropriate reference signals that derive duty cycle (D_{SC}) for the semiconductors of the SC bidirectional converter using PWM (Equation 4.4). However, a novel switching strategy is introduced in the proposed work where the switching of Q_{1SC} is only allowed during the boost mode and remaining time instants it is made off and the Q_{2SC} is provided with duty ratio only during buck mode when regenerative braking appears in the bus. The modified control strategy ensures the reduction of the switch stresses and eventually minimizes the switching losses. The PI controllers of each loop provide the desired phase margin (PM) at

the required bandwidth (BW) for ensuring system stability based on frequency domain specifications [Cabrane et al., 2020]. PI controller parameter design is implemented using the MATLAB SISO tool with the small signal model equations for the converter [Erickson and Maksimovic, 2007]. P & O MPPT algorithm generates switching pulses for PV boost converter [Zineb et al., 2021]. The stability analysis is analyzed with the bode and phase plots, where the gain margin and phase margin are selected to ensure the system's stability which is followed from literature [Arunkumar et al., 2022]. However, the criterion of the PI design in the proposed work is to fasten the current control loop of SC so that the fluctuations in the load and PV side must not disturb the stability of the DC bus. Hence the BW and PM are selected as 50 krad/sec and 62.1° for the SC current loop and 4.7 krad/sec and 63° for the outer voltage loop. The SC reference current generation equations are shown in Equation 4.3 Finally, the total current (I_T) supplied by the hybrid sources is shown in Equation 4.5.

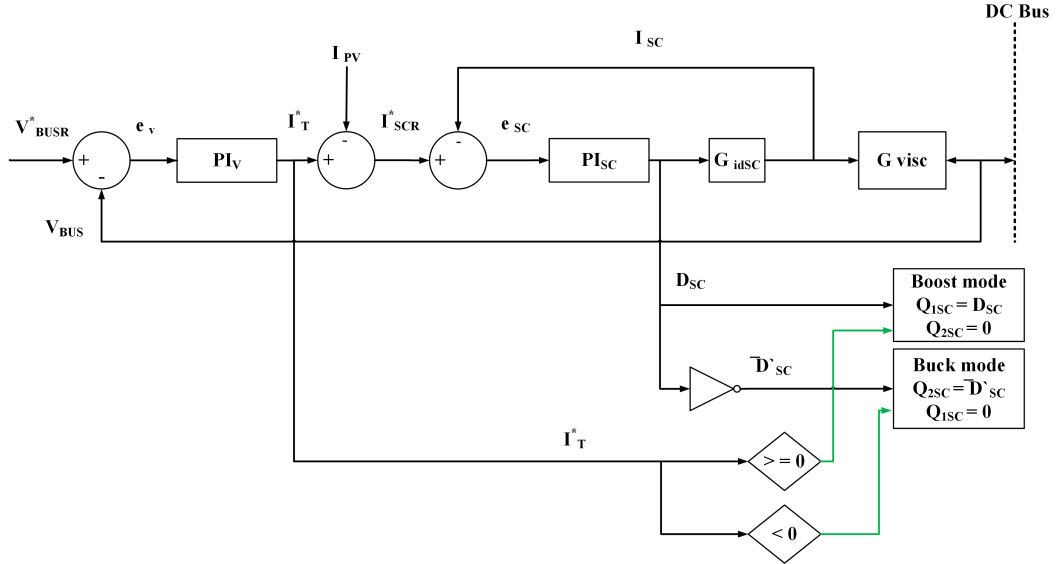


Figure 4.3: Control block diagram of the SC reference current calculation under proposed modified EMS

$$I_T^* = (V_{BUSR} - V_{BUS}) \cdot (K_{pv} + \frac{K_{iv}}{s}); I_{SCR}^* = I_T^* - I_{PV} \quad (4.3)$$

where K_{pV} and K_{iV} are the parameters of proportional and integral constants of the outer voltage loop, $V_{BUSR} = 48V$, and V_{BUS} are reference and actual DC bus voltage.

$$e_{SC} = I_{SCR}^* - I_{SC}; D_{SC} = e_{SC} \cdot (K_{pSC} + \frac{K_{iSC}}{s}) \cdot G_{idSC} \quad (4.4)$$

where K_{pSC} and K_{iSC} are the parameters of proportional and integral constants

of SC current loop, G_{idSC} is the duty to control transfer function of SC.

$$I_T = I_{PV} + I_{SC} \quad (4.5)$$

4.4 Simulation Results

The EMA of the proposed EMS for HSEV is detailed in Section 3.4. The proposed algorithm ensures a stabilized and optimal operation of the hybrid source system that exhibits EMA's significance in ensuring high energy-dense SC's availability during sudden fluctuations due to three different conditions. The first condition is the varying irradiance cases throughout the drive detailed in section 4.4.1. The next condition discussed in section 4.4.2 investigates the variations in load power demand under different road terrain (locations), and the last condition considers the varying driving behavior or style, which is discussed in section 4.4.3. The EMA handles the impacts of varying driving and environmental conditions on the EV. Hence the result analysis is described with various initial conditions. Three different driving profiles are selected to test the proposed system response towards fluctuating load power (varying driving conditions), and shown in Figure 4.10b, 4.11b, 4.12b. Investigation of varying PV irradiance describes three cases of EV runs considering the different locations (varying environmental conditions). The following initial conditions of the proposed work ($SC_{SOC} = 85\%$). The PV irradiance and temperature remain highly fluctuating, indicating the varying environmental conditions. The conversion efficiency of the PV panels is considered as 60%, as per the discussions in section 3.2.1. A three-wheeler's daily average driving distance is 100 km with the varying sunshine hour. The proposed EMA allocates the power between SC and solar PV considering the variations in driving, environmental, and source conditions and is realized with MATLAB/Simulink environment. Moreover, the effects of variation in solar irradiance and driving fluctuations are mitigated by SC and regulate the bus voltage with reduced fluctuations. Overall discussion and analysis on proposed HSEV and BEV are included in the section 4.4.1-4.4.3. In sections 4.4.4, the technical and economic parameters are detailed with the impact of driving conditions on EVs.

4.4.1 Cases of EV run under varying PV irradiance

Different cases are considered to analyze the effect of varying environmental conditions throughout the day. Three PV irradiance conditions are chosen for the hybrid system analysis. Based on the energy consumption patterns from each case [European, 2022], the parameters of each case are shown in Table 4.2. The PV panels are installed over the EV and experience losses during the vehicle run and parking in shades [Shemin et al., 2022]. Centeno et al. 2021 depicted the driving and parking irradiance losses as 20% and 50%, respectively, which is followed in this work [Brito et al., 2021]. Repeated driving cycles are used for the analysis to effectuate a daily standard average distance of 100 km per day [Niu et al., 2022] and different cases are classified as: 1) **Case-I:** Daily average PV

Irradiance is available for charging.2) **Case-II:** Half of a daily average PV Irradiance is available for charging. 3) **Case-III:** Zero daily average PV Irradiance is available for charging.

In the first case, an average drive of a 3W is 100 km under a full sunshine hour (PV power = $W_p = 2.88$ kW). The driving schedule scenario and energy consumption of case 1 are shown in Table 4.2. 20 % additional energy consumption for varying driving profiles (driver/route/road terrain Etc.,) is considered in the analysis. In the second case, an average drive of 100 km under a half sunshine hour (PV power = $0.5 W_p = 1.44$ kW). In the third case, an average drive of 100 km during night time (PV power = 0). Table 4.2 summarizes different cases, and it is clear that when compared with a BEV, the proposed HSEV can achieve higher vehicle performance and energy efficiency with a lower main source size utilizing the PV energy. All the environmental and driving conditions considered in this work satisfies the actual EV scenario.

Table 4.2: Cases of electric vehicle drive

Parameters	Case-I	Case-II	Case-III	BEV
Daily energy demand (Wh)	3,100	3,100	3,100	3,100
Monthly energy demand (additional 20% load changes) (Wh)	1,11,600	1,11,600	1,11,600	1,11,600
Monthly PV energy generation (Wh)	95,478	47,739	0	0
Monthly source energy consumption (Wh)	16,122	63,861	1,11,600	1,11,600
Monthly electricity cost (INR)	161.22	638.61	1,116.00	1,116.00
Monthly source capacity loss (%)	0.0012	0.00053	0.0004	0.335
Daily 3W EV drive distance(km)	100	100	100	100
Daily PV range (km)	85	42	0	0
Monthly grid charging instants	6	22	30	20

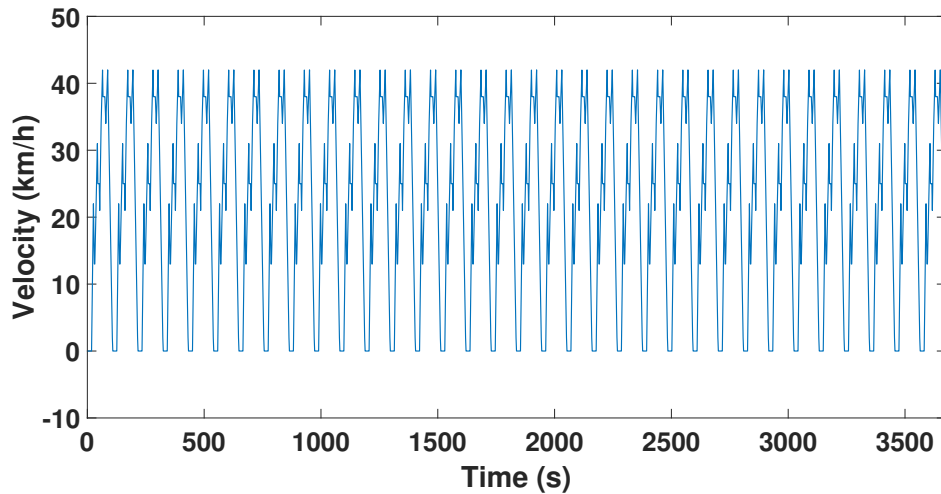
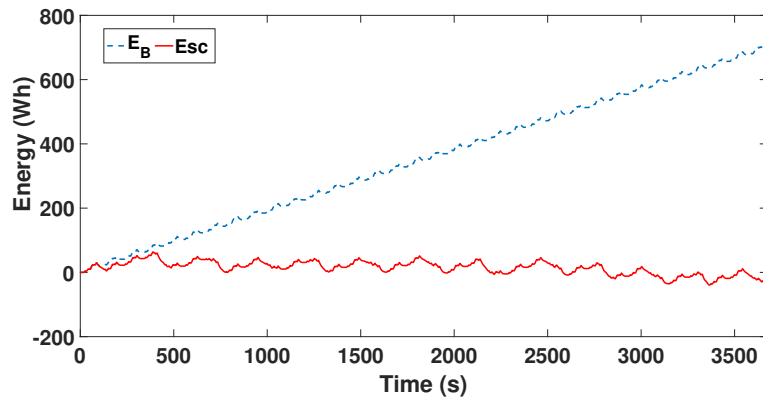
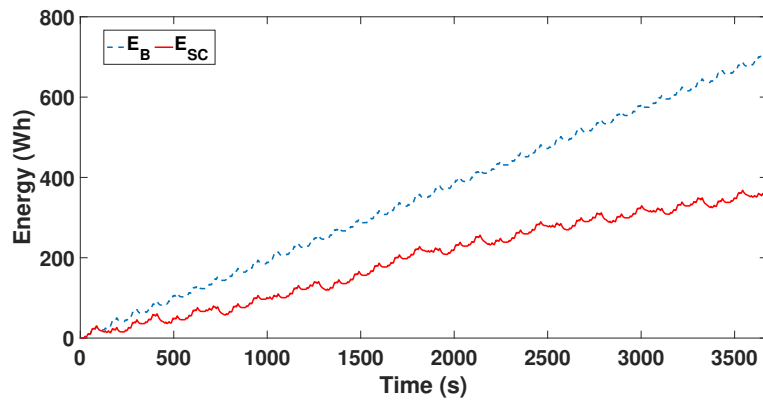


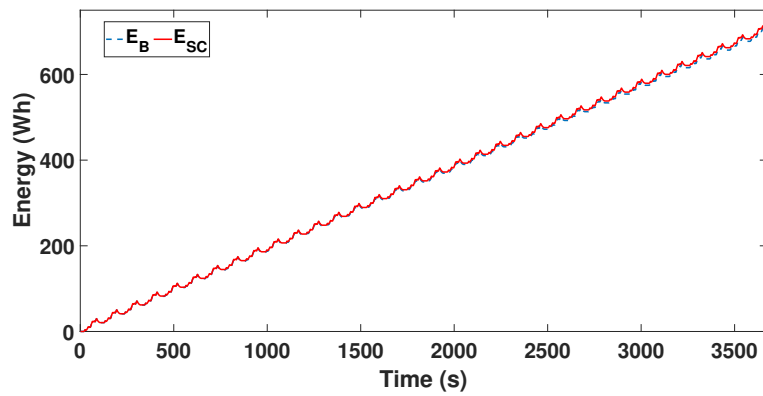
Figure 4.4: Combined 34 repeated IDC test profile



(a)

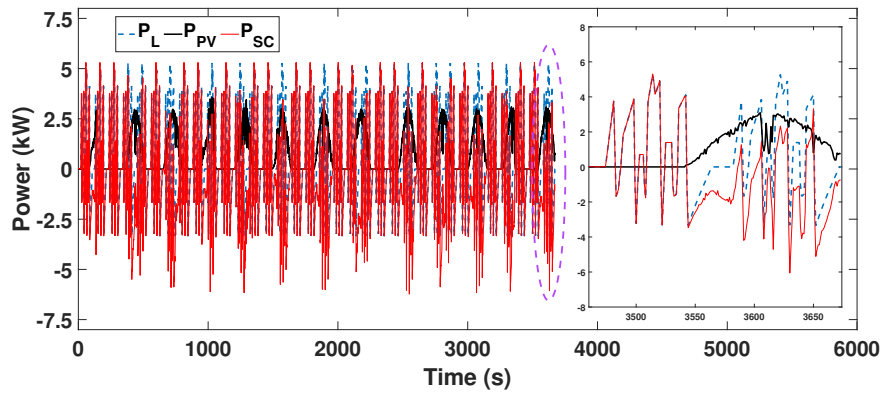


(b)

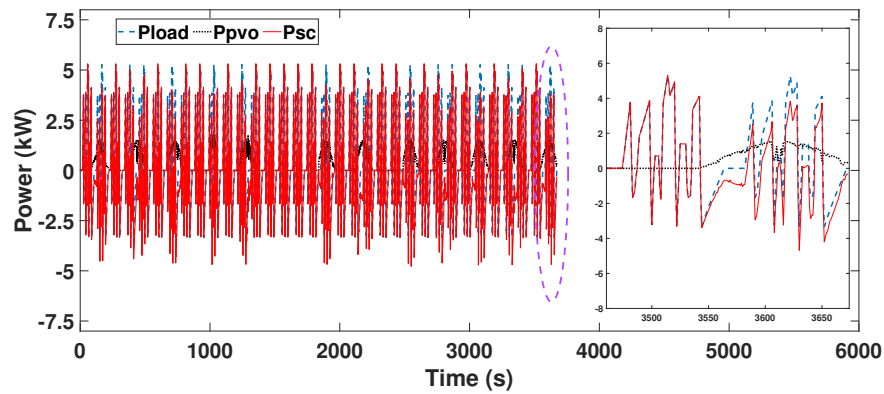


(c)

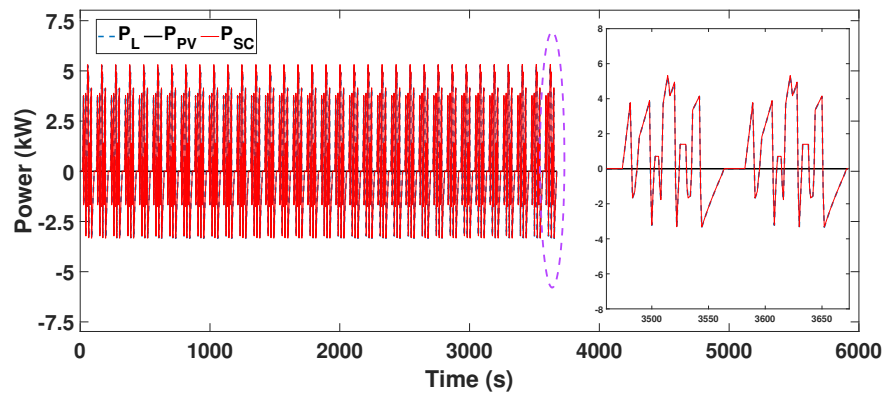
Figure 4.5: Energy consumption comparison for varying PV irradiance cases under 34 IDC cycles (a) Case-I (b) Case-II (c) Case-III.



(a)

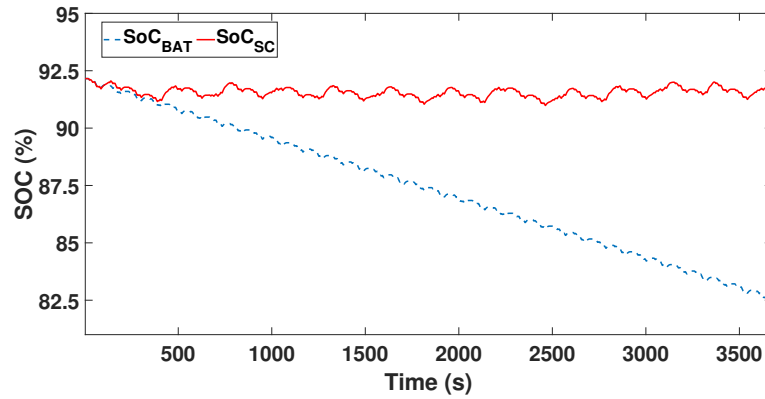


(b)

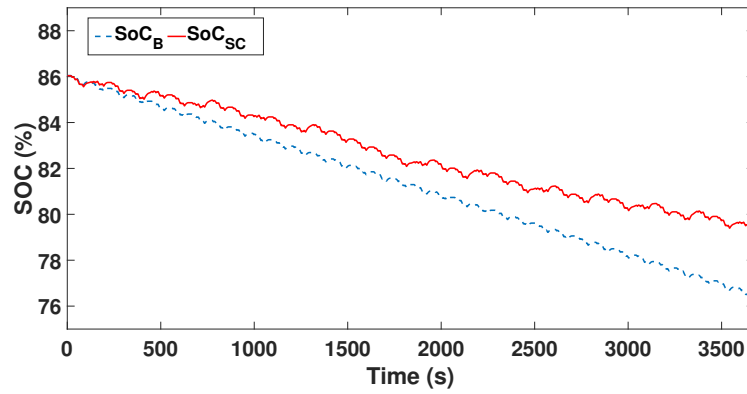


(c)

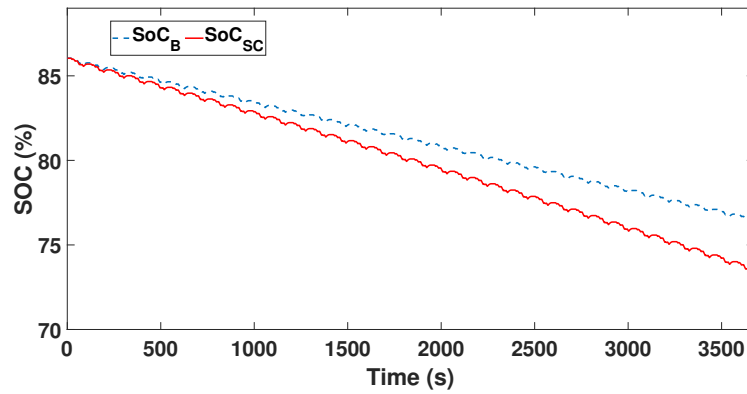
Figure 4.6: Power flow analysis for varying PV irradiance cases under 34 IDC cycles (a) Case-I (b) Case-II (c) Case-III .



(a)



(b)

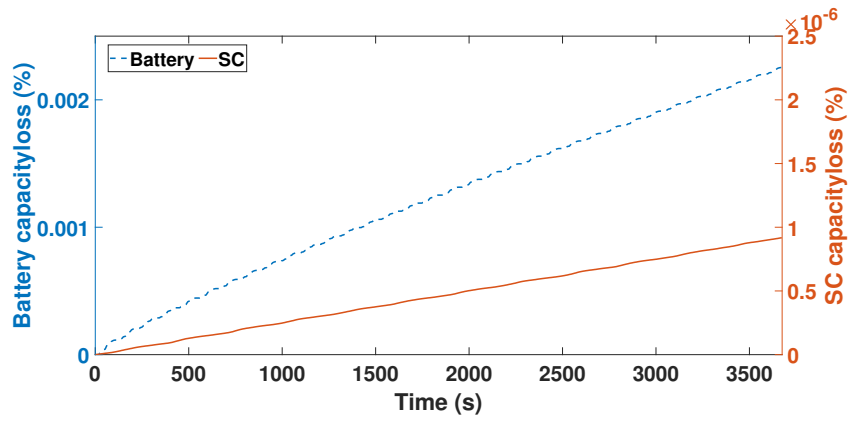


(c)

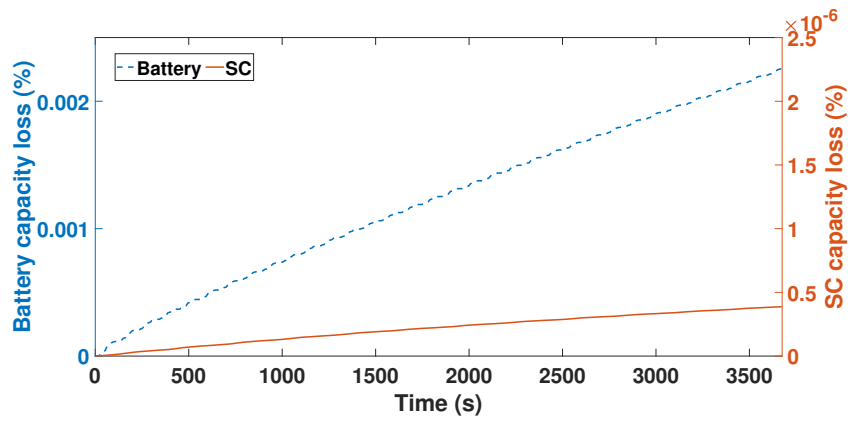
Figure 4.7: SOC comparison for varying PV irradiance cases under 34 IDC cycles (a) Case-I (b) Case-II (c) Case-III.

Comparison results of the proposed SC-PV vehicle and BEV run under varying irradiance cases are illustrated in figure 4.5-4.9 for each case under similar driving conditions (IDC). AIS-039 (Rev1):2015 details the application of 34 cycles of IDC (108 sec each) to evaluate the electrical energy consumption for the L category of

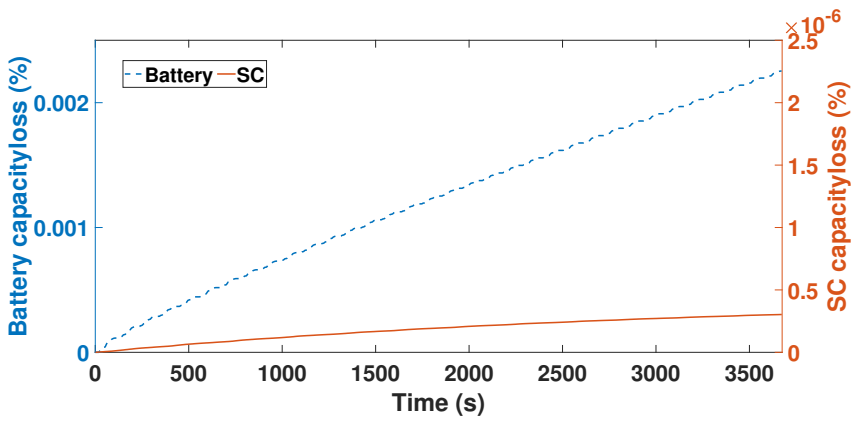
vehicles followed in the analysis. Figure 4.4 shows the combined driving velocity profile of 34 repeated test IDC cycles. Hence a total drive distance of 22.372 km (34 IDC cycles-1.02 hours of vehicle run) is considered the test drive for the analysis of each case [consumption ARAI, 2021]. Energy consumption (EC) of the primary source, i.e., Li-ion battery in BEV and SC in SC-PV vehicle, during the three different cases are shown in Figure 4.5. The average energy consumption of the main source SC in SC-PV vehicle is reduced by 85.56 % and 42.78 % compared to the Battery in BEV for Case-I and II, respectively. The utilization of PV energy is significant for EVs and is clear from the analysis. Figure 4.6 shows an analysis of the BEV and SC-PV vehicle's power flow and highlights the importance of the proposed EMA in SC-PV vehicles. In each case, the EMA achieves the impact of PV energy with the adaptive variation of SC power usage considering the irradiance conditions. In case I, PV power contributes a high portion of the load power, improving the SC-PV vehicle range, and in case III, SC handles a major portion of load power since PV power is lower. The EMA ensures the availability of SC during the peak and sudden variations in environmental conditions (irradiance), as discussed in this section. The SPM and DPM modes are switched throughout the drive, exhibiting the significance of EMA. The range of the vehicle is detailed with the SOC plots in figure 4.7. SOC of the battery (BEV) and SC (SC-PV) are discussed, and the final SOC of the proposed HSEV is improved for case-I (initial SOC=92%) and II (initial SOC=86%) by 11.21 % and 4.5 %. Due to the non-availability of PV energy during case-III (initial SOC=86%), the final SOC of the SC-PV vehicle is reduced by 4.4 % compared to BEV.



(a)

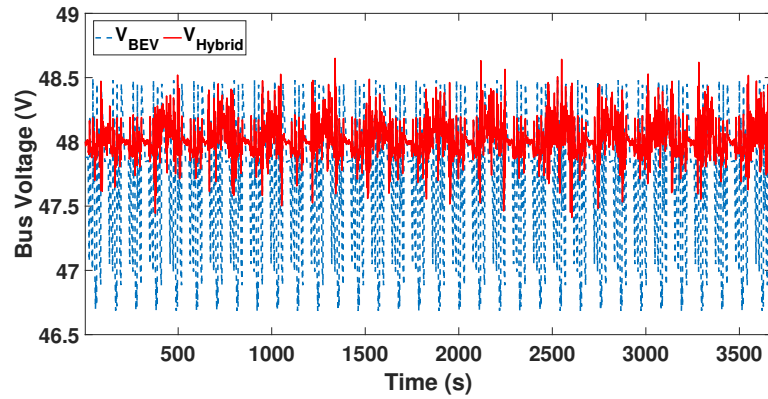


(b)

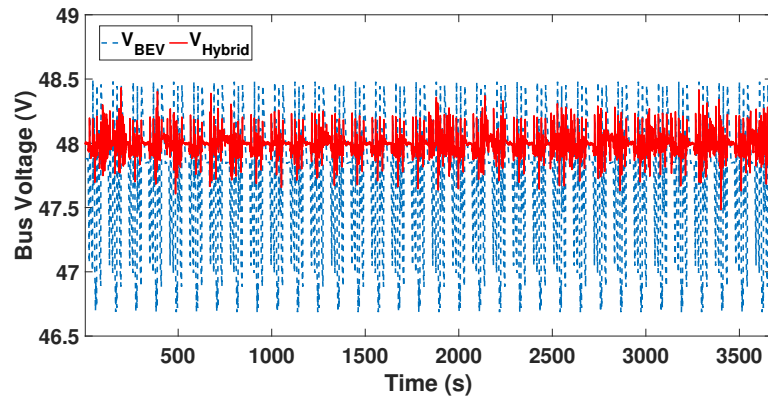


(c)

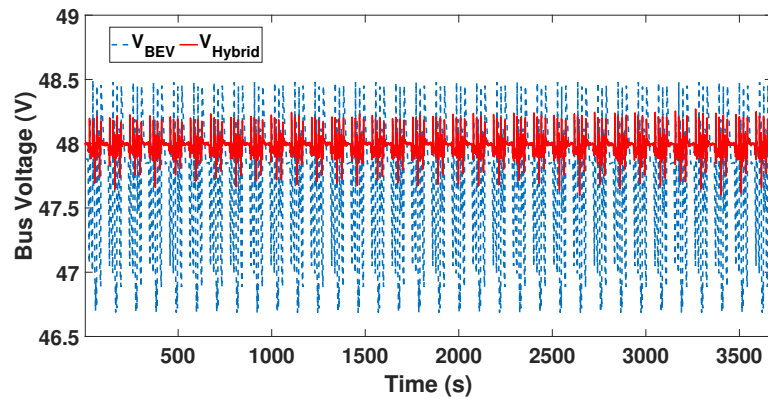
Figure 4.8: Capacity loss comparison for varying PV irradiance cases under 34 IDC cycles (a) Case-I (b) Case-II (c) Case-III.



(a)



(b)



(c)

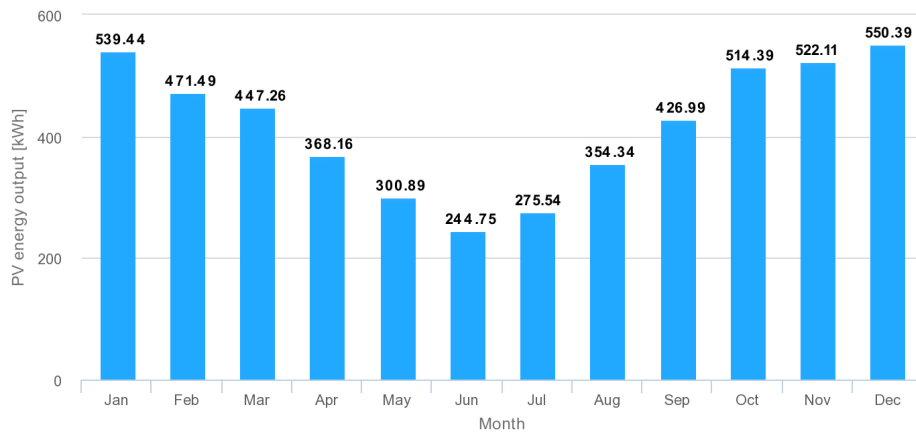
Figure 4.9: DC bus voltage comparison for varying PV irradiance cases under 34 IDC cycles (a) Case-I (b) Case-II (c) Case-III.

Moreover, the lower SC capacity loss is the significant impact of employing SC as the primary source in EV. Battery capacity loss is higher than the SC due to the chemical compositions in the battery. The battery Arrhenius model and SC degradation model are employed for the analysis of capacity losses (Section

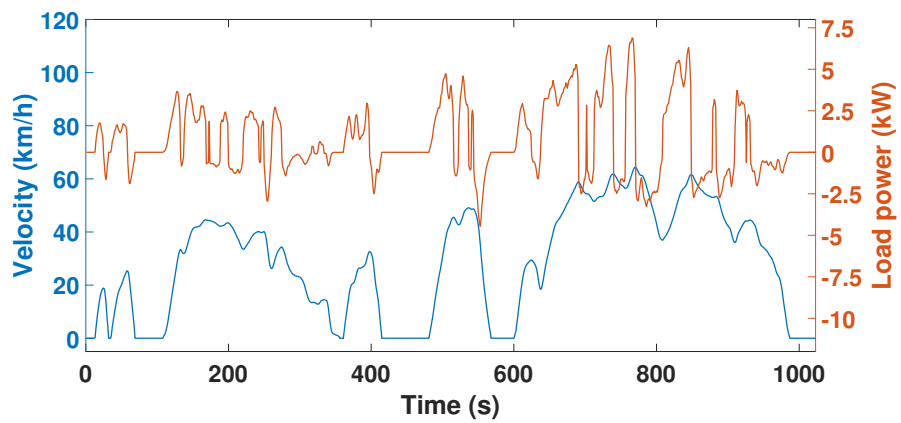
1.3.1, 1.3.2). Degradation of battery and SC for each case are discussed in figure 4.8. For all the cases, SC experiences lower capacity losses. Due to the higher fluctuations in PV energy in case-I and case-II, SC capacity loss is the lowest in case-III. Similarly, DC bus voltage fluctuations for each case are explained in figure 4.9. Bus voltage fluctuations of the proposed SC-PV vehicle are lower compared to BEV. All the comparative analysis with BEV and proposed HSEV is tabulated in Table 4.2. The study on varying irradiance cases exhibits the significance of PV energy and SC in the EV source and highlights the role of hybrid sources in future sustainable transportation modes.

4.4.2 Cases of EV run under varying driving locations

In tropical countries with high irradiance throughout the year, the EV source charging from the grid could be reduced. As a real-world analysis of each irradiance case, EV drives at different locations/terrains (driving profiles) are selected, which display the significance of the proposed EMS. EMA manages the energy management of hybrid sources based on the varying driving conditions (terrain/profiles). The locations are selected based on the variations in PV energy generation and the driving conditions (terrain/profiles). Firstly the energy generation is selected from New South Wales, Australia (31.2532° S, 146.9211° E) under a WLTP class-1 driving profile, Bangalore, India (12.9716° N, 77.5946° E) under an Indian driving cycle (IDC) and finally Scotland, Europe (56.4907° N, 4.2026° W) under ECE driving profile. Monthly PV energy generation of real locations with their maps and respective driving profiles are shown in figure 4.10-4.12 respectively. The yearly average PV generation from New South Wales is 5040 kWh. An average monthly PV energy generation is expected to be 420 kWh in New South Wales. Similarly, Bangalore, India, and Scotland generate monthly PV generation of 360 kWh and 155 kWh, respectively.

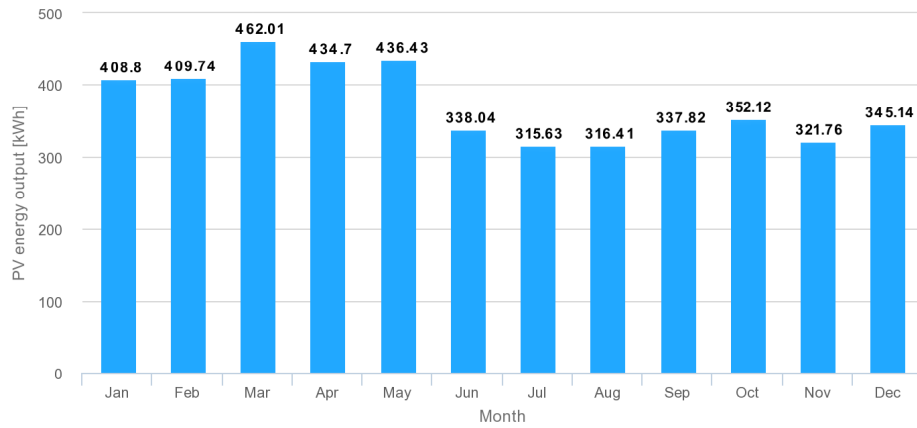


(a) Monthly PV energy generation (kWh) at New South Wales

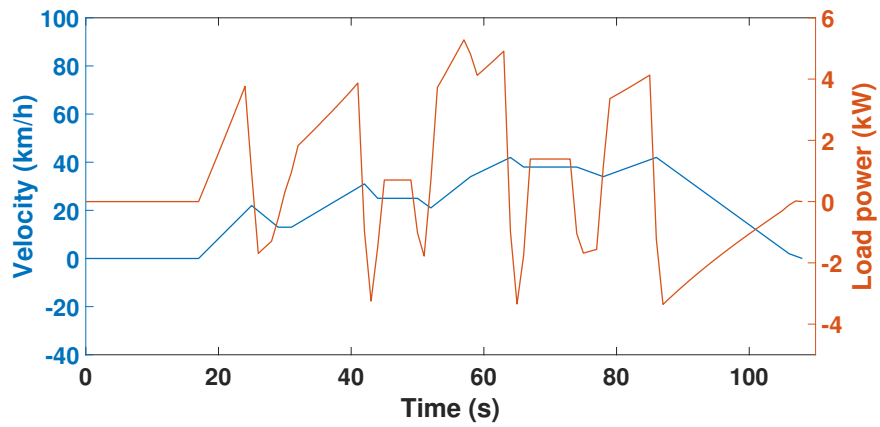


(b) Velocity and load power under WLTP class-1 driving profile

Figure 4.10: PV energy generation (kWh) and standard driving profile (WLTP class-1) in New South Wales, Australia (31.2532° S, 146.9211° E).

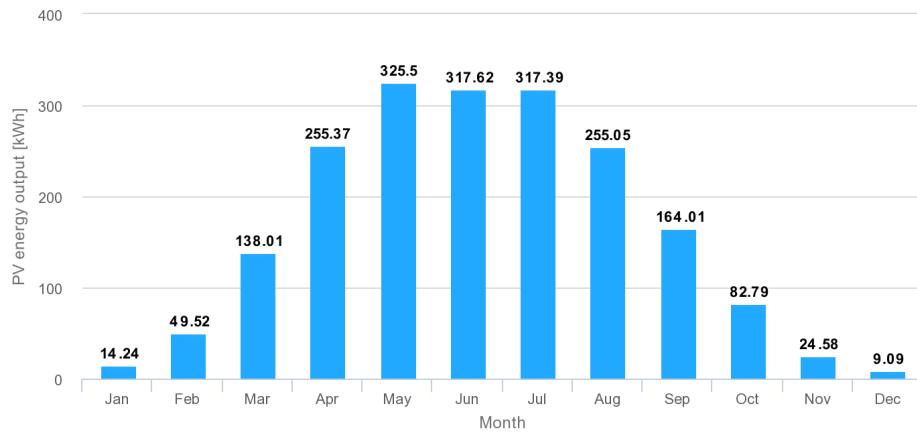


(a) Monthly PV energy generation (kWh) at Bangalore, India

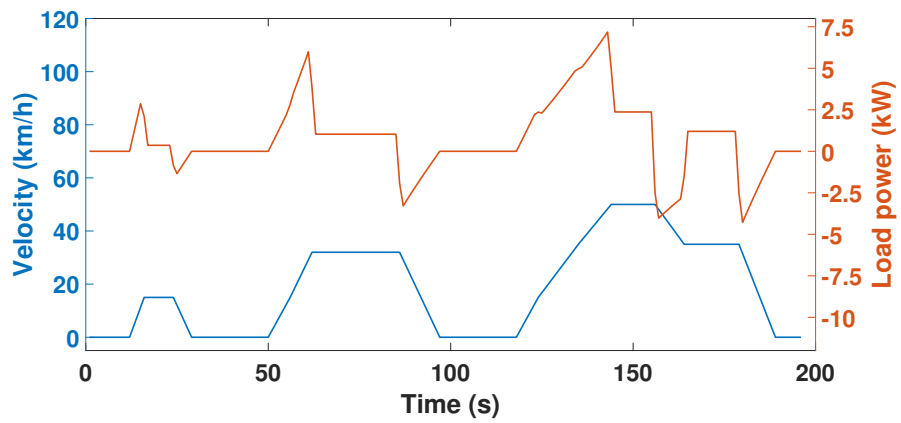


(b) Velocity and load power under IDC

Figure 4.11: PV energy generation (kWh) and standard driving profile (IDC) in Bangalore, India (12.9716° N, 77.5946° E).



(a) Monthly PV energy generation (kWh) at Scotland, Europe



(b) Velocity and load power under ECE driving profile

Figure 4.12: PV energy generation (kWh) and ECE driving profile in Scotland (56.4907° N, 4.2026° W).

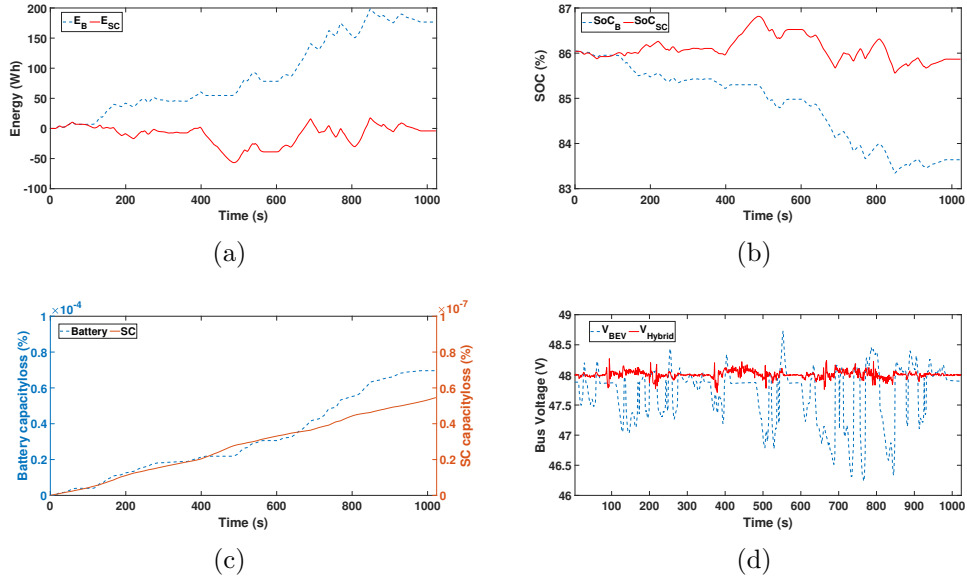


Figure 4.13: EV Performance analysis of BEV and SC-PV vehicle at New South Wales, Australia under WLTP class-1 driving cycle (a) Energy consumption (b)Source SOC (c) Source capacity loss (d) DC bus voltage.

Result analysis of the proposed SC-PV vehicle and BEV are illustrated in figure 4.13-4.16 for each location (Australia, India, Scotland) under respective different driving conditions (WLTP class-1, IDC, ECE) selected based on the locations. Battery degradation under varying driving behaviors and terrains is discussed in this section. Table 4.3 tabulates all the result analyses in this section with varying driving locations. The BEV is selected as a benchmark to compare with SC-PV vehicle in each location with similar charge states and driving conditions. Proposed EMA is significant and ensures an optimal operation of the HSEV under selected driving conditions based on locations. The results show the impact of the control algorithm by switching the hybrid source system operation into different modes (SPM and DPM).

The degradation models for battery and SC discussed in (Section 1.3.1, 1.3.2) are employed in the proposed work. The capacity loss of battery (BEV) and SC (SC-PV vehicle) for each location are discussed in figure 4.13c, 4.14c and 4.15c and exhibit the significance of using the proposed vehicle for varying conditions under different locations with their respective terrains and driving profiles. SC capacity is least affected due to the varying load conditions, and there is less chance of replacement and maintenance than the battery, which reflects positive effects in the economic and environmental aspects of the proposed vehicle. The EC of the primary source, i.e., Li-ion battery in BEV and SC in SC-PV vehicle, under Australia, India, and Scotland are shown in Figure 4.13a, 4.14a and 4.15a respectively. PV energy is highest under New South Wales, and EC from the primary source is 40 % less compared to the BEV under a single WLTP class-1 driving cycle, which enables the proposed vehicle to get recharged from the grid less frequently.

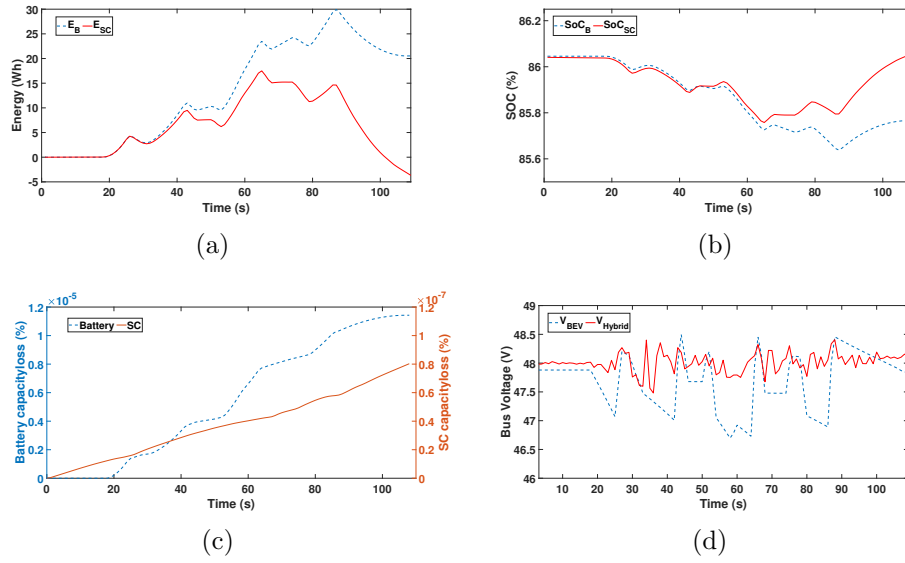


Figure 4.14: EV Performance analysis of BEV and SC-PV vehicle at Bangalore, India under Indian driving cycle (a) Energy consumption (b)Source SOC (c) Source capacity loss (d) DC bus voltage.

Similarly, the monthly energy consumption of the proposed vehicle under repeated

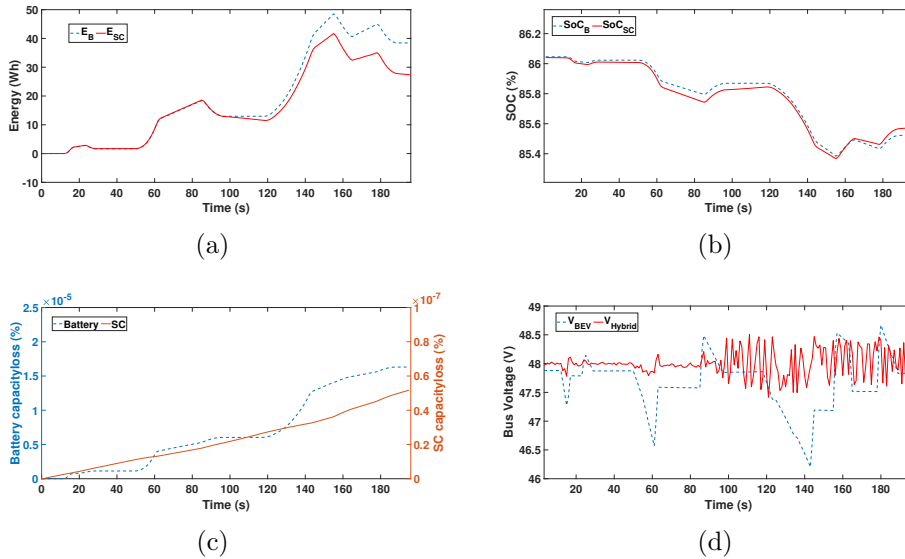
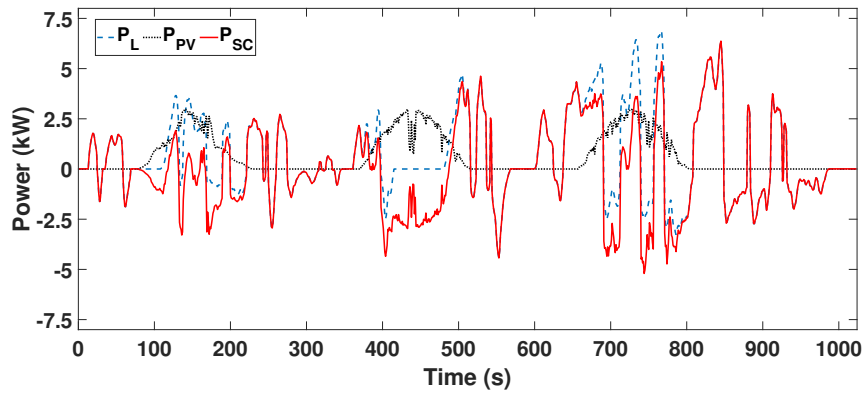


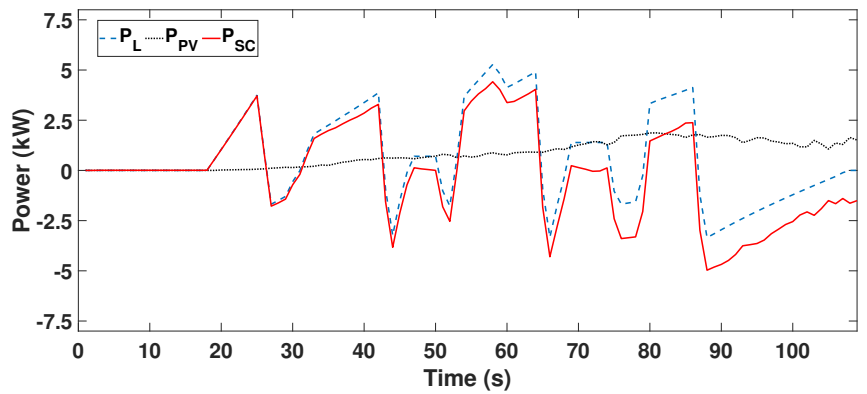
Figure 4.15: Performance analysis of BEV and SC-PV vehicle at Scotland under ECE driving cycle (a) Energy consumption (b)Source SOC (c) Source capacity loss d) DC bus voltage.

driving cycles of IDC and ECE reduces the overall energy consumption by 25% and 10% in India and Scotland, respectively. The effect of energy efficiency is reflected in the technical aspect (higher battery life) and economic aspect (fewer instants of charging from the grid). Detailed improvements of each aspect are tabulated

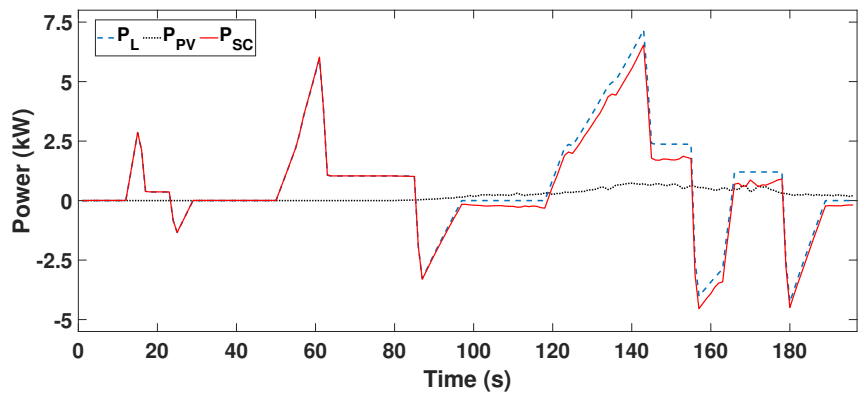
in Table 4.3. SOC of the battery and SC are discussed in figure 4.13b, 4.14b, and 4.15b, respectively, for each location. DC bus voltage regulation is shown under various locations compared with BEV in figure 4.13d, 4.14d, and 4.15d. The proposed HSEV reduces the DC bus voltage fluctuations under Australia, India, and Scotland when compared to a BEV driving in the respective locations under same conditions. A comparison of DC bus voltage fluctuations with BEV under similar conditions are detailed in Table 4.3. The significance of SC response in handling sudden variations in load power regulates the DC bus voltage. Figure 4.16 shows an analysis of the BEV and SC-PV vehicle's power flow and highlights the significance of the proposed EMA. For each location, the PV power improves the energy efficiency based on their respective irradiance. The proposed EMA manages the power flow among PV and SC to meet the P_L and SC absorbs the PV fluctuations (charging or discharging) in quick instants, which does not allow the fluctuations to affect the EV motor drive.



(a)



(b)

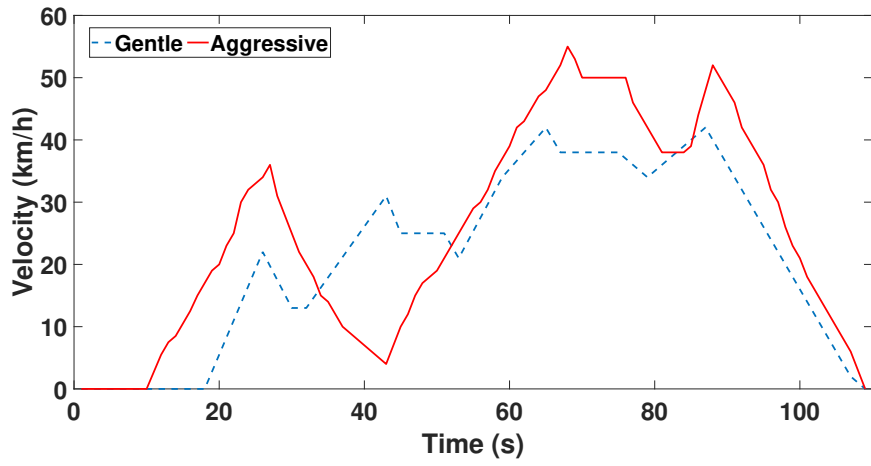


(c)

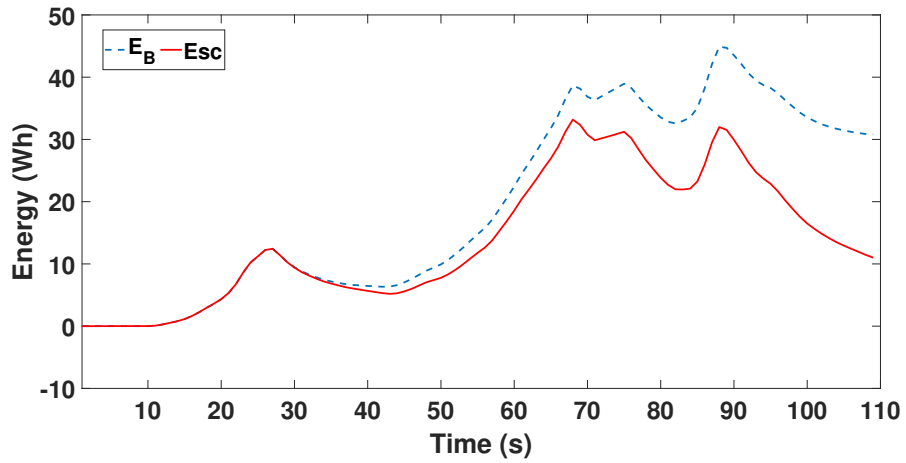
Figure 4.16: Power flow analysis for varying driving locations cases (a) NSW (b) Bangalore (c) Scotland.

4.4.3 Cases of sudden load demand fluctuations in EV drive

Electric vehicles are trending worldwide, and their sales shares are expected to reach around 60 % by 2030 to reach the Net Zero CO₂ in 2050 [IEA-EV, 2022]. The increasing adoption rate of EVs worldwide needs detailed investigations on the energy management systems due to the highly varying nature of the driving conditions (vehicle-related, driver-related, and environmental-related [Vishnu et al.,]. The significant concept to analyze is the sudden variation in driving profiles under different road terrain (locations) and driving behaviors. Proposed SC-PV vehicles exhibit an improved performance during varying or fluctuating unexpected driving variations. An (Indian driving cycle) IDC is chosen as a base driving cycle to investigate the sudden load demand fluctuations. The velocity profiles tested under the unexpected load demand fluctuations with the standard IDC profile are shown in figure 4.17a. The energy consumption of the main source in BEV and the proposed vehicle is analyzed in figure 4.17b. The plot shows the increase (50 % increase) in energy consumption due to unexpected load variations in the IDC profile due to aggressive driving. Such sudden load variations increase the C-rates and highly affect the battery capacity, as shown in figure 4.18. The analysis exhibits the significance of the EMA by maximizing the utilization of SC as the primary source in EVs during the peak and fluctuating load instants since, in BEV, the battery gets sudden high C-rates and increased operating temperature, accelerating its deterioration. The control diagram of the proposed modified EMS reduces the stress on switches of the converter and ensures the immediate action of SC during a dip or rise in the load power demand due to the aggressive driving scenarios. Such an effective control algorithm improves the performance of the vehicle.



(a) Gentle and aggressive velocity profiles



(b) Energy consumption of BEV and SC-PV vehicle

Figure 4.17: Comparison of BEV and SC-PV vehicle under sudden load fluctuations.

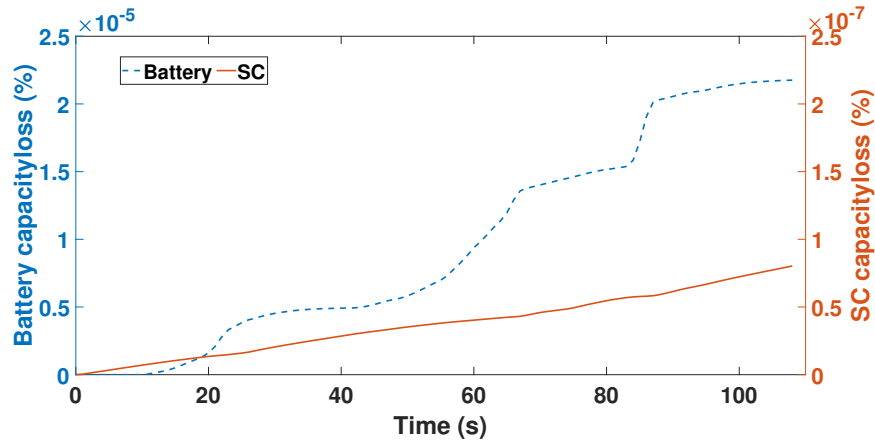


Figure 4.18: Comparison of source capacity loss for BEV and SC-PV vehicle under unexpected load demand fluctuations

4.4.4 Technical parametric analysis

The overall analysis of the proposed EV is summarized in the section, and a comparison with BEV on technical and economic aspects is tabulated in Table 4.3. Since the EV users are highly diverse, three different driving locations are selected considering their location, terrain, and environmental conditions, as discussed in the previous section 4.4.2 (Australia, India, and Scotland). Daily driving distance of 100 km is considered for each location with repeated similar driving cycles (12 repeated (8.1 km per cycle) cycles of WLTP class-1, 154 repeated (0.65 km per cycle) cycles of IDC, 99 repeated (1.01 km per cycle) cycles of ECE). Table 4.3 discusses the following technical parameters: Capacity, EC, Peak power under respective driving cycles, Capacity loss (100 km run), Lifespan improvement, DC bus voltage fluctuations, and Monthly grid charging instants. A reduction of 51.15% in the capacity of the main source is achieved for similar performance BEV. PV energy improves the energy efficiency of the proposed system. Total daily (100 km run) energy consumption of the main source under each driving cycle for respective locations shows a reduction of 86.79%, 57.91%, and 15.3% for Australia, India, and Scotland, respectively, compared to BEV.

Capacity loss is a significant aspect since it is very low for the SC compared to lithium-ion battery; hence, the former can easily handle varying charge-discharge, road terrain, driving profile, and environmental conditions. Equations described in section 1.3.2 and 1.3.1 are employed for the calculations. In the analysis of 100 km run (daily), the capacity loss of the main source under each location (Australia, India, and Scotland) is detailed and lowest for the Australia case due to the high energy contribution from PV and driving profile pattern. In turn, the SC lifespan improvements are 1296, 143, and 129 times higher compared to BEV under each location and profile. These huge improvements provide the edge for SC in the longer run. Moreover, the DC bus voltage fluctuations are lowest for SC-PV vehicles compared to BEV (5.2% and 1.16 %, 3.75% and 1.91 %, 5.15 %

Table 4.3: Performance analysis of EMSs under various locations

Parameters	BEV	AUS	IND	SCO
Main source capacity (kWh)	7.37	3.6	3.6	3.6
Reduction (compared to BEV %)	-	51.15	51.15	51.15
Daily source energy consumption (kWh)	2.12/3.16/3.8	0.28	1.33	3.225
Reduction (compared to BEV %)	-	86.79	57.91	15.13
Source Capacity Loss (%)	$0.85 \text{ e}^{-3}/1.77 \text{ e}^{-3}/0.64 \text{ e}^{-3}$	6.6 e^{-7}	1.23 e^{-5}	$4.95 \text{ X } 10^{-6}$
Source Life Span Improvement (times)	-	1296.87	143.54	129.41
DC bus voltage fluctuations (%)	5.2/3.75/5.15	1.16	1.91	2.28
Monthly grid charging instants (times)	10-19	3	13	32

and 2.28 %). PV energy in countries with higher solar irradiance can reduce EV grid charging. In Australia, monthly grid charging to meet the repeated WLTP cycle with the PV energy considered limits to 3. A daily commute with minimum daytime drive can further reduce the intervals of grid charging.

Table 4.4: Economic analysis of energy storage in electric vehicle [Eaton, 2022]

Parameters	BEV	SC-PV	
		SC	PV
Energy source cost (INR-Lakhs.)	1.10	7.29	0.92
Energy storage replacement	2	0	0
Total maintenance cost for 10 years (INR-Lakhs.)	4.40	0	0
Annual efficiency losses (INR-Lakhs.)	2.22	0.66	0.046
Annual cooling costs (INR-Lakhs.)	0.44	0.067	0.01
Total efficiency Cost for 10 years (INR-Lakhs.)	26.71	7.30	0.56
Total operations cost for 10 years (INR-Lakhs.)	31.11	7.30	0.56
10-year total cost of ownership (INR-Lakhs.)	32.22	14.59	1.49

Economic analysis is essential for emerging energy technologies. Hence the investigation is conducted for the total cost of ownership (TCO) for 10 years of vehicle usage [Sharma et al., 2012] [Eaton, 2022]. The proposed SC-PV vehicle is compared with the BEV, and all the parameters that need to be validated are detailed in Table 4.4. The replacement and maintenance of a lithium-ion battery is a critical issue that increases the cost of ownership in the longer run. The reduction in capacity loss of SC discussed in Table 4.3 reflects the outcome in the maintenance-free operation of SC. Similarly, the efficiency of SC is higher

compared to the lithium-ion battery (Table 1.2) which reduces the efficiency cost of SC. However total energy source cost of SC-PV vehicle includes that of both PV and SC. Even though the initial cost of an SC-PV vehicle is higher when compared with BEVs, the TCO analysis shows that in a long run, the cost of SC-PV vehicles is less than half of that of the BEVs to operate in similar driving conditions.

4.5 Summary

In this work, a high energy dense SC and PV based HSEV is introduced with the future trends of improvements in renewable energy sources and analyzing their significance of sustainable transportation. The proposed EMS manages the power flow among the hybrid source. It avoids the impacts of driving (load current) and environmental fluctuations under various locations (Australia, India, Scotland) and driving intervals (day, night). EMA is considered under two power modes 1) Surplus Power Mode and 2) Deficit power mode considering the power flow in the system. Modified dual loop controller reduces the stress and power loss of switches. The degradation of SC is evaluated in work and compared with Battery (BEV) to show the significance of the proposed HSEV structure. The results confirm the proposed HSEV model's effectiveness, which improves energy efficiency, reduces source maintenance/ replacements, improves lifespan, and reduces DC bus voltage fluctuations. Proposed HSEV exhibits a maximum impact in all aspects of the analysis in Australia, where average PV energy generation is highest throughout the year. Charging from the grid for the tested profile is reduced to 3 instants which shows the significance of PV energy-based solar vehicles. The major result analysis outcomes are as follows:

- The main source capacity of the proposed HSEV is reduced by 51.15 % compared to BEV (7.37 kWh to 3.6 kWh) to achieve a minimum range of 100 km per day.
- The source capacity loss is reduced in the proposed HSEV as SC is least affected by the fluctuating loads and thus does not requires any replacement throughout the vehicle life.
- Source energy consumption is significantly reduced in the proposed HSEV compared with BEV under similar driving conditions. It shows a reduction of 86.79%, 57.91%, and 15.13% under Australia (WLTP), India (IDC), and Scotland (ECE), respectively.
- DC bus voltage fluctuations are limited near to 2 % under all the driving locations and profiles considered, thus improving the motor drive performance.
- Analysis of unexpected driving variations due to terrain/traffic/driver behavior is discussed, and the proposed HSEV shows improved performance compared to BEV.
- Technical and economic parameter assessments are conducted to highlight

the significance of the proposed HSEV over the existing BEVs. The economic comparison reveals that initial costs on hybrid source vehicles cross the break-even point before half-life in a longer run.

The proposed HSEV concept enlightens the following topics of EV research: 1)As a future work, improvement in energy density and cost reduction in research for SC manufacturing can speed up the SC-based EVs in the market. 2)Similarly, improving PV cell conversion efficiency to higher levels can shift a complete transformation of the transportation sector towards a sustainable and green mode.

Chapter 5

Conclusion and Future Scope

The major share of the rise in CO₂ emissions is from the transportation industry, which accelerates global warming. Moreover, the rise in fossil fuel prices and their shortage in availability are other major issues that enable the development of a green and clean transportation mode. Transition to EVs from IC engine vehicles can be achieved by developing accurate solutions to the current problems. Recent implementation and development of intelligent transport systems into the EV sector have improved the adoption of EVs. In the context of the expected growth of EVs in the current scenario, keen attention must be invested in the improvement of EV sources.

5.1 Conclusion

Globally, witness to a sustainable economy depends on the rapid development of renewable energy applications. In this context, a hybrid source with a renewable background plays a crucial role in transportation. The present work highlights the importance of EMS for hybrid source EVs with the design and simulation modeling. The proposed Intelligent Hybrid Source Energy Management Strategy (IHSEMS) allocates the load power to enhance the performance of the EV. The IHSEMS effectively manages the effects of varying driving conditions by using an absolute energy sharing algorithm (AESA). Incorporating solar and supercapacitors with existing BEVs improves battery life and energy efficiency. The SMC and FDS strategies are analyzed in the comparative study. With this thought, the main contributions of this thesis are the proposal, investigation, and verification of different hybrid source system models and respective energy management strategies to ensure optimal source operations. The proposed energy management algorithm outcomes an optimal and intelligent power allocation among each source. A detailed technical and economic investigation is reported to validate the reliability and significance of the proposed hybrid source EV system. The general conclusion of each chapter has been collected as follows:

Chapter 1 briefly introduced the current transportation scenarios where the extensive background study is conducted. The issues of lithium-ion batteries due to the varying driving and environmental conditions are detailed, followed by the significance of hybrid sources in EVs. Moreover, the importance of renewable energy sources in the current energy scenario is also highlighted. Energy management plays a vital role in improving the performance of hybrid source EVs and ensuring optimal source operations.

Chapter 2 comprehensively reviews the drawbacks of existing electric vehicles, characteristics and comparison of hybrid sources, DC-DC converter topologies, and energy management strategies (EMSs). The significance and drawbacks of each topology, EMSs, are detailed throughout the chapter. As an outcome, it was learned that despite many solutions capable of efficient energy management with complex modeling and huge data collections, an opportunity for developing an alternative way of achieving the same endures with improved optimality and safe operation of sources.

Chapter 3 proposed a hybrid source system with battery, SC, and PV as the sources. An Intelligent Hybrid Source Energy Management Strategy (IHSEMS) with an absolute energy sharing algorithm (AESAs) is designed and developed to optimize the energy sharing among each source considering the driving and environmental conditions employing a fuzzy logic controller. The IHSEMS also ensures the availability of SC during each instants of driving and braking to discharge and charge respectively throughout the driving period. A techno-economic assessment that includes battery capacity loss, battery life, DC bus voltage fluctuations, battery degradation cost, and total cost of operation is conducted, which compares the existing EMSs (State machine control, Frequency decoupling strategy) and BEVs to highlight the significance of the proposed hybrid model and IHSEMS.

Chapter 4 proposed a hybrid source combination with high energy-dense SC and high conversion efficient PV panels. A modified Energy Management Algorithm (EMA) considers various modes and sub modes to ensure the safety and performance of the vehicle throughout the drive. A detailed techno-economic investigation is preformed with proposed hybrid EV and existing BEVs and the impact of SC-PV vehicles are higher for tropical countries. It achieves high improvement in terms of source life time, vehicle performance and reduction in charging from grid and recharging time which eventually shifts towards a complete green and sustainable transportation sector and improves the user interests respectively. Moreover, the economic comparison reveals that initial costs on SC-PV vehicles cross the break-even point before half-life in a longer run when compared to BEVs of similar type.

5.2 Contributions

This dissertation presents the modeling, design, and analysis of a hybrid source energy management strategy with various hybrid source electric vehicle (HSEV) models. The methodology of each proposed hybrid models and their respective energy management algorithm are described in the dissertation. The main contributions of this research are outlined as follows:

- A hybrid source system is proposed which includes Li-ion Battery, Supercapacitor (SC), Photovoltaic (PV) panels for an Electric 3W which improves the energy efficiency, range, safety and life cycle of the sources.
- An intelligent absolute energy sharing algorithm (AESA) is developed to allocate the power among each sources at varying driving and environmental conditions without any complex modeling and data collection.
- The energy optimization is ensured along with the availability of SC to support the battery throughout the driving interval by the AESA which implemented using fuzzy logic controller.
- A new hybrid energy vehicle is proposed with a high energy dense SC and high conversion efficient PV panels and an Energy Management Algorithm (EMA) is developed to ensure the safety and energy efficiency of the sources.
- Techno-economic assessment is conducted for both the proposed hybrid source systems and EMSs for EVs and compared with BEVs and existing EMSs that highlights the significance of proposed system.

5.3 Future Scope of Work

From this dissertation, the following are suggestions for future research.

- The next step of this work includes the extension of the proposed methodology into larger vehicles to highlight the PV capabilities to adequately cover the modern BEV's energy needs under normal consumption conditions (200-300 km per week).
- Hardware implementation of the proposed hybrid source electric vehicle and testing the vehicle on the real drive.
- The key to the success of hybrid source in EVs is the combination of eco-friendly driving behavior (e.g., smooth accelerations and decelerations, low average speeds, daytime driving, parking, and charging outdoors) with the use of marginally sufficient electric motors for the actual transportation needs which require a fundamental change of the current automotive industry way of marketing and thinking.
- The future of electrified transportation is based on a smart city where mo-

bility can be used as a service, connected vehicles, Advanced Driver Assistance Systems and automated driving system employing V2X infrastructures. Such intelligent aspects improves the level of energy management in hybrid source electric vehicles (HSEV).

Appendix A

Resistive Forces Opposing Electric Vehicle Motion

Further analysis of the EV modeling discussed in Chapter 3 is presented here. The longitudinal mathematical model of electric vehicles is discussed below with necessary equations of motion and resistive forces. The longitudinal motion of the vehicle in the forward direction with slope is illustrated in figure 3.2 in Chapter 3. The following are the resistive forces that need to be overcome by the vehicle traction unit to achieve the required acceleration for the vehicle.

A.1 Frictional Force

Frictional forces, F_{roll} occur due to the friction between the tire and the road. Reference values of rolling coefficient f_r vary for different road types as shown in Table A.1. Therefore, the resistive force is expressed as in Equation A.1 [NPTEL:, 2018]:

$$F_{ad} = M_T \cdot g \cdot f_r \cdot \cos(\alpha) \quad (\text{A.1})$$

where M_T is the gross weight of the vehicle, g is the acceleration due to gravity, f_r the rolling resistance coefficient, α the gradeability angle.

A.2 Aerodynamic Drag Force

The aerodynamic drag force, F_{ad} is the resistive force due to wind opposition during the motion. The force varies based on wind velocity, the frontal area A_f of the vehicle, and the drag coefficient, C_D which varies for different vehicles. The opposing force is expressed in terms of Equation A.2 shown below [NPTEL:, 2018]:

Table A.1: Reference values for the rolling resistance coefficient .

Conditions	Rolling resistance coefficient (f_r)
Tire on smooth tarmac road	0.01
Tire on concrete road	0.011
Tire on a rolled gravel road	0.02
Tar macadam road	0.025
Unpaved road	0.05
Bad earth tracks	0.16
Loose sand	0.15-0.3
Truck tire on concrete or asphalt road	0.006-0.01
Wheel on iron rail	0.001-0.002

$$F_{roll} = \frac{1}{2} \cdot \rho \cdot A_f \cdot C_D \cdot V^2 \quad (\text{A.2})$$

where ρ the air density, A_f the frontal area of the vehicle, C_D the drag coefficient, V the velocity of the vehicle.

A.3 Grading Force

The grading force, F_g is the resistive force that occurs during the uphill of the vehicle on a slope road. It opposes the tractive force during the uphill slope and aids during the downhill slope. The main parameter that defines grading force is the angle of the uphill which varies based on road conditions or terrains. The grading force is represented using the equation A.3, [NPTEL:, 2018]:

$$F_g = M_T \cdot g \cdot \sin(\alpha) \quad (\text{A.3})$$

where M_T is the gross weight of the vehicle, g is the acceleration due to gravity, α the gradeability angle.

A.4 Acceleration Force

The acceleration force, F_a , is significant in moving the vehicle forward at the required speed the driver decides. It varied with the driver behavior and expressed as in equation A.4, [NPTEL:, 2018]:

$$F_a = \lambda \cdot M_T \cdot \frac{dV}{dt} \quad (\text{A.4})$$

where λ the rotational inertia constant, M_T is the gross weight of the vehicle, V the velocity of the vehicle.

The total resistive force which opposes the motion of the vehicle is the summation of all the forces as shown in Equation A.5. The motor must deliver the power in order to overcome these opposing forces as discussed in Equation 3.1-3.3 in Chapter 3.

$$F_{res} = F_{roll} + F_{ad} + F_g + F_a \quad (\text{A.5})$$

Bibliography

- [Abdul et al., 2022] Abdul, Ghani, O., Qaisar, A., Ahmed, Al, M., and Mohammad, Ali, A. (2022). Supercapacitors as next generation energy storage devices: Properties and applications. *Energy*, 248(2022):1–8.
- [Agrawal and Pandey, 2008] Agrawal, R. C. and Pandey, G. P. (2008). Solid polymer electrolytes: materials designing and all-solid-state battery applications: an overview. *Journal of Physics D: Applied Physics*, 41:1–18.
- [Ahmadi et al., 2014] Ahmadi, L., Fowler, M., Young, S. B., Fraser, R. A., Gaffney, B., and Walker, S. B. (2014). Energy efficiency of li-ion battery packs re-used in stationary power applications. *Sustainable Energy Technologies and Assessments*, 8:9–17.
- [Akar et al., 2017] Akar, F., Tavlasoglu, Y., and Vural, B. (2017). An energy management strategy for a concept battery/ultracapacitor electric vehicle with improved battery life. *IEEE Trans Transp Electr*, 3:191–200.
- [Alobeidli and Khadkikar, 2018] Alobeidli, K. and Khadkikar, V. (2018). A new ultracapacitor state of charge control concept to enhance battery lifespan of dual storage electric vehicles. *IEEE Transactions on Vehicular Technology*, 67(11):10470–10481.
- [Amin et al., 2017] Amin, M. A., Apostolos, P., Srithar, R., Ricardo, M.-B., and Vahid, E. (2017). A review of battery electric vehicle technology and readiness levels. *Renewable and Sustainable Energy Reviews*, 78:414–430.
- [Amine et al., 2020] Amine, L., Riadh, A., Ahmed, Chiheb, A., Ali, S., and Pascal, V. (2020). Reinforcement learning based adaptive power sharing of battery/supercapacitors hybrid storage in electric vehicles. *Energy Sources, Part A: Recovery, Utilization, and Environmental Effects*, pages 1–22.
- [Arunkumar et al., 2022] Arunkumar, C., Udaya, Bhasker, M., and Srinivas, P. (2022). Supercapacitor voltage based power sharing and energy management strategy for hybrid energy storage system. *Journal of Energy Storage*, 50:104232.
- [Bernard et al., 2006] Bernard, J., Delprat, S., Buechi, F., and Guerra, T. (2006). Global optimisation in the power management of a fuel cell hybrid vehicle (fchv).

- In *2006 IEEE Vehicle Power and Propulsion Conference*, pages 1–6. IEEE.
- [Blanes et al., 2013] Blanes, J. M., Gutiérrez, R., Garrigós, A., Lizán, J. L., and Cuadrado, J. M. (2013). Electric vehicle battery life extension using ultracapacitors and an fpga controlled interleaved buck–boost converter. *IEEE Transactions on Power Electronics*, 28(12):5940–5948.
- [Bonfiglio and Roessler, 2009] Bonfiglio, C. and Roessler, W. (2009). A cost optimized battery management system with active cell balancing for lithium ion battery stacks. *IEEE Vehicle Power and Propulsion Conference*, pages 304–309.
- [Boulanger et al., 2011] Boulanger, A. G., Chu, A. C., Maxx, S., and Waltz, D. L. (2011). Vehicle electrification: Status and issues. *proceedings of the IEEE*, 99(6):1116–1138.
- [Brida et al., 2021] Brida, V. M., Lennert, V., Klaas, T., and Geert, D. (2021). A hybrid policy gradient and rule-based control framework for electric vehicle charging. *Energy and AI*, 4(2021):12416–12429.
- [Brito et al., 2021] Brito, M. C., Santos, T., Moura, F., Pera, D., and Rocha, J. (2021). Urban solar potential for vehicle integrated photovoltaics. *Transportation Research Part D: Transport and Environment*, 94. <https://doi.org/10.1016/j.trd.2021.102810>.
- [Cabrane et al., 2020] Cabrane, Z., Batool, D., Kim, J., and Yoo, K. (2020). Design and simulation studies of battery-supercapacitor hybrid energy storage system for improved performances of traction system of solar vehicle. *Journal of Energy Storage*, 32:5540–5550. <https://doi.org/10.1016/j.est.2020.101943>.
- [Cao and Emadi, 2012] Cao, J. and Emadi, A. (2012). A new battery/ultracapacitor hybrid energy storage system for electric, hybrid, and plug-in hybrid electric vehicles. *IEEE Transactions on Power Electronics*, 27(1):122–132.
- [Capasso and Veneri, 2015] Capasso, C. and Veneri, O. (2015). Experimental study of a dc charging station for full electric and plug in hybrid vehicles. *Appl Energy*, 152:131–142.
- [Chan et al., 2009] Chan, C., Wong, Y. S., Bouscayrol, A., and Chen, K. (2009). Powering sustainable mobility: roadmaps of electric, hybrid and fuel cell vehicles. *proceedings of the IEEE*, 97(4).
- [Charging Stations-Gemamex., 2022] Charging Stations-Gemamex., . (2022). Charging stations by gemamex motion co. (2022) <https://chariot-electricbus.com/cmproduct/charging-stations-gemamex/>.
- [Chen et al., 2016] Chen, Z., Xiong, R., and Cao, J. (2016). Particle swarm optimization-based optimal power management of plug-in hybrid electric vehicles considering uncertain driving conditions. *Energy*, 96:197–208.

- [Chenghui et al., 2007] Chenghui, Z., Qingsheng, S., Naxin, C., and Wuhua, L. (2007). Particle swarm optimization for energy management fuzzy controller design in dual-source electric vehicle. In *2007 IEEE Power Electronics Specialists Conference*, pages 1405–1410. IEEE.
- [consumption ARAI, 2021] consumption ARAI, E. E. (2021). Electric power train vehicles—measurement of electrical energy consumption, the automotive research association of india, ministry of road transport & highways. <https://morth.nic.in/ais>.
- [Correa et al., 2017] Correa, F. C., Eckert, J. J., Santiciolli, F. M., Silva, L. C. A., Costa, E. S., and Dedini, F. G. (2017). Electric vehicle battery-ultracapacitor energy system optimization. In *2017 IEEE Vehicle Power and Propulsion Conference (VPPC)*, pages 1–6. IEEE.
- [Demircali and Koroglu, 2022] Demircali, A. and Koroglu, S. (2022). Modular energy management system with jaya algorithm for hybrid energy storage in electric vehicles. *Int J Energy Res*, 28:1–14. doi:10.1002/er.7848.
- [Dhar et al., 2017] Dhar, S., Pathak, M., and Shukla, P. (2017). Electric vehicles and india's low carbon passenger transport: a long-term co-benefits assessment. *J. Cleaner Prod.*, 146:139–148.
- [Djamila et al., 2014] Djamila, R., Samia, B., and Nabila, B. (2014). Development of hybrid photovoltaic-fuel cell system for stand-alone application. *International Journal of Hydrogen Energy*, 39(3):1604–1611.
- [Dougal et al., 2002] Dougal, R., Liu, S., and White, R. (2002). Power and life extension of battery-ultracapacitor hybrids. *IEEE Transactions on Components and Packaging Technologies*, 25(1):120–131.
- [Du et al., 2022] Du, G., Zou, Y., Zhang, X., Guo, L., and Guo, N. (2022). Energy management for a hybrid electric vehicle based on prioritized deep reinforcement learning framework. *Energy*, 241:122523.
- [Dusmez and Khaligh, 2014] Dusmez, S. and Khaligh, A. (2014). A supervisory power-splitting approach for a new ultracapacitor–battery vehicle deploying two propulsion machines. *IEEE Transactions on Industrial Informatics*, 10(3):1960–1971.
- [Eaton, 2022] Eaton (2022). Tco - energy storage 2022, energy storage total cost of ownership calculator-eaton, <https://www.eaton.com/us/en-us/products/electronic-components/supercapacitor-tco-tool.html>.
- [Eckert et al., 2020] Eckert, J. J., de Alkmin Silva, L. C., Dedini, F. G., and Corrêa, F. C. (2020). Electric vehicle powertrain and fuzzy control multi-objective optimization, considering dual hybrid energy storage systems. *IEEE Transactions on Vehicular Technology*, 69(4):3773–3782.

- [Elia et al., 2021] Elia, A., Kamidelivand, M., Rogan, F., and Gallachóir, B. (2021). Impacts of innovation on renewable energy technology cost reductions. *Renewable and Sustainable Energy Reviews*, 138:1–31.
- [Erickson and Maksimovic, 2007] Erickson, R. W. and Maksimovic, D. (2007). *Fundamentals of power electronics*. Springer Science & Business Media.
- [European, 2022] European, C. (2022). Photovoltaic geographical information system. <https://ec.europa.eu/jrc/en/pvgis>.
- [EV Battery, 2020] EV Battery, c.-. (2020). Electric vehicle battery cost. <https://auto.economictimes.indiatimes.com/news/auto-components/evs-to-close-in-on-icevehicles-in-few-years-as-battery-costs-expected-to-plummet-to-100/kwh-by-2023/79764942>.
- [Fathabadi, 2018] Fathabadi, H. (2018). Novel fuel cell/battery/supercapacitor hybrid power source for fuel cell hybrid electric vehicles. *Energy*, 145:467–477.
- [Fazelpour et al., 2014] Fazelpour, F., Vafaeipour, M., Rahbari, O., and Rosen, M. (2014). Intelligent optimization to integrate a plug-in hybrid electric vehicle smart parking lot with renewable energy resources and enhance grid characteristics. *Energy Convers Manage.*, 77:250–261.
- [Florescu et al., 2015] Florescu, A., Bacha, S., Munteanu, I., Brateu, A., and Rumeau, A. (2015). Adaptive frequency-separation-based energy management system for electric vehicles. *J Power Sources*, 280:410–421.
- [Fu et al., 2019] Fu, Z., Li, Z., Si, P., and Tao, F. (2019). A hierarchical energy management strategy for fuel cell/battery/supercapacitor hybrid electric vehicles. *International Journal of Hydrogen Energy*, 44(39):22146–22159.
- [Gao et al., 2016] Gao, C., Zhao, J., Wu, J., and Hao, X. (2016). Optimal fuzzy logic based energy management strategy of battery/supercapacitor hybrid energy storage system for electric vehicles. In *2016 12th World Congress on Intelligent Control and Automation (WCICA)*, pages 98–102. IEEE.
- [Gao, 2005] Gao, W. (2005). Performance comparison of a fuel cell-battery hybrid powertrain and a fuel cell-ultracapacitor hybrid powertrain. *IEEE Trans Veh Technol.*, 54(3):846–855.
- [García et al., 2013] García, P., Torreglosa, J. P., Fernández, L. M., and Jurado, F. (2013). Control strategies for high-power electric vehicles powered by hydrogen fuel cell, battery and supercapacitor. *Expert Systems with Applications*, 40(12):4791–4804.
- [GE0, 2020] GE0 (2020). Resources for the future. (2020, may). global energy outlook 2020: energy transition or energy addition?. available online: <https://www.rff.org/publications/reports/global-energy-outlook-2020> (accessed on 22 may 2021).

- [Geetha and Subramani,] Geetha, A. and Subramani, C. A comprehensive review on energy management strategies of hybrid energy storage system for electric vehicles. *International Journal of Energy Research*, 41(13):1817–1834.
- [Global EV, 2020] Global EV, m.-. (2020). Global ev market. <https://www.virta.global/global-electricvehicle-market>.
- [Golchoubian and Azad, 2017] Golchoubian, P. and Azad, N. (2017). Real-time nonlinear model predictive control of a battery–supercapacitor hybrid energy storage system in electric vehicles. *IEEE Trans Veh Technol*, 66(11):9678–9688.
- [Gomozov et al., 2017] Gomozov, O., Trovão, J. P. F., Kestelyn, X., and Dubois, M. R. (2017). Adaptive energy management system based on a real-time model predictive control with nonuniform sampling time for multiple energy storage electric vehicle. *IEEE Transactions on Vehicular Technology*, 66(7):5520–5530.
- [Guang et al., 2017] Guang, H., Jili, T., Ridong, Z., and Xiangming, C. (2017). Improved ga based fc-uc hybrid power management considering prolong lifetime. In *2017 36th Chinese Control Conference (CCC)*, pages 4150–4155. IEEE.
- [Hao et al., 2020] Hao, X., Wang, H., Lin, Z., and Ouyang, M. (2020). Seasonal effects on electric vehicle energy consumption and driving range: A case study on personal, taxi, and ridesharing vehicles. *Journal of Cleaner Production*, 249:119403.
- [He et al., 2020] He, H., Quan, S., Sun, F., and Wang, Y.-X. (2020). Model predictive control with lifetime constraints based energy management strategy for proton exchange membrane fuel cell hybrid power systems. *IEEE Transactions on Industrial Electronics*, 67(10):9012–9023.
- [He et al., 2013] He, H., Xiong, R., Zhao, K., and Liu, Z. (2013). Energy management strategy research on a hybrid power system by hardware-in-loop experiments. *Applied Energy*, 112:1311–1317.
- [Hegazy et al., 2012] Hegazy, O., Van, M. J., Barrero, R., Omar, N., and Lataire, P. (2012). Pso algorithm-based optimal power flow control of fuel cell/supercapacitor and fuel cell/battery hybrid electric vehicles. *COMPEL Int J Comput Math Electr Electron Eng.*, 32:86–107.
- [Hegazy and Van Mierlo, 2010] Hegazy, O. and Van Mierlo, J. (2010). Particle swarm optimization for optimal powertrain component sizing and design of fuel cell hybrid electric vehicle. In *2010 12th International Conference on Optimization of Electrical and Electronic Equipment*, pages 601–609. IEEE.
- [Hegde et al., 2020] Hegde, B., Ahmed, Q., and Rizzoni, G. (2020). Velocity and energy trajectory prediction of electrified powertrain for look ahead control. *Applied Energy*, 279:115903.
- [Hemi et al., 2013] Hemi, H., Ghouili, J., and Cheriti, A. (2013). A real time

- energy management for electrical vehicle using combination of rule-based and ecms. In *2013 IEEE Electrical Power Energy Conference*, pages 1–6. IEEE.
- [Hemi et al., 2015] Hemi, H., Ghouili, J., and Cheriti, A. (2015). Combination of markov chain and optimal control solved by pontryagin’s minimum principle for a fuel cell/supercapacitor vehicle. *Energy Conversion and Management*, 91:387–393.
- [Hemmati and Saboori, 2016] Hemmati, R. and Saboori, H. (2016). Emergence of hybrid energy storage systems in renewable energy and transport applications – a review. *Renewable Sustainable Energy Rev.*, 65:11–23.
- [Hredzak et al., 2015] Hredzak, B., Agelidis, V. G., and Demetriades, G. (2015). Application of explicit model predictive control to a hybrid battery-ultracapacitor power source. *Journal of Power Sources*, 277:84–94.
- [Hredzak et al., 2014] Hredzak, B., Agelidis, V. G., and Jang, M. (2014). A model predictive control system for a hybrid battery-ultracapacitor power source. *IEEE Transactions on Power Electronics*, 29(3):1469–1479.
- [Hsu et al., 2016] Hsu, R. C., Chen, S.-M., Chen, W.-Y., and Liu, C.-T. (2016). A reinforcement learning based dynamic power management for fuel cell hybrid electric vehicle. In *2016 Joint 8th International Conference on Soft Computing and Intelligent Systems (SCIS) and 17th International Symposium on Advanced Intelligent Systems (ISIS)*, pages 460–464. IEEE.
- [Hu et al., 2016] Hu, S., Liang, Z., and He, X. (2016). Ultracapacitor-battery hybrid energy storage system based on the asymmetric bidirectional zsource topology for ev. *IEEE Trans Power Electron.*, 31:7489–7498.
- [Hussain et al., 2019] Hussain, S., Ali, M., Park, G.-S., Nengroo, S., Khan, M., and Kim, H.-J. (2019). A real-time bi-adaptive controller-based energy management system for battery–supercapacitor hybrid electric vehicles. *Energies*, 12(24):1–24.
- [IEA, 2020] IEA (2020). International energy agency. outlook for biogas and biomethane: Prospects for organic growth 2020.available online: <https://www.iea.org/reports/outlook-for-biogas-and-biomethane-prospects-for-organic-growth> (accessed on 12 january 2022).
- [IEA-EV, 2022] IEA-EV (2022). Iea (2022), by 2030 evs represent more than 60% of vehicles sold globally, and require an adequate surge in chargers installed in buildings, iea, paris. <https://www.iea.org/reports/by-2030-evs-represent-more-than-60-of-vehicles-sold-globally-and-require-an-adequate-surge-in-chargers-installed-in-buildings>, License: CC BY 4.0.
- [IEA-India, 2021] IEA-India (2021). International energy agency. india energy outlook 2021. [online].available online: <https://www.iea.org/reports/india-energy-outlook-2021/energy-in-india-today> (accessed on 25 april 2022).

- [IEA-Oil and Gas, 2020] IEA-Oil and Gas (2020). The oil and gas industry in energy transitions. available online: <https://www.iea.org/reports/the-oil-and-gas-industry-in-energy-transitions> (accessed on 10 november 2021).
- [IEA-REA, 2019] IEA-REA (2019). International renewable energy agency. (2019, apr). global energy transformation: A roadmap to 2050 (2019 edition). [online]. available online: <https://www.irena.org/publications/2019/apr/global-energytransformation-a-roadmap-to-2050> (accessed on 15 april 2021).
- [IEA-World, 2021] IEA-World (2021). International energy agency. world energy outlook 2021. available online: <https://www.iea.org/reports/india-energy-outlook-2021> (accessed on 18 may 2022).
- [Jafari et al., 2018] Jafari, M., Gauchia, A., Zhao, S., Zhang, K., and Gauchia, L. (2018). Electric vehicle battery cycle aging evaluation in real-world daily driving and vehicle-to-grid services. *IEEE Transactions on Transportation Electrification*, 4(1):122–134.
- [Jangid et al., 2019] Jangid, M. K., Mukhopadhyay, A., and Mater, J. (2019). Real-time monitoring of stress development during electrochemical cycling of electrode materials for li-ion batteries: overview and perspectives. *Chem. A*, 7(41):23679 —23726.
- [Jia et al., 2021a] Jia, L., Ma, J., Cheng, P., and Liu, Y. (2021a). A perspective on solar energy-powered road and rail transportation in china. *Journal of Power and Energy Systems*, 6(4):760–771.
- [Jia et al., 2021b] Jia, L., Ma, J., Cheng, P., and Liu, Y. (2021b). A perspective on solar energy-powered road and rail transportation in china. *Journal of Power and Energy Systems*, 6(4):760–771.
- [Jiahao et al., 2022] Jiahao, H., Zhiwu, H., Yue, W., Yongjie, L., Heng, L., Fu, J., and Jun, P. (2022). Sizing optimization research considering mass effect of hybrid energy storage system in electric vehicles. *Journal of Energy Storage*, 48(1):72–80. <https://doi.org/10.1016/j.est.2021.103892>.
- [Jiang et al., 2019] Jiang, H., Xu, L., Li, J., Hu, Z., and Ouyang, M. (2019). Energy management and component sizing for a fuel cell/battery/supercapacitor hybrid powertrain based on two-dimensional optimization algorithms. *Energy*, 177:386–396.
- [Jing et al., 2018] Jing, W., Lai, C., WSH, W., and MLD, W. (2018). A comprehensive study of battery-supercapacitor hybrid energy storage system for standalone pv power system in rural electrification. *Appl Energy*, 224:340–356.
- [Jiquan et al., 2018] Jiquan, W., Igo, B., and Henk, N. (2018). Battery electric vehicle energy consumption prediction for a trip based on route information. *Proceedings of the Institution of Mechanical Engineers, Part D: Journal of Automobile Engineering*, 232(11):1528–1542.

- [John et al., 2011] John, W., Ping, L., Jocelyn, H.-G., Elena, S., Souren, S., Mark, V., Harshad, T., James, M., and Peter, F. (2011). Cycle-life model for graphite-lifepo4 cells. *Journal of Power Sources*, 196(8):3942–3948.
- [key,] key. Bloombergnev. hitting the ev inflection point. 2020, (3.2.1). <https://www.transportenvironment.org/discover/hitting-the-ev-inflection-point/>.
- [key, 2019] key (2019). Guide to ev adoption. (2019, dec). [online]. available: <https://www.wbcsd.org/programs/cities-and-mobility/transforming-urban-mobility/mobility-decarbonization/coalitions/resources/india-business-guide-to-ev-adoption>.
- [Kouchachvili et al., 2018] Kouchachvili, L., Yaïci, W., and Entchev, E. (2018). Hybrid battery/supercapacitor energy storage system for the electric vehicles. *J Power Sources*, 374:237–248.
- [Koziel and Yang, 2011] Koziel, S. and Yang, X. (2011). *Computational Optimization, Methods and Algorithms*, volume 356. Springer.
- [Kreczanik et al., 2014] Kreczanik, P., Venet, P., Hijazi, A., and Clerc, G. (2014). Study of supercapacitor aging and lifetime estimation according to voltage, temperature, and rms current. *IEEE Transactions on Industrial Electronics*, 61(9):4895–4902.
- [Laldin et al., 2013] Laldin, O., Moshirvaziri, M., and Trescases, O. (2013). Predictive algorithm for optimizing power flow in hybrid ultracapacitor/battery storage systems for light electric vehicles. *IEEE Transactions on Power Electronics*, 28(8):3882–3895.
- [Lee et al., 2020] Lee, H., Kang, C., Park, Y.-I., Kim, N., and Cha, S. W. (2020). Online data-driven energy management of a hybrid electric vehicle using model-based q-learning. *IEEE Access*, 8:84444–84454.
- [Li et al., 2017a] Li, H., Ravey, A., N’Diaye, A., and Djerdir, A. (2017a). Equivalent consumption minimization strategy for fuel cell hybrid electric vehicle considering fuel cell degradation. *IEEE Transportation Electrification Conference and Expo (ITEC)*, pages 540–544.
- [Li et al., 2018a] Li, H., Ravey, A., N’Diaye, A., and Djerdir, A. (2018a). A novel equivalent consumption minimization strategy for hybrid electric vehicle powered by fuel cell, battery and supercapacitor. *Journal of Power Sources*, 395:262–270.
- [Li et al., 2019] Li, H., Ravey, A., N’Diaye, A., and Djerdir, A. (2019). Online adaptive equivalent consumption minimization strategy for fuel cell hybrid electric vehicle considering power sources degradation. *Energy Conversion and Management*, 192:133–149.

- [Li et al., 2015] Li, J., Gee, A. M., Zhang, M., and Yuan, W. (2015). Analysis of battery lifetime extension in a smes-battery hybrid energy storage system using a novel battery lifetime model. *Energy*, 86:175–185.
- [Li et al., 2016] Li, Q., Yang, H., Han, Y., Li, M., and Chen, W. (2016). A state machine strategy based on droop control for an energy management system of pemfc-battery-supercapacitor hybrid tramway. *International Journal of Hydrogen Energy*, 41(36):16148–16159. Special Issue: 16th China Hydrogen Energy Conference (CHEC 2015), November 2015, Zhenjiang City, Jiangsu Province, China.
- [Li et al., 2017b] Li, Y., He, H., Peng, J., and Zhang, H. (2017b). Power management for a plug-in hybrid electric vehicle based on reinforcement learning with continuous state and action spaces. *Energy Procedia*, 142:2270–2275. Proceedings of the 9th International Conference on Applied Energy.
- [Li et al., 2018b] Li, Z., Zhu, L., Tao, F., and Fu, Z. (2018b). Energy management strategy based on model prediction control for hybrid batteries/ supercapacitors electrical vehicle. In *2018 Chinese Automation Congress (CAC)*, pages 2463–2468. IEEE.
- [Lin et al., 2004] Lin, C.-C., Peng, H., and Grizzle, J. (2004). A stochastic control strategy for hybrid electric vehicles. In *Proceedings of the 2004 American Control Conference*, volume 5, pages 4710–4715 vol.5. IEEE.
- [Lin et al., 2010] Lin, X., Banvait, H., Anwar, S., and Chen, Y. (2010). Optimal energy management for a plug-in hybrid electric vehicle: Real-time controller. In *Proceedings of the 2010 American Control Conference*, pages 5037–5042. IEEE.
- [Lin et al., 2015] Lin, X., Bogdan, P., Chang, N., and Pedram, M. (2015). Machine learning-based energy management in a hybrid electric vehicle to minimize total operating cost. In *2015 IEEE/ACM International Conference on Computer-Aided Design (ICCAD)*, pages 627–634. IEEE.
- [Lithium ion Battery cost, 2022] Lithium ion Battery cost, I. (2022). Iea, average pack price of lithium-ion batteries and share of cathode material cost, 2011-2021, iea, paris <https://www.iea.org/data-and-statistics/charts/average-pack-price-of-lithium-ion-batteries-and-share-of-cathode-material-cost-2011-2021>, iea. license: Cc by 4.0.
- [Liu et al., 2016] Liu, S., Peng, J., Li, L., Gong, X., and Lu, H. (2016). A mpc based energy management strategy for battery-supercapacitor combined energy storage system of hev. In *2016 35th Chinese Control Conference (CCC)*, pages 8727–8731. IEEE.
- [Liu et al., 2015] Liu, T., Zou, Y., Liu, D., and Sun, F. (2015). Reinforcement learning of adaptive energy management with transition probability for a hybrid electric tracked vehicle. *IEEE Transactions on Industrial Electronics*,

62(12):7837–7846.

- [Lu et al., 2013] Lu, L., Han, X., Li, J., Hua, J., and Ouyang, M. (2013). A review on the key issues for lithium-ion battery management in electric vehicles. *Journal of Power Sources*, 226:272–288.
- [Madhusudhanan and Na, 2020] Madhusudhanan, A. K. and Na, X. (2020). Effect of a traffic speed based cruise control on an electric vehicle s performance and an energy consumption model of an electric vehicle. *IEEE/CAA Journal of Automatica Sinica*, 7(2):386–394.
- [Martinez et al., 2017] Martinez, C., Hu, X., Cao, D., Velenis, E., Gao, B., and Wellers, M. (2017). Energy management in plug-in hybrid electric vehicles: recent progress and a connected vehicles perspective. *IEEE Trans. Veh. Technol.*, 66(6):4534–4549.
- [Marzougui et al., 2017] Marzougui, H., Amari, M., Kadri, A., Bacha, F., and Ghouili, J. (2017). Energy management of fuel cell/battery/ultracapacitor in electrical hybrid vehicle. *International Journal of Hydrogen Energy*, 42(13):8857–8869. Hydrogen Fuel Cell Renewable Energy Techniques: The 8th International Conference on Renewable Energy (CIER-2015), 21-23 December 2015, Sousse, Tunisia.
- [Masih-Tehrani et al., 2013] Masih-Tehrani, M., Ha’iri-Yazdi, M.-R., Esfahanian, V., and Safaei, A. (2013). Optimum sizing and optimum energy management of a hybrid energy storage system for lithium battery life improvement. *Journal of Power Sources*, 244:2–10. 16th International Meeting on Lithium Batteries (IMLB).
- [Mellincovsky et al., 2014] Mellincovsky, M., Kuperman, A., Lerman, C., Gadelovits, S., Aharon, I., Reichbach, N., and et al. (2014). Performance and limitations of a constant power-fed supercapacitor. *IEEE Trans. Energy Convers*, 29(2):445–452. <https://doi.org/10.1016/j.scs.2021.103117>.
- [Mesbahi et al., 2017] Mesbahi, T., Rizoug, N., Bartholomeüs, P., Sadoun, R., Khenfri, F., and Le Moigne, P. (2017). Optimal energy management for a li-ion battery/supercapacitor hybrid energy storage system based on a particle swarm optimization incorporating nelder–mead simplex approach. *IEEE Transactions on Intelligent Vehicles*, 2(2):99–110.
- [Min HT, 2017] Min HT, Lai CL, Y. Y. Z. T. Z. C. (2017). Comparison study of two semi-active hybrid energy storage systems for hybrid electric vehicle applications and their experimental validation. *Energies.*, 10(3):1–20.
- [Moreno et al., 2006] Moreno, J., Ortuzar, M., and Dixon, J. (2006). Energy-management system for a hybrid electric vehicle, using ultracapacitors and neural networks. *IEEE Transactions on Industrial Electronics*, 53(2):614–623.
- [Murphey et al., 2011] Murphey, Y. L., Chen, Z., Kiliaris, L., and Masrur, M. A.

- (2011). Intelligent power management in a vehicular system with multiple power sources. *Journal of Power Sources*, 196(2):835–846.
- [Nguyen et al., 2014] Nguyen, A., Lauber, J., and Dambrine, M. (2014). Optimal control based algorithms for energy management of automotive power systems with battery/supercapacitor storage devices. *Energy Conversion and Management*, 87:410–420.
- [Nguyen et al., 2019] Nguyen, B.-H., German, R., Trovão, J. P. F., and Bouscayrol, A. (2019). Real-time energy management of battery/supercapacitor electric vehicles based on an adaptation of pontryagin’s minimum principle. *IEEE Transactions on Vehicular Technology*, 68(1):203–212.
- [Nguyen et al., 2017] Nguyen, B.-H., Trovao, J. P., German, R., and Bouscayrol, A. (2017). An optimal control-based strategy for energy management of electric vehicles using battery/supercapacitor. In *2017 IEEE Vehicle Power and Propulsion Conference (VPPC)*, pages 1–6. IEEE.
- [Nguyen et al., 2021] Nguyen, H.-L., Nguyn, B.-H., Vo-Duy, T., and Trovão, J. (2021). A comparative study of adaptive filtering strategies for hybrid energy storage systems in electric vehicles. *Energies*, 14(12):3373.
- [Niu et al., 2022] Niu, J., Zhuang, W., Ye, J., Song, Z., Yin, G., and Zhang, Y. (2022). Optimal sizing and learning-based energy management strategy of ncr/lto hybrid battery system for electric taxis. *Energy*, 257. <https://doi.org/10.1016/j.energy.2022.124653>.
- [NPTEL:, 2018] NPTEL: (2018). Hybrid and electric vehicles. (accessed january 2020). <https://nptel.ac.in/courses/108/103/108103009/>.
- [P K Singha et al., 2021] P K Singha, R., Karayaka, H. B., He, J., and Yu, Y. H. (2021). Economic comparison between battery and supercapacitor for hourly dispatching wave energy converter power. *52nd North American Power Symposium (NAPS)*, (2021):1–6.
- [Pedro et al., 2019] Pedro, M., Rita, G., Luiz, K., and Fausto, F. (2019). Comparative life cycle assessment of lithium-ion batteries for electric vehicles addressing capacity fade. *Journal of Cleaner Production*, 229:787–794.
- [Pei and Leamy, 2013] Pei, D. and Leamy, M. (2013). Dynamic programming-informed equivalent cost minimization control strategies for hybrid-electric vehicles. *J Dyn Syst Meas Control*, 135:051013.
- [Peter et al., 2018] Peter, R., Gregor, K., Timur, G., Wolfgang, S., Janusz, C., Zbigniew, K., Pallav, P., Chris, H., Markus, A., Jens, B.-K., and Laura, C. (2018). Outlook for clean air in the context of sustainable development goals. *Global Environmental Change*, 53:1–11.
- [PV-NREL, 2022] PV-NREL (2022). Solar photovoltaic research by nrel (2022)

<https://www.nrel.gov/pv/cell-efficiency.html>.

- [Rahbari et al., 2017] Rahbari, Oand Vafaeipour, M., Omar, N., and et al. (2017). An optimal versatile control approach for plug-in electric vehicles to integrate renewable energy sources and smart grids. *Energy.*, 134:1053–1067.
- [Raman et al., 2021] Raman, S., Cheng, K.-W., Xue, X.-D., Fong, Y.-C., and Cheung, S. (2021). Hybrid energy storage system with vehicle body integrated super-capacitor and li-ion battery: Model, design and implementation, for distributed energy storage. *Energies*, 14(20):6553. <https://doi.org/10.3390/en14206553>.
- [Ranganath and Debasis, 2021] Ranganath, N. and Debasis, S. (2021). Life cycle costing analysis of solar photo voltaic generation system in indian scenario. *International Journal of Sustainable Engineering*, 14(6):1698–1713.
- [Rodatz et al., 2005] Rodatz, P., Paganelli, G., Sciarretta, A., and Guzzella, L. (2005). Optimal power management of an experimental fuel cell/supercapacitor-powered hybrid vehicle. *Control Engineering Practice*, 13(1):41–53.
- [Romaus et al., 2010] Romaus, C., Gathmann, K., and Böcker, J. (2010). Optimal energy management for a hybrid energy storage system for electric vehicles based on stochastic dynamic programming. In *2010 IEEE Vehicle Power and Propulsion Conference*, pages 1–6. IEEE.
- [Rui et al., 2020] Rui, X., Yue, P., Weixiang, S., Hailong, L., and Fengchun, S. (2020). Lithium-ion battery aging mechanisms and diagnosis method for automotive applications: Recent advances and perspectives. *Renewable and Sustainable Energy Reviews*, 131. <https://doi.org/10.1016/j.rser.2020.110048>.
- [S. Njoya Motapon and Al-Haddad, 2014] S. Njoya Motapon, L. A. D. and Al-Haddad, K. (2014). A comparative study of energy management schemes for a fuel-cell hybrid emergency power system of more-electric aircraft. *IEEE Transactions on Industrial Electronics*, 61(3):1320–1334. doi: 10.1109/TIE.2013.2257152.
- [Samad et al., 2015] Samad, N. A., Kim, Y., Siegel, J. B., and Stefanopoulou, A. G. (2015). Influence of battery downsizing and soc operating window on battery pack performance in a hybrid electric vehicle. *IEEE Vehicle Power and Propulsion Conference (VPPC)*, pages 1–6. doi: 10.1109/VPPC.2015.7352966.
- [Santucci et al., 2014] Santucci, A., Sorniotti, A., and Lekakou, C. (2014). Power split strategies for hybrid energy storage systems for vehicular applications. *Journal of Power Sources*, 258:395–407.
- [Schuster et al., 2017] Schuster, S. F., Brand, M. J., Philipp, B., Markus, G., and Andreas, J. (2017). Lithium-ion cell-to-cell variation during battery electric vehicle operation. *Journal of Power Sources*, 297:242–251.

- [Sellali et al., 2019a] Sellali, M., Abdeddaim, S., Betka, A., Djerdir, A., Drid, S., and Tiar, M. (2019a). Fuzzy-super twisting control implementation of battery/super capacitor for electric vehicles. *ISA Transactions*, 95:243–253. <https://doi.org/10.1016/j.isatra.2019.04.029>.
- [Sellali et al., 2019b] Sellali, M., Betka, A., Drid, S., Djerdir, A., Allaoui, L., and Tiar, M. (2019b). Novel control implementation for electric vehicles based on fuzzy -back stepping approach. *Energy*, 178:644–655.
- [Sharma et al., 2012] Sharma, R., Manzie, C., Bessede, M., Brear, M., and Crawford, R. (2012). Conventional, hybrid and electric vehicles for australian driving conditions – part 1: Technical and financial analysis. *Transportation Research Part C: Emerging Technologies*, 25:238–249.
- [Shemin et al., 2022] Shemin, S., Gonçalo, D., Diana, N., and Patricia, B. (2022). Photovoltaic integrated electric vehicles: Assessment of synergies between solar energy, vehicle types and usage patterns. *Journal of Cleaner Production*, 348. <https://doi.org/10.1016/j.jclepro.2022.131402>.
- [Shen et al., 2020] Shen, D., Lim, C.-C., Shi, P., and Bujlo, P. (2020). Energy management of fuel cell hybrid vehicle based on partially observable markov decision process. *IEEE Transactions on Control Systems Technology*, 28(2):318–330.
- [Shen and Khaligh, 2015] Shen, J. and Khaligh, A. (2015). A supervisory energy management control strategy in a battery/ultracapacitor hybrid energy storage system. *IEEE Transactions on Transportation Electrification*, 1(3):223–231.
- [Singh et al., 2019] Singh, K., Bansal, H., and Singh, D. (2019). A comprehensive review on hybrid electric vehicles: architectures and components. *J Mod Transport.*, 27:77–107.
- [Sinoquet et al., 2011] Sinoquet, D., Rousseau, G., and Milhau, Y. (2011). Design optimization and optimal control for hybrid vehicles. *Optim Eng*, 12:199–213.
- [Solar, 2020] Solar, P, V. (2020). Solar photovoltaic power potential by country (2020, july). <https://www.worldbank.org/en/topic/energy/publication/solar-photovoltaic-power-potential-by-country>.
- [Sonali et al., 2021] Sonali, G., Renu, S., and Akshay Kumar, R. (2021). A review on barrier and challenges of electric vehicle in india and vehicle to grid optimisation. *Transportation Engineering*, 4(2021):1–14.
- [Song et al., 2015a] Song, Z., Hofmann, H., Li, J., Han, X., and Ouyang, M. (2015a). Optimization for a hybrid energy storage system in electric vehicles using dynamic programming approach. *Appl Energy*, 139:151–162.
- [Song et al., 2015b] Song, Z., Hofmann, H., Li, J., Han, X., Zhang, X., and Ouyang, M. (2015b). A comparison study of different semi-active hybrid energy

- storage system topologies for electric vehicles. *J Power Sources*, 274:400–411.
- [Song et al., 2014a] Song, Z., Hofmann, H., Li, J., Hou, J., Han, X., and Ouyang, M. (2014a). Energy management strategies comparison for electric vehicles with hybrid energy storage system. *Applied Energy*, 134:321–331.
- [Song et al., 2014b] Song, Z., Li, J., Han, X., Xu, L., Lu, L., Ouyang, M., and Hofmann, H. (2014b). Multi-objective optimization of a semi-active battery/supercapacitor energy storage system for electric vehicles. *Applied Energy*, 135:212–224.
- [Song et al., 2018] Song, Z., Li, J., Hou, J., Hofmann, H., Ouyang, M., and Du, J. (2018). The battery-supercapacitor hybrid energy storage system in electric vehicle applications: A case study. *Energy*, 154:433–441. <https://doi.org/10.1016/j.apenergy.2020.115408>.
- [Spotnitz, 2003] Spotnitz, R. (2003). Simulation of capacity fade in lithium-ion batteries. *J. Power Sources*, 113(1):72–80.
- [Subhash and Reinhard, 2016] Subhash, K. and Reinhard, M. (2016). Co2 emission reduction potential assessment using renewable energy in india. *Energy*, 97:273–282.
- [Sun et al., 2015] Sun, C., Moura, S. J., Hu, X., Hedrick, J. K., and Sun, F. (2015). Dynamic traffic feedback data enabled energy management in plug-in hybrid electric vehicles. *IEEE Transactions on Control Systems Technology*, 23(3):1075–1086.
- [Sun and Xiong, 2015] Sun, F. and Xiong, R. (2015). A novel dual-scale cell state-of-charge estimation approach for series-connected battery pack used in electric vehicles. *Journal of Power Sources*, 274:582–594.
- [Sun et al., 2020] Sun, H., Fu, Z., Tao, F., Zhu, L., and Si, P. (2020). Data-driven reinforcement-learning-based hierarchical energy management strategy for fuel cell/battery/ultracapacitor hybrid electric vehicles. *Journal of Power Sources*, 455:227964.
- [Sun et al., 2017] Sun, L., Feng, K., Chapman, C., and Zhang, N. (2017). An adaptive power-split strategy for battery–supercapacitor powertrain—design, simulation, and experiment. *IEEE Transactions on Power Electronics*, 32:9364–9375.
- [Sundstrom and Stefanopoulou, 2006] Sundstrom, O. and Stefanopoulou, A. (2006). Optimal power split in fuel cell hybrid electric vehicle with different battery sizes, drive cycles, and objectives. In *2006 IEEE Conference on Computer Aided Control System Design, 2006 IEEE International Conference on Control Applications, 2006 IEEE International Symposium on Intelligent Control*, pages 1681–1688. IEEE.

- [Sunrunmotors, 2022] Sunrunmotors (2022). <http://www.sunrunmotors.com/> (accessed on 02 november 2022).
- [Supercapacitor-AOWEI, 2022] Supercapacitor-AOWEI, T. (2022). <http://www.aowei.com/en/program/product.html>.
- [Syahbana and Trilaksono, 2019] Syahbana, D. F. and Trilaksono, B. R. (2019). Mpc and filtering-based energy management in fuel cell/ battery/ supercapacitor hybrid source. In *2019 International Conference on Electrical Engineering and Informatics (ICEEI)*, pages 122–127. IEEE.
- [Tashakori Abkenar et al., 2017] Tashakori Abkenar, A., Nazari, A., Jayasinghe, S. D. G., Kapoor, A., and Negnevitsky, M. (2017). Fuel cell power management using genetic expression programming in all-electric ships. *IEEE Transactions on Energy Conversion*, 32(2):779–787.
- [Tie and Tan, 2013] Tie, S. and Tan, C. (2013). A review of energy sources and energy management system in electric vehicles. *Renewable Sustainable Energy Rev.*, 20:82–102.
- [Tran et al., 2020] Tran, D.-D., Vafaeipour, M., El Baghdadi, M., Barrero, R., Van Mierlo, J., and Hegazy, O. (2020). Thorough state-of-the-art analysis of electric and hybrid vehicle powertrains: Topologies and integrated energy management strategies. *Renewable and Sustainable Energy Reviews*, 119:109596.
- [Tremblay et al., 2007] Tremblay, O., Dessaint, L., and Dekkiche., A. (2007). A generic battery model for the dynamic simulation of hybrid electric vehicles. *IEEE Vehicle Power and Propulsion Conference*, 43(2007):284–289.
- [Trovao et al., 2013] Trovao, J., Pereirinha, P., Jorge, H., and Antunes, C. (2013). A multilevel energy management system for multi-source electric vehicles-an integrated rule-based meta-heuristic approach. *Appl Energy*, 105:304–318.
- [Trovão et al., 2017] Trovão, J. P. F., Roux, M., Ménard, , and Dubois, M. R. (2017). Energy- and power-split management of dual energy storage system for a three-wheel electric vehicle. *IEEE Transactions on Vehicular Technology*, 66(7):5540–5550. doi: 10.1109/TVT.2016.2636282.
- [Uddin et al., 2016] Uddin, K., Moore, A. D., Barai, A., and Marco, J. (2016). The effects of high frequency current ripple on electric vehicle battery performance. *Applied Energy*, 178:142–154.
- [US-EPA, 2019] US-EPA (2019). Us epa dynamometer drive schedules [online]. <https://www.epa.gov/vehicle-and-fuel-emissions-testing/dynamometer-drive-schedules> (accessed january 2019).
- [USEP-Agency, 2022] USEP-Agency (2022). Dynamometer drive schedules. 4.1, <https://www.epa.gov/vehicle-and-fuel-emissions-testing/dynamometer-drive-schedule>.

- [Vishnu and Kashyap, 2020] Vishnu, S. P. and Kashyap, Y. (2020). Brushless dc hub motor drive control for electric vehicle applications. In *First International Conference on Power, Control and Computing Technologies (ICPC2T)*, pages 448–453. IEEE.
- [Vishnu et al.,] Vishnu, S. P., Kashyap, Y., and Castelino, R. V. Adaptive intelligent hybrid energy management strategy for electric vehicles. *Energy Storage*, n/a(n/a):e436.
- [Vukajlović et al., 2020] Vukajlović, N., Milićević, D., Dumnić, B., and Popadić, B. (2020). Comparative analysis of the supercapacitor influence on lithium battery cycle life in electric vehicle energy storage. *Journal of Energy Storage*, 31:101603.
- [Wang et al., 2022] Wang, C., Liu, R., and Tang, A. (2022). Energy management strategy of hybrid energy storage system for electric vehicles based on genetic algorithm optimization and temperature effect. *Journal of Energy Storage*, 51. <https://doi.org/10.1016/j.est.2022.104314>.
- [Wang et al., 2021] Wang, L., Niu, J., Zhao, W., Li, G., and Zhao, X. (2021). Study on electrochemical and thermal characteristics of lithium-ion battery using the electrochemical-thermal coupled model. *Int J Energy Res.*, 43(2019):2086–2107.
- [Wang et al., 2020] Wang, L., Wang, Y., Liu, C., Yang, D., and Chen, Z. (2020). A power distribution strategy for hybrid energy storage system using adaptive model predictive control. *IEEE Transactions on Power Electronics*, 35(6):5897–5906.
- [Wang et al., 2019] Wang, Y., Wang, W., Zhao, Y., Yang, L., and Chen, W. (2019). A fuzzy-logic power management strategy based on markov random prediction for hybrid energy storage systems. *Energies*, 9(1):1–20.
- [Wanlu et al., 2022] Wanlu, Z., Ye, Y., Pengfei, Z., and Zhenghuo, L. (2022). A control strategy of photovoltaic hybrid energy storage system based on adaptive wavelet packet decomposition. *Int. J. Electrochem. Sci.*, 17(2022):1–18.
- [Wen et al., 2012] Wen, H., Xiao, W., Li, H., and Wen, X. (2012). Analysis and minimisation of dc bus surge voltage for electric vehicle applications. *IET Electrical Systems in Transportation*, 2(2):68–76. DOI:10.1049/iet-est.2011.0035.
- [Wieczorek and Lewandowski, 2017] Wieczorek, M. and Lewandowski, M. (2017). A mathematical representation of an energy management strategy for hybrid energy storage system in electric vehicle and real time optimization using a genetic algorithm. *Appl Energy*, 192:222–233.
- [Wu et al., 2015] Wu, G., Zhang, X., and Dong, Z. (2015). Powertrain architectures of electrified vehicles: review, classification and comparison. *J Franklin Inst.*, 352:425–448.

- [Xi et al., 2014] Xi, J., Li, M., and Xu, M. (2014). Optimal energy management strategy for battery powered electric vehicles. *Applied Energy*, 134:332–341.
- [Xie et al., 2018a] Xie, J., Yang, P., Wang, Y., Qi, T., Lei, Y., and Li, C. M. (2018a). Puzzles and confusions in supercapacitor and battery: Theory and solutions. *Journal of Power Sources*, 401:213–223.
- [Xie et al., 2017] Xie, S., He, H., and Peng, J. (2017). An energy management strategy based on stochastic model predictive control for plug-in hybrid electric buses. *Applied Energy*, 196:279–288.
- [Xie et al., 2018b] Xie, S., Hu, X., Xin, Z., and Li, L. (2018b). Time-efficient stochastic model predictive energy management for a plug-in hybrid electric bus with an adaptive reference state-of-charge advisory. *IEEE Transactions on Vehicular Technology*, 67(7):5671–5682.
- [Xiong et al., 2018a] Xiong, R., Cao, J., and Yu, Q. (2018a). Reinforcement learning-based real-time power management for hybrid energy storage system in the plug-in hybrid electric vehicle. *Applied Energy*, 211:538–548.
- [Xiong et al., 2018b] Xiong, R., Chen, H., Wang, C., and Sun, F. (2018b). Towards a smarter hybrid energy storage system based on battery and ultracapacitor - a critical review on topology and energy management. *J. Cleaner Prod.*, 202:1228–1240.
- [Yavasoglu et al.,] Yavasoglu, H. A., Tetik, Y. E., and Ozcan, H. G. Neural network-based energy management of multi-source (battery/uc/fc) powered electric vehicle. *International Journal of Energy Research*, 44(15):12416–12429.
- [Yin et al., 2016] Yin, H., Zhou, W., Li, M., Ma, C., and Zhao, C. (2016). An adaptive fuzzy logic-based energy management strategy on battery/ultracapacitor hybrid electric vehicles. *IEEE Transactions on Transportation Electrification*, 2(3):300–311.
- [Ying et al., 2020] Ying, Z., Ting, Z., Dongxue, H., Wei, Y., Yuanyuan, Z., Qijin, W., and Nianjun, Y. (2020). High-energy-density supercapacitors from dual pseudocapacitive nanoelectrodes. *ACS Appl. Energy Mater.*, 3(11):10685–10694.
- [Yuqing et al., 2021] Yuqing, C., Yuqiong, K., Yun, Z., Li, W., Jilei, L., Yanxi, L., Zheng, L., Xiangming, H., Xing, L., Naser, T., and Baohua, L. (2021). A review of lithium-ion battery safety concerns: The issues, strategies, and testing standards. *Journal of Energy Chemistry*, 59(2021):83–99.
- [Zhang et al., 2020] Zhang, J., Wang, Z., Liu, P., and Zhang, Z. (2020). Energy consumption analysis and prediction of electric vehicles based on real-world driving data. *Applied Energy*, 275:115408.
- [Zhang et al., 2019] Zhang, R., Tao, J., and Zhou, H. (2019). Fuzzy optimal en-

- ergy management for fuel cell and supercapacitor systems using neural network based driving pattern recognition. *IEEE Transactions on Fuzzy Systems*, 27(1):45–57.
- [Zhang et al., 2017] Zhang, S., Luo, Y., Wang, J., Wang, X., and Li, K. (2017). Predictive energy management strategy for fully electric vehicles based on preceding vehicle movement. *IEEE Transactions on Intelligent Transportation Systems*, 18(11):3049–3060.
- [Zhang et al., 2021] Zhang, Y., Wei, C., Liu, Y., Chen, Z., Hou, Z., and Xu, N. (2021). A novel optimal power management strategy for plug-in hybrid electric vehicle with improved adaptability to traffic conditions. *Journal of Power Sources*, 489:229512.
- [Zhou et al., 2017] Zhou, D., Gao, F., Ravey, A., Al-Durra, A., and Simões, M. G. (2017). Online energy management strategy of fuel cell hybrid electric vehicles based on time series prediction. In *2017 IEEE Transportation Electrification Conference and Expo (ITEC)*, pages 113–118. IEEE.
- [Zhou et al., 2014] Zhou, W., Li, M., Yin, H., and Ma, C. (2014). An adaptive fuzzy logic based energy management strategy for electric vehicles. In *2014 IEEE 23rd International Symposium on Industrial Electronics (ISIE)*, pages 1778–1783. IEEE.
- [Zhu et al., 2018] Zhu, X., Xiang, Z., Quan, L., Chen, Y., and Mo, L. (2018). Multi-mode optimization research on a multi-port magnetic planetary gear permanent magnet machine for hybrid electric vehicles. *IEEE Trans. Ind. Electron.*, 65(11):9035–9046.
- [Zineb et al., 2021] Zineb, C., Jonghoon, K., Kisoo, Y., and Mohammed, O. (2021). Hess-based photovoltaic/batteries/supercapacitors: Energy management strategy and dc bus voltage stabilization. *Solar Energy*, 216:551–563. <https://doi.org/10.1016/j.solener.2021.01.048>.
- [Ziyou et al., 2015] Ziyou, S., Heath, H., Jianqiu, L., Jun, H., Xiaowu, Z., and Minggao, O. (2015). The optimization of a hybrid energy storage system at subzero temperatures: Energy management strategy design and battery heating requirement analysis. *Applied Energy*, 159(8):576–588.
- [Zou et al., 2016] Zou, Y., Liu, T., Liu, D., and Sun, F. (2016). Reinforcement learning-based real-time energy management for a hybrid tracked vehicle. *Applied Energy*, 171:372–382.

Publications based on the thesis

Patents

1. Yashwant Kashyap, **Vishnu Sidharthan P**, Roystan Vijay Castelino., Universal Hybrid Energy Management Controller for Electric Vehicle with Emulator, *Application No:202341048198, Patent filed & published :01-09-2023.*

Papers published in refereed journals

1. **Sidharthan Panaparambil, V**, Kashyap, Y, Vijay Castelino, R. A review on hybrid source energy management strategies for electric vehicle. *Int J Energy Res.*, 45(14): 19819- 19850, 2021, doi:10.1002/er.7107.
2. **Sidharthan VP**, Kashyap Y, Kosmopoulos P. Adaptive-Energy-Sharing-Based Energy Management Strategy of Hybrid Sources in Electric Vehicles. *Energies*,16(3):1214, 2023, doi:10.3390/en16031214.
3. **Vishnu, SP**, Kashyap, Y, Castelino, RV. Adaptive intelligent hybrid energy management strategy for electric vehicles. *Energy Storage*,2023;e436, 2023, doi:10.1002/est2.436.
4. **Vishnu, Sidharthan P**, Yashwant, Kashyap. Investigation of performance and technical assessments of hybrid source electric vehicles under different locations and driving conditions. *International Journal of Green Energy*, doi: 10.1080/15435075.2023.2200545.

Papers published in conference proceedings

1. **P. Vishnu Sidharthan** and Y. Kashyap. Brushless DC Hub Motor Drive Control for Electric Vehicle Applications. *2020 First International Conference on Power, Control and Computing Technologies (ICPC2T)*, 2020, pp.448-453,doi:10.1109/ICPC2T48082.2020.9071469.
2. **P. Vishnu Sidharthan** and Y. Kashyap. Intelligent Power Allocation Strategy of Hybrid Source System in Solar Electric Vehicle. *6th International Conference on Green Energy and Applications (ICGEA) Singapore*, 2022, pp. 93-98,doi:10.1109/ICGEA54406.2022.9791973.

Bio-Data

Name : Vishnu Sidharthan P

Date of birth: 08-11-1989

Marital status: married

E-mail: vishnusidharthanp.187ee013@nitk.edu.in

Mobile: +91 8639248423

Address:

Research Scholar

Department of Electrical and Electronics Engineering

National Institute of Technology Karnataka

Surathkal, Mangaluru, India-575025, India.

Education:

- **M.Tech.**, Power Electronics, Amrita School of Engineering, Coimbatore, Tamilnadu, CGPA - 6.94, 2015.
- **B.Tech**, Electrical & Electronics Engineering, Government Engineering College Idukki, Mahatma Gandhi University, Kerala, Percentage - 67.80, 2012.

